2012

Identification of a Novel Regulator of ER Stress-Induced Apoptosis

Genevieve S. Joseph

IDENTIFICATION OF A NOVEL REGULATOR OF ER STRESS-INDUCED APOPTOSIS

A Thesis Presented to the Faculty of

The Rockefeller University

in Partial Fulfillment of the Requirements for

the degree of Doctor of Philosophy

by

Genevieve S. Joseph

June 2012

IDENTIFICATION OF A NOVEL REGULATOR OF ER STRESS-INDUCED APOPTOSIS

Genevieve S. Joseph, Ph.D.
The Rockefeller University 2012

The survival and development of a multicellular organism is reliant upon proper cell and organelle function, and the tight regulation of cell number. The endoplasmic reticulum (ER) is the cellular compartment where membrane and secretory pathway proteins are folded and modified for transport within or outside of the cell. When the ER becomes overwhelmed by the accumulation of unfolded or misfolded proteins, it enters a state of "ER stress" and the organelle activates the unfolded protein response (UPR) to alleviate the strain. One prominent event during ER stress and the UPR is the Ire1-mediated splicing of unspliced *xbp1* (*xbp1U*) into the potent transcription factor spliced Xbp1 (Xbp1S). If the ER cannot return to homeostasis, the apoptotic program is activated. Programmed cell death (apoptosis) is an evolutionarily conserved, genetically controlled program which eliminates excess or irreparably damaged cells and it is necessary to maintain tissue integrity. The failure to properly activate or suppress cell death can greatly impact the health and survival of an organism. Cancer is caused by the failure to remove compromised cells leading to the generation of highly-proliferative and renegade cells which are harmful the animal. In contrast, excessive cell death in neuronal tissues is associated with a variety of neurodegenerative diseases. Research conducted by several groups has led to the identification of the primary regulators of the UPR and apoptosis in

Drosophila. However, limited studies have taken place to isolate genes which specifically affect both the proximal event of the UPR and the distal event of apoptosis. In order to identify novel regulators of ER stress-induced apoptosis, an *ex vivo* assay was developed to screen 452 p-element lethal FRT lines generated by the UCLA Undergraduate Consortium in Functional Genomics. *Drosophila* is amenable for a modifier screen using the FLP/FRT technique, in which mitotic recombination is used to generate loss-of-function clones in specific tissues. In particular, the use of the FLP/FRT system allows clonal analysis of mutant genes in dispensable tissues of the fly when a gene cannot be easily studied in the homozygous condition. Eye imaginal discs, dissected from the progeny of selected p-element lethal FRT allele males mated to females with GFP-marked wild-type chromosomes were cultured in ER stress inducing conditions and analyzed for differential cleaved caspase 3 activity. *CG8108* was identified in the screen as a strong loss-of-function suppressor of ER stress-induced apoptosis and the gene was selected for further study. This thesis shows that CG8108 is necessary for efficient splicing of *xbp1* during the early phase of the UPR and for the activation of caspases at the final stages of ER stress-induced apoptosis. The function and protein expression pattern of *CG8108* is currently unknown and this work provides the initial characterization of CG8108 localization during development.

This dissertation is dedicated to my family, closest supporters, and…

In memoriam

"*… Dad! Dad! A fly! A fly! ...*"

Acknowledgements

I would like to express my gratitude to my advisor Dr. Hermann Steller for inviting me to join his lab and for his advice during my graduate studies. In addition, I extend my appreciation to my committee members Dr. Shai Shaham and Dr. Michael Young for their direction and input during my FAC meetings and to Dr. Claude Desplan for accepting my outside committee member request.

I am indebted to my undergraduate developmental genetics lab instructor Dr. J. Peter Gergen for encouraging me to delve into *Drosophila* research under the watchful eye of his then graduate student Pegine Walrad and his suggestion to apply to The Rockefeller University. With Dr. Gergen's and Peg's guidance and patience, I learned the basics of fly pushing, *in situ* hybridization, and using Photoshop to process my images. I am also appreciative of the opportunity to work as a research coordinator for Dr. Leslie Pick. Dr. Pick taught me the fundamentals of molecular biology such as cloning; without her instruction, I would have been lost in the Steller lab.

I am grateful for the technical assistance and/or suggestions from: Sigi Benjamin-Hong, Anshuman Kelkar, Jose Rodriguez, Cristinel Sandu, Brieann Fant, Alana Bhajan Persaud, Samara Brown, and my summer student Zuwena Plata.

Thanks are due to Pedro Domingos for initially designing the screen to identify modifiers of ER stress-induced apoptosis and for his technical assistance to tediously fine-dissect thousands of eye-antennal imaginal discs.

Finally, I would like to thank my mom, my siblings, my extended family members, and fellow musicians for their supplications, encouragement, and well wishes.

Table of Contents

List of Figures

List of Tables

Chapter 1

Introduction to Programmed Cell Death

1.1 Programmed cell death

The survival of a multicellular organism is contingent upon nutrient availability, proper cell function, and the tight regulation of cell number. Programmed cell death (PCD) is an evolutionarily conserved, genetically controlled program which eliminates excess or irreparably damaged cells and is necessary to maintain tissue homeostasis. The distinct morphological characteristics of PCD such as membrane blebbing, cell shrinkage, chromosome condensation, and engulfment of cell corpses by macrophages, were described by Kerr *et al*., after observations of normal embryonic and malignant tissues and were classified as apoptosis (Kerr *et al*., 1972). During apoptosis, the release of potentially caustic cellular material into the surrounding area is prevented and corpses are cleared by phagocytosis. In contrast, during necrotic cell death, damaged cells swell, lyse, and subsequently release cytosolic material into the surrounding area, triggering an inflammatory response (Steller, 1995; Thompson, 1995; Fuchs and Steller, 2011; Yuan and Kroemer, 2010). Proper execution of the PCD pathway in metazoans contributes to the overall survival of an organism by ensuring accurate shaping of an organism during early development, eliminating deleterious or damaged cells, and opposing proliferation. In contrast, dysregulated apoptosis caused by retarded or increased cell death can have pathological consequences.

The regulation of apoptosis is necessary for proper development of diverse organisms such as the worm, fly, and mammals. In the nematode *C. elegans*, the reproducible death of 131 out of the roughly 1000 somatic cells of the hermaphrodite is a consequence of a genetically controlled program regulating cell number (Ellis and Horvitz, 1986). In the fly and mammals, the number of neurons in the central nervous

system is controlled by target-dependent trophic factor availably and cells which do not make proper connections are eliminated (Zhou *et al*., 1995; Sonnenfeld and Jacobs, 1995; Bergmann *et al*., 2002; Yuan and Yanker, 2002). During mammalian development, PCD fashions the tubular structure of the gut and mammary glands and sculpts digits by removing interdigital cells (Abud, 2004).

Apoptosis maintains tissue homeostasis and promotes organismal survival by eliminating cells which are potentially harmful to the animal. Ionizing radiation can induce DNA damage, causing catastrophic mutations and organism mortality. PCD is initiated after x-ray, gamma-ray, or UV radiation and leads to the elimination of cells with DNA damage (Zhou *et al*., 1999; Zhou *et al*., 2003).

Dysregulated apoptosis can lead to either inappropriate cell survival or cell death causing an increase or decrease in the cell population, respectively. B-cell lymphomas in humans stem from the failure of cells to die, while retinitis pigmentosa and Fuchs Dystrophy are examples of human ocular diseases caused by increased activation of the apoptotic program. Follicular B-cell lymphomas result from the translocation of the Bcl-2 gene from chromosome 18 onto the heavy chain locus of chromosome 14. The translocation event leads to markedly increased expression of the apoptosis antagonist Bcl-2, conferring apoptosis resistance in B-cells (Tsujimoto *et al*., 1985; Thompson, 2005). The retinal degenerative disease retinitis pigmentosa is caused by photoreceptor death due to the misfolding of photoreceptor proteins such as rhodopsin (Davidson and Steller, 1998; Ryoo *et al*., 2007; Kang and Ryoo, 2009). Fuchs dystrophy is degenerative disease of the eye caused by increased cell death of corneal endothelial cells leading to corneal edema and eventual vision loss (Borderie *et al*., 2000).

1.2 Initial investigations into the genetics of apoptosis

The generic underpinnings of PCD were fully appreciated after the elegant studies of cell fate specification in the nematode worm, *C. elegans*. Sulston and Horvitz noted that 131 out of roughly 1000 hermaphrodite somatic cells underwent death in stereotypic fashion (Sulston and Horvitz, 1977). Based on the premise that cell death is genetically controlled, an EMS mutagenesis screen was conducted to identify genes required for controlling the number of somatic cells in the hermaphrodite. *ced-3* and *ced-4* mutants possessed extra somatic cells and the *ced-3* and *ced-4* genes were classified as necessary for cell death (Ellis and Horvitz, 1986 and Yuan and Horvitz, 1990). *ced-3* was subsequently cloned and its sequence was found to show similarity to the human cysteine protease interleukin-1β converting enzyme (ICE) (Yuan *et al*., 1993). In addition, ectopic expression of *ced-3* induced cell death; solidifying the notion that cells have an intrinsic, gene-directed cell death program (Shaham and Horvitz, 1996).

The revelation that components of cell death machinery are conserved between mammals and *C. elegans* led to intensive efforts to identify and mechanistically characterize additional PCD proteins in the worm. After ced-3 and ced-4 were identified, subsequent experiments led to the elucidation of the core cell death machinery in *C. elegans* and other model systems (Figure 1.1). The central apoptotic pathway in the worm is composed of Egl-1, ced-9, ced-4, and ced-3 (Horvitz *et al*., 1994; Hengartner and Horvitz, 1994). Egl-1 is a proapoptotic Bcl-2 family protein which disrupts the ced-9-ced-4 complex, thereby liberating ced-4 and permitting the activation of apoptosis (Conradt and Horvitz, 1998; del Peso *et al*., 2000; del Peso *et al*., 1998). ced-9 is a Bcl-2-like protein that inhibits apoptosis by binding to ced-4 and preventing its oligomerization

Figure 1.1: The core apoptotic pathway in the fly, worm, and mammals

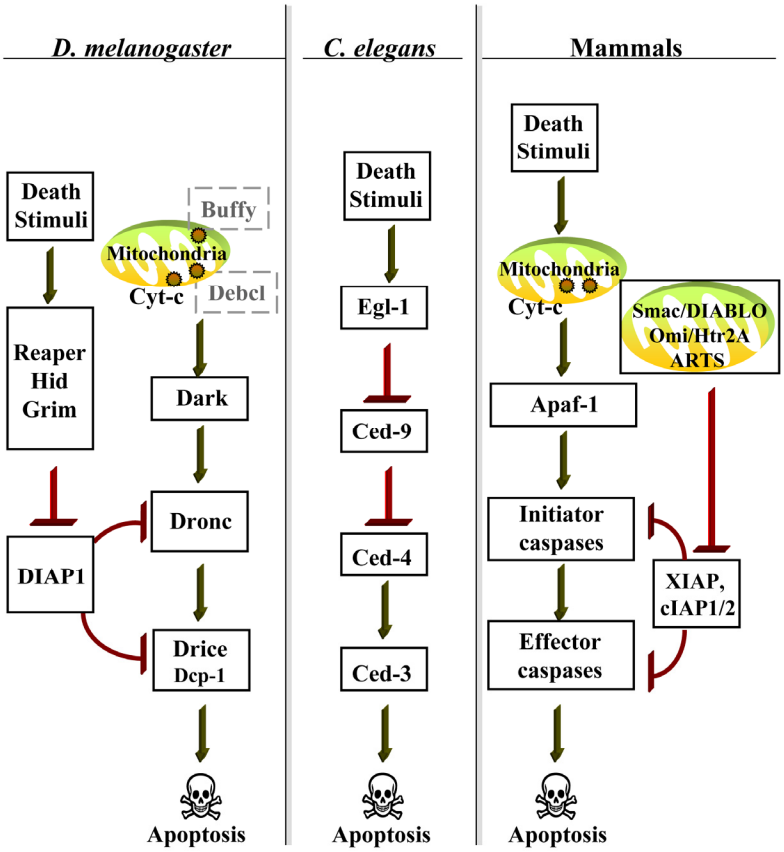

Figure 1.1: An apoptotic stimulus leads to the formation of an 'apoptosome' consisting of Dark/ced-4/Apaf-1, Dronc/ced-3/caspase-9 and cytochrome c in some instances. The apoptosome facilitates the activation of initiator caspases which in turn activate effector caspases. Inhibitors of apoptosis such as Diap1//ced-9//XIAP/cIAP1/cIAP2/ARTS promote cell survival by sequestering and/or degrading caspases such as Dronc/drice in the fly, ced-3 in worms, and caspase 3, 7, and 9 (not depicted) in mammals. IAP antagonists such as Reaper, Hid and Grim (RHG)//Egl-1//Smac/DIABLO/Omi/Htr2 promote cell death after apoptotic stimuli by dislodging caspases.

with and activation of ced-3 (Hengartner *et al*., 1992; Yang *et al*., 1998). Recent publications indicating that ced-9 and ced-4 rarely co-localize and may not bind, have called the nature of the ced-9 and ced-4 interaction into question; however, the initial assumptions regarding ced-9 and ced-4 physical association initiated the exploration for additional PCD components in the worm (Pourkarimi *et al*., 2011). The potential for caspases to both promote and inhibit cell death was highlighted by experiments showing ced-4 had anti- and pro-apoptotic properties (Shaham and Horvitz, 1996).

1.3 Cell death regulation in *Drosophila*

1.3.1 Identification of cell death genes in the fly

The utility of studying PCD in the fly was initially demonstrated in a deficiency screen for regulators of embryonic cell death (White *et al*., 1994). Homozygous embryos from a set of deletions, including *Df(3L)H99* (also referred to as *H99*), were devoid of developmental cell death and ectopic cell death due to either genetic defects, or ionizing radiation (White *et al*., 1994). The genes *reaper* (*rpr*), *head involution defective* (*hid*), and *grim* (collectively referred to as *RHG*) map to *Df(3L)H99* and are proximal regulators of PCD (White *et al*., 1994; Grether *et al*., 1995; Chen *et al*., 1996). Although *RHG* do not share significant sequence homology across their proteins, they share a common motif in the N-terminus (IBM) which is essential for their efficient cell killing (Olson *et al*., 2003; Wang *et al*., 1999; Wu *et al*., 2001; further discussed in section 1.3.6). The identification and characterization of *RHG* made it possible to conduct genetic modifier screens to isolate additional *Drosophila* cell death genes (McCall and Steller, 1997; Goyal *et al*., 2000; Xu *et al*., 2005; Xu *et al*., 2006).

1.3.2 The proximal cell death inducers RHG and RHG-like proteins

Rpr is a small 65 amino acid protein capable of inducing apoptosis when ectopically expressed in fly tissues and mammalian cells (White *et al.*, 1994; White *et al*., 1996; Fraser and Evan, 1997; Vucic *et al*., 1997; McCarthy and Dixit, 1998). *rpr* is transcriptionally induced in response to many different apoptotic stimuli, and its expression is detected significantly before doomed cells show any morphological changes (White *et al.*, 1994; Nordstrom *et al*., 1996; Zhou *et al*., 2003; Jiang *et al*., 2000). Ectopic killing by *rpr* is suppressed by co-expression of anti-apoptotic proteins such as baculovirus p35 and by the loss-of-function mutations in cell death effectors (Clem *et al*. 1991; Hay *et al*., 1995; Vucic *et al*., 1997; Kanuka *et al*., 1999; Zhou *et al*., 1999; Xu *et al*., 2005; Xu *et al*., 2006, Muro *et al*., 2006). Due to the partially redundant function of RHG proteins, *rpr* null mutants display nearly wild-type numbers of apoptotic cells during embryogenesis and are viable, but they are male sterile and have an enlarged central nervous system (CNS) (Peterson *et al*., 2002; Zhou *et al.*, 1997; Tan *et al.*, 2011).

Mutations in *head involution defective (hid)* were originally noted to affect rotation of the male genitalia, wing formation, and embryonic head involution (Abbott and Lengyel, 1991). *hid* was subsequently shown to encode a 410 amino acid protein that maps within the H99 deletion and plays an important role in the induction of apoptosis (Grether *et al.*, 1995). *hid* null mutants have reduced viability, reduced cell death and contain extra cells (Grether *et al*., 1995; Suzanne *et al.*, 2010). *hid* mRNA and protein is expressed during embryogenesis, in both dying cells and many living cells. Hid is negatively regulated by the RAS/MAPK pathway; phosphorylation of Hid by MAPK suppresses its killing ability, thereby explaining how cells that express Hid can survive

(Kurada *et al*., 1998; Bergmann *et al*., 1998; Gafuik and Steller, 2011). Ectopic over-expression of *hid* induces apoptosis in fly tissues and cells, as well as mammalian cells (Grether *et al*., 1995; Haining *et al*., 1999). Like *rpr*, death induced by ectopic *hid* can be suppressed by p35 and mutations in downstream cell death effectors (Hay *et al*., 1995; Zhou *et al*., 1999; Kanuka *et al*., 1999; Xu *et al*., 2005; Leulier *et al*., 2006; Xu *et al*., 2006; Muro *et al*., 2006).

grim is expressed during embryonic development in regions where death occurs and encodes a 138 amino acid protein that induces cell death when over expressed in the adult fly, midline-glia, and insect cell lines. *Grim*-induced apoptosis is suppressed by p35 and by abrogated activity of distal cell death components (Chen *et al*., 1996; Wing *et al*., 1998). *grim* null animals are viable, fertile, and do not show overt developmental defects. Analysis of *grim* mutants indicated it is not necessary for the pruning of ommatidial cells, but is required for microchaete glial cell death. Grim-mediated microchaete death is dependent upon the Bcl-2-like protein, Buffy (Wu *et al*., 2010). Although Grim does not have significant homology to human proteins it can utilize the mammalian cell death machinery and mediate degradation of XIAP via ubiquitination (Silke *et al*., 2004).

sickle, *Jafrac2*, and *Drosophila Omi* (*dOmi)* are proposed to function in proximal events of the apoptosis pathway like *RHG*. Sickle, Jafrac2, and dOmi possess an IBM and utilize mechanisms analogous to RHG to elicit cell death (Srinivasula *et al*., 2002; Tenev *et al*., 2002; Challa *et al*., 2007; Khan *et al*., 2008). In contrast to RHG, Sickle, Jafrac2 and dOmi require proteolytic cleavage to expose their IBMs.

sickle over-expression is sufficient to induce cell death in mammalian and fly cells and its cell killing can be inhibited by p35 (Srinivasula *et al*., 2002). *Jafrac2* is an

ER localized thioredoxin peroxidase which translocates to the cytoplasm in apoptotic cells. *dOmi* is the fly homologue of the mammalian serine protease *Omi/Htr2A* and localizes to the mitochondria in living cells (Tenev *et al*., 2002). Upon apoptotic stimuli, *dOmi* translocates from the mitochondria to the cytoplasm where it may activate *dronc* and facilitate cell death. *dOmi* expression is sufficient to kill S2 cells and fly tissues and is subject to inhibition by p35 (Challa *et al*., 2007; Khan *et al*., 2008).

1.3.3 Caspases

Caspases are executioners of the apoptotic program and responsible for the characteristic morphological features of apoptosis. Caspases are an evolutionarily conserved family of cysteine aspartyl-specific proteases which cleave cellular targets including cytoskeletal proteins, the nuclear lamina, and chromatin, leading to cell shrinkage, nuclear condensation, and DNA laddering, respectively (Hengartner, 2000; Ju *et al*., 2007). Caspases are produced as inactive zymogens and are composed of three domains: the prodomain, a large subunit ("p20"), and a small subunit ("p10") (Walker *et al*., 1994; Wilson *et al*., 1994).

Caspases are classified as "initiator" or "executioner" caspases depending upon the size of their prodomain and the presumed mechanism of their activation. Initiator caspases have a long prodomain, and are the proximal components of the proteolytic caspase cascade that are activated upon apoptotic stimuli. Effector caspases have short prodomains and are activated by initiator caspases after cleavage at specific Asp residues and are considered the executioners of apoptosis (Reed *et al*., 2004; Boatright *et al*., 2003; Kuida *et al*., 1998; Miura *et al*., 1993; Chai *et al*., 2001). Initiator caspases utilize protein-protein interactions via the caspase activation recruitment domain (CARD) or

death effector domain (DED) in their long prodomains. Initiator caspases form complexes with adaptor molecules and autoactivate to become mature caspases (Yang *et al*., 1998; Shi, 2002; Renatus *et al*., 2001; Rodriguez *et al*., 1999; Boatright *et al*., 2003). In mammals, the CARD of Caspase-9 is used to form a cell death-inducing complex in concert with the adaptor proteins Apaf-1 and cytochrome c, called the apoptosome. The apoptosome facilitates activation and Caspase-9 and allows it to activate downstream caspases such as Caspase-3 and Caspase-7 (Zou *et al*., 1999; Li *et al*., 1997; Acehan *et al*., 2002). In the fly, the CARD-containing apical caspase Dronc, associates with Dark, the *Drosophila* homologue of Apaf-1, and sometimes with cytochrome c to activate caspases (Kanuka *et al*., 1999).

1.3.4 The *Drosophila* caspases

The *Drosophila* genome contains seven caspases: *dronc*, *dredd*, *drice*, *dcp-1*, *decay*, *damm* and *strica* (Figure 1.1). *dronc* and *dredd* are classified as initiator caspases and *drice*, *dcp-1*, *decay*, *damm* and *strica* are effector caspases.

Dronc (Drosophila Nedd2-like caspase) contains an N-terminal CARD and is expressed throughout embryonic and larval development and in the ovary of the adult fly. Dronc is an ecdysone inducible protein and is upregulated in the mid-gut and salivary glands of late third instar larvae (Dorstyn *et al*., 1999). Dronc's integral role in cell killing is evidenced by its death induction capabilities in yeast, fly, and mammalian cells (Meier *et al.*, 2000). Dronc is a strong cell death inducer and its cell death is weakly suppressed by p35 (Meier *et al*., 2000; Quinn *et al*., 2000). When placed in trans with mutations in *RHG* or *dark* and by ectopic co-expression or the *Drosophila* cell death inhibitor proteins Diap1 and Diap2*,* apoptosis by ectopic Dronc can be dominantly suppressed (Quinn *et*

al., 2000). Cell culture experiments subsequently demonstrated Dronc cleavage of caspase substrates requires Dark (Harvey *et al*., 2001; Dorstyn *et al*., 2002). The dominant suppression of Dronc killing by Dark, the *Drosophila* homologue of human Apaf-1, indicates Dronc may be processed in an apoptosome-like complex akin to Caspase-9. Loss-of-function *dronc* mutants are sickly and die within a few days of eclosing. *dronc* mutants have opaque wings due to the failure of wing cells to die after adults eclose, contain extra cells in the eye, exhibit little embryonic cell death when generated by germline clones, and do not have overt defects in oogenesis (Xu *et al*., 2005; Baum *et al*., 2007).

Insight into the mechanism of Dronc killing was furthered by studies focused on protein-protein interactions mediated by *dronc*. Dronc co-immunoprecipitates with and proteolytically processes both Drice and Diap1, confirming *dronc's* classification as an initiator caspase (Meier *et al*., 2000; Muro *et al*., 2005).

Dredd (death-related ced-3/Nedd2-like gene) is an apical caspase with a long, DED-containing prodomain. *Dredd* encodes three splice variants, two of which contain long prodomains baring similarities to Caspase-8, implicating *dredd* as an initiator caspase. The initial evidence classifying *dredd* as an effector of cell death was based on data showing that *dredd* is upregulated in cells expressing ectopic *rpr*, *hid*, and *grim* and that its transcript is suppressed in *H99* mutant embryos. Dredd's interaction with Dark and the ability of a deficiency uncovering *dredd* to dominantly suppress cell killing by *GMRrpr* and *GMRhid* implicated *dredd* as a regulator apoptosis (Chen *et al*., 1998; Rodriguez *et al*., 1999). Interestingly, Dredd was determined to have a non-apoptotic role in immunity. *Dredd* mutants were isolated in a screen for genes necessary for providing

resistance to Gram-negative bacteria in the fly. *dredd* null animals are viable and fertile, but display defective induction of genes encoding proteins which confer an immune response to a Gram-negative bacterial infection (Leulier *et al*., 2000). Dredd is currently categorized as being functionally more relevant for immunity than for cell death regulation as it poorly induces ectopic cell death.

drIce (Drosophila ICE) is an important effector caspase responsible for executing cell death in the fly. *drice* is expressed throughout development and it has a role in oogenesis, elimination of vCrz neurons, and ectopic cell death due to RNAi-mediated knockdown of Diap1, the primary cell death suppressor (Fraser and Evan, 1997; Leulier *et al*., 2006; Lee *et al*., 2011). *drice* hypomorphic and null mutants have reduced viability, mis-rotated terminalia, extra interommatidial cells, and display defects in spermatid individualization (Arama *et al*., 2003; Muro *et al*., 2006). Loss of *drice* function leads to increased numbers of midline glia and can suppress ectopic cell deaths due to *RHG* overexpression in the eye or loss of Diap1 activity (Wang *et al*., 2006; Muro, 2006).

The effector caspase Dcp-1 (Drosophila caspase-1) is expressed in embryonic tissues and in the developing ovary and can cleave caspase substrates in mammalian cell culture (Song *et al*., 1997; Song *et al.*, 2000; Laundrie *et al*., 2003). *dcp-1* mutant flies are viable and fertile, but females have cell death defects during mid-oogenesis (Laundrie *et al*., 2003). *dcp-1* mutants also display a delay in vCrz neuron death (Lee *et al*., 2011).

Decay (Drosophila executioner caspase related to Apopain/Yama) has sequence homology to Caspase-3, Caspase-7, Caspase-8, and Caspase-10 and is capable of cleaving caspase substrates (Dorstyn *et al*., 1999; Harvey *et al*., 2001). Decay is a

putative effector caspase with a short prodomain and its misexpression in the testis leads to sterility. However, a significant role for *decay* in controlling cell death seems unlikely, as null mutants are viable, fertile, and do not have defects in developmental apoptosis (Kondo *et al*., 2006; Lee *et al*., 2011).

damm (death *associated molecule related to Mch2*) is expressed during most of development and induces apoptosis when over-expressed, but the physiological function of this gene remains to be determined (Harvey *et al*., 2001).

Strica (Ser/Thr-Rich caspase) is an atypical caspase containing a long serine-threonine rich prodomain devoid of a CARD, DED, or protein-protein domain capable to stimulating oligomerization. Ectopic expression of *strica* in SL2 cells induces apoptosis and it is not inhibited by p35. *strica* mRNA is expressed during all stages of development and Strica protein localizes to the cytoplasm. Strica is capable of binding both Diap1 and Diap2, but it is only inhibited by Diap1 (Doumanis *et al*., 2001). RNAi knockdown of s*trica* delays interommatidial cell death suggesting it may have a role in patterning of the eye. *strica* functions during developmental apoptosis and homozygous null mutants display defects in oogenesis (Leulier *et al*., 2006; Baum *et al*., 2007; Lee *et al*., 2011).

1.3.5 RHG proteins and caspase regulation

Protecting cells from excessive caspase activation necessitates sequestering RHG and caspases from their downstream targets. Inhibitor of apoptosis (IAP) proteins inhibit cell death by binding to and blocking the activity of caspases, thereby preventing cells from unwanted death. IAPs contain at least one baculovirus IAP repeat (BIR) domain and may contain a RING domain. BIR domains possess a zinc-binding fold that facilitates protein-protein interactions. The BIR domains of IAPs bind to both caspases

and IAP antagonists, preventing the activation of apoptosis. The RING domains of IAPs ubiquitinate target proteins or themselves for either degradation or inactivation (Reed *et al*., 2004). *Diap1*, *Diap2*, *dBruce*, and *deterin* are the four fly IAPs (Hay *et al*., 1995; Vernooy *et al*., 2002; Jones *et al*., 2000).

Diap1 is the most important and best-studied IAP in the fly, and is composed of two BIR domains and a single RING domain. The BIR domains are essential for caspase binding and the RING domain functions as an E3 ubiquitin protein ligase (Ryoo *et al.*, 2002; Wilson *et al.*, 2002). Diap1 is a potent inhibitor of cell death and its function is vital for the survival of the fly. The elimination of Diap1 protein leads to unbridled caspase activation in the embryo, developmental defects, and animal lethality (Wang *et al.*, 1999; Lisi *et al*., 2000; Goyal *et al*., 2000). The dramatic increase of cell death in Diap1 null animals highlights the importance of this protein for controlling the ever present and active cell death cascade. Ectopic expression of Diap1 is sufficient to inhibit naturally occurring and ectopic RHG-mediated cell death (Goyal *et al*., 2000; Hay *et al*., 1995; Yin and Thummel, 2004). Diap1 prevents caspase activation by simultaneously binding the active effector caspases, Drice and Dcp-1, and the initiator caspase Dronc via its BIR1 and BIR2 domains, along with the removal of its N-terminal 20 amino acids (Zachariou *et al*., 2003; Tenev *et al*., 2005). The ability of Diap1 to bind both initiator and effector caspases is an elegant means of curtailing caspase activation by blocking the initiation and propagation of the caspase cascade. Mutational analysis of the Diap1 BIR domains revealed the requirement of the BIR1-BIR2 linker region for binding to Drice and Dcp-1 for suppression of apoptosis (Zachariou *et al*., 2003). The Diap1 BIR1 is the primary region required for physical binding to Drice and Dcp-1, and alterations to

Drice/Dcp-1 binding to BIR1 have significant consequences for Diap1 activity (Lisi *et al*., 2000; Zachariou *et al*., 2003; Yan *et al*., 2004).

While the BIR1 domain is important for effector caspase binding, the BIR2 domain of Diap1 is crucial for inhibition of Dronc activity (Wilson *et al*. 2002; Chai *et al*., 2003; Meier *et al*., 2000). A twelve amino acid stretch of Dronc in the linker region between its CARD and protease domains is sufficient for binding to Diap1-BIR2 and mutations preventing this interaction enhance Dronc killing (Chai *et al*., 2003). Structural analysis of this region revealed the BIR2 pocket bound by Dronc is the same surface used by RHG proteins. RHG proteins compete for binding to Diap1 and free Dronc to activate the apoptotic pathway. Once Dronc is bound to Diap1, the Diap1 RING ubiquitinates and inactivates Dronc (Wilson *et al*., 2002; Chai *et al*., 2003; Lee *et al*., 2011). When Dronc is free of Diap1 inhibition, it is thought to cleave Diap1 and leave it in an autoinhibited state where it can no longer function as potent *drice* inhibitor, thus allowing cell death to proceed (Yan *et al.*, 2004).

The Diap2 protein contains three BIR domains and one RING domain. Ectopic expression of Diap2 in the eye is sufficient to suppress cell death due to *GMRrpr* and *GMRhid*. Diap2 physically interacts with Rpr, Hid, Strica, and Drice (Hay *et al*., 1995; Doumanis *et al*., 2001; Vucic *et al*., 1997; Vucic *et al.,* 1998). Diap2 null animals are homozygous viable and fertile, but they are compromised in their ability to mount an immune response. The Diap2 immune response is dependent on a functional RING domain (Huh *et al*., 2007; Gesellchen *et al*., 2005). Rpr and Hid antagonize Diap2 by degrading Diap2 (Huh *et al*., 2007). Deterin is a single BIR containing IAP and it lacks a RING domain. Deterin is similar to mammalian Survivin, an IAP which does not contain

a RING domain and contains a single BIR (Jones *et al*., 2000). Deterin function depends on its BIR domain and C-terminus. Transfection of *deterin* into insect cell lines exposed to liposomes or *rpr* expression exhibit less cell death compared to cells transfected with the vector alone. RNAi-mediated knockdown of endogenous *deterin* in SF9 cells causes reduced viability (Jones *et al*., 2000).

dBruce is a very large, 530kDa IAP that contains a single BIR domain and a C-terminal ubiquitin conjugation domain (E2) (Vernooy *et al*., 2002). The BIR of dBruce directly binds to wild-type rpr, but it weakly suppress *rpr* killing. DBruce has a relatively minor role in suppressing apoptosis in the fly and it cannot mitigate *GMRdronc, GMRdark* or *GMRhid* mediated killing (Vernooy *et al*., 2002; Domingues and Ryoo, 2011). Homozygous loss-of-function mutants for *dBruce* are viable and male sterile (Arama *et al*., 2003; Domingues and Ryoo, 2011).

dBruce regulates the levels of Rpr expression; *dBruce*$^{-/-}$ animals have elevated levels of ectopically expressed Rpr and lysine deficient Rpr compared to wild-type animals (Domingues and Ryoo, 2011). Lysine residues are the primary targets of ubiquitination and allow degradation or modification function of proteins (Bergmann, 2010).

1.3.6 Antagonizing IAPs

RHG proteins promote cell death by antagonizing inhibitor of apoptosis proteins (IAPs). RHG killing depends on their N-terminal IAP binding motif (IBM); amino acids of 1-15 of RHG share homology and the first four amino acids after the initiator methionine are vital for IAP binding, inhibition and caspase liberation (Olson *et al*., 2003; Wang *et al*., 1999; Wu *et al*., 2001). RHG proteins reduce Diap1 protein levels by

ubiquitin-proteasome-mediated degradation, and Diap1 degradation is RING domain dependent (Ryoo *et al*., 2002; Yoo *et al*., 2003; Olson *et al*., 2003; reviewed in Bader and Steller, 2009). The ability of Rpr to fully inactivate Diap1 depends on the E3 ubiquitin ligase activity of the Diap1 RING (Ryoo *et al*., 2002).

Sickle is another IAP-binding protein that contains an IBM. Sickle physically associates with full length Diap1 and Diap2 in an IBM-dependent manner (Srinivasula et al., 2002). Jafrac2 and dOmi differ from RHG and Sickle since their IBMs are exposed after proteolytic cleavage and targeting to the ER or mitochondria, respectively. Jafrac2 is released from the ER and into the cytosol upon apoptotic stimuli where it induces apoptosis by competing for the BIR2 binding pocket of Diap1 used to sequester Dronc (Tenev et al., 2002). dOmi consists of an IBM, a serine protease domain, and PDZ domain. After apoptotic stimulation, dOmi is translocated from the mitochondria to the cytosol where dOmi binds both BIR domains of Diap1 and can stimulate Diap1 ubiquitination and proteolytic cleavage (Challa *et al.*, 2007; Khan *et al.*, 2008). dOmi cleavage of Diap1 between BIR1 and BIR2 leads to the degradation of the BIR1 domain and the freeing of BIR1 bound effector caspases Drice and Dcp-1 in S2 cells (Khan *et al*., 2008). In contrast to the other IAP antagonists, dOmi is able to kill without an intact IBM domain due to its serine protease activity. Additionally, removal of the dOmi PDZ domain increases its killing efficiency indicating the PDZ domain acts to restrain its activity (Challa *et al.*, 2007; Khan *et al.*, 2008).

Additional requirements for RHG killing include mitochondrial localization and self association (Claveria *et al*., 2002; Olson *et al*., 2003; Abdelwahid *et al*., 2007; Freel *et al*., 2008; Sandu *et al*., 2010). The expression of *rpr* and *hid* in S2 cells leads to

cytochrome c release and mitochondrial membrane permeabilization in a caspase-dependent manner (Abdelwahid *et al*., 2007).

Grim contains three regions which are predicted to form helical structures called GH1, GH2, GH3 for Grim helix 1, 2, and 3. The GH3 domain of Grim is required for its mitochondrial localization and cell killing, but not its physical association with IAPs (Claveria *et al*., 2002). The Hid C-terminus contains a domain necessary for its mitochondrial localization and for ectopically-induced *hid* cytochrome c release (Haining *et al*., 1999; Abdelwahid *et al*., 2007). Mutations truncating the Hid C-terminus result in animal lethality indicating the importance of that region for proper Hid function (Haining *et al*., 1999). Initial cell culture experiments indicated Rpr localizes in the mitochondria due to the amphipathic region similar to the Grim GH3 domain. The Rpr GH3 domain is necessary for its localization and effective killing (Olson *et al*., 2003; Freel *et al*., 2008). The fusion of the Rpr GH3 domain to GFP is sufficient to target GFP to the mitochondria leading researchers to assume Rpr independently transports to the mitochondria. Deletion of the Rpr GH3 domain (RprΔGH3) does not affect Rpr binding to Diap1, but results in cytoplasmic localization of Rpr, reduced RING domain-mediated degradation of Diap1, and mitigates its killing in cell culture and *Drosophila* tissues (Olson *et al*., 2002; Freel *et al*., 2008). Replacement of the Rpr GH3 domain with mitochondria targeting sequences such as Bcl-x_L tail or the C-terminus of Hid restored Rpr localization and IAP destruction. The experiments studying Diap1 and RprΔGH3 interaction revealed that binding of Rpr to Diap1 is necessary but not sufficient to elicit cell death.

Recent studies indicate that both Rpr self-association and binding to Hid are important for cell killing (Sandu *et al.*, 2010). Replacement of the Rpr GH3 domain with

the yeast GCN4 leucine zipper (RprLZ) which promotes parallel dimerization was capable of efficient killing and Diap1 degradation, while replacement of the Rpr GH3 domain with the antiparallel domain of *E. coli* ProP was a poor killer (Sandu *et al*., 2010). The ability for RprLZ to kill with nearly sixty percent of the protein replaced with sequences from yeast shows that the power of *rpr* killing resides in its ability to self associate. Hid binds to and transports Rpr to the mitochondria. In the absence of Hid expression, Rpr has a diffuse expression pattern and compromised function. Suppression of Hid localization in the mitochondria or its total repression leads to Rpr stabilization in S2 cells and mitigates *rpr* killing when ectopically expressed in the eye (Sandu *et al*., 2010). In addition, forced targeting of wild-type or GH3 defective Rpr to the mitochondria with the Hid mitochondrial targeting sequence enhances *rpr* killing (Sandu *et al.,* 2010). Collectively, these studies indicate that Hid recruits Rpr to the mitochondrial outer membrane (MOM) for efficient cell killing.

1.3.7 Non-apoptotic functions for apoptotic pathway components

The activation of caspases and cytochrome c are necessary for terminal sperm differentiation (Arama *et al*., 2003; Arama *et al*., 2006; Arama *et al*., 2007). In the fly, sperm are produced in a bulk cytoplasm and caspases are locally activated to extrude excess cytoplasm allowing the formation of individual, functional sperm in the process of terminal individualization. During individualization, caspase activity can be detected with anti-cleaved Caspase-3 or anti-Drice antibodies. There are two forms of cytochrome c in *Drosophila*, *cyt-c-p* which is primarily found in the soma and is necessary for respiration and *cyt-c-d* which is mostly expressed in the male germline and is required for the individualization process. Loss of *cyt-c-d* function leads to suppression of caspase

activation, failed individualization, and sterility. The importance of proper caspase activation for individualization is also indicated by the presence of defective individualization complexes and sterility phenotypes of *dronc* and *dark* mutant males (Arama *et al*., 2003; Arama *et al*., 2006). The IAP dBruce is also required for proper individualization and *dBruce*$^{-/-}$ males exhibit reduced fertility. dBruce forms a protective gradient which opposes caspase activity allowing the skillful removal of cellular material from developing sperm while maintaining a functional entity (Arama *et al*., 2003; Arama *et al*., 2007; Kaplan *et al*., 2010).

During neuronal pruning in the fly, caspases are locally activated at the ends of dendrites after being severed and tagged by phagocytes. The activation is site-specific and the soma of the neuron is spared. Neuronal pruning can be suppressed by the overexpression of *Diap1* or the suppression of apoptosis regulators such as *dronc* or *dark*; whilst overexpression of *hid* leads to neuronal cell death (Williams *et al*., 2006). As previously mentioned, the initiator caspase *dredd* functions in a non-apoptotic manner to regulate the immune response by upregulating the expression of drosomycin and metchnikowin during Gram-negative bacterial challenge (Leulier *et al*., 2000).

1.4 Comparison of *Drosophila* and mammalian apoptosis

Intrinsic mammalian PCD depends on cytochrome c and apoptosome formation (Zou *et al*., 1999). Apaf-1, cytochrome c and Caspase-9 come together in a complex to activate downstream caspases. Mammalian cytochrome c release depends upon Bcl-2 family proteins. Anti-apoptotic Bcl-2 proteins preserve mitochondrial membrane integrity and prevent permeabilization due to apoptotic stimuli. In contrast, pro-apoptotic Bcl-2

proteins stimulate membrane permeabilization, allowing cytochrome c release and the propagation of apoptosis signaling (Manion and Hockenbery, 2003).

Drosophila melanogaster has the capability to form an apoptosome-like complex and contains two Bcl-2-like genes (Figure 1.1). *Dark/hac-1/Dapaf-1* is the *Drosophila* homologue of human *Apaf-1* (Kanuka *et al*., 1999; Zhou *et al*., 1999; Rodriguez *et al*., 1999). Dark contains a ced-4/Apaf-1 homologous region (CARD/ced-4 domains) and WD repeats capable of interacting with cytochrome c. *dark* expression is induced by apoptotic stimuli such as UV irradiation, and ectopic *dark* expression leads to caspase activation and killing in SL2 cells and fly tissues (Zhou *et al*., 1999; Rodriguez *et al*., 1999; Kanuka *et al*., 1999). *dark* mutants have reduced apoptosis and reduced ectopic killing by *RHG* in the fly eye (Kanuka *et al*., 1999; Zhou *et al*., 1999; Rodriguez *et al*., 1999).

The fly contains two Bcl-2-like proteins, Buffy and Debcl. Debcl is a proapoptotic Bcl-2 homologue and its ectopic expression induces apoptosis in SL2 cells and fly tissues. Debcl can be inhibited by p35 indicating it functions by activating caspases (Colussi *et al*., 2000). *Debcl* killing is reduced by heterozygosity for *H99*, as well as the loss of *dark*. *Debcl*-induced apoptosis is enhanced by the loss of Diap1 activity. Unlike the pro-apoptotic Bcl-2 family members in mammals which simulate cytochrome release, *Debcl* does not induce significant cytochrome c release in BG2 cells. However, Debcl killing depends on its BH3 domain and it is capable of binding human Bcl-2 and its proapoptotic homologues (Colussi *et al*., 2000). Buffy is Bcl-2-like protein with pro- and anti-apoptotic properties and can bind Debcl (Quinn *et al*., 2003; Wu *et al*., 2010). Buffy contains three Bcl-2 homology domains (BH) and C-terminal hydrophobic

membrane anchor and localizes in mitochondria in normal and apoptotically stimulated cells. Buffy is required for preventing embryonic cell death. dsRNA for *buffy* leads to ectopic cell death; whilst ectopic expression of *buffy* inhibits cell death by *Debcl*, gamma-irradiation, and *GMR-RHG*, but not *GMRdronc* (Quinn *et al*., 2003).

Mammals contain several IAPs, including XIAP, cIAP1, and cIAP2, which act to curtail uncontrolled apoptosis in the cell by suppressing Caspase-3, Caspase-7, and Caspase-9 (Deveraux *et al*., 1998; Deveraux *et al*., 1996; Roy *et al*., 1997). Individual null mutations in *XIAP*, *cIAP1*, or *cIAP2* do not affect animal viability (Harlin *et al*., 2001; Schile *et al*., 2008; Conze *et al*., 2005; Conte *et al*., 2006). XIAP-null mice do not exhibit decreased animal viability or a grossly compromised apoptotic response; however deletion of the XIAP-RING domain sensitizes XIAP null MEFs to apoptotic stimuli and leaves sympathetic neurons in a competent state rendering them susceptible to spurious cytochrome c induced cell death (Harlin *et al*., 2001; Potts *et al*., 2003; Schile *et al*., 2008). cIAP2 null animals also appear outwardly healthy, but produce macrophages which are susceptible to apoptosis induced by lipopolysaccharide (Conte *et al*., 2006). The conservation of IAP/IAP antagonist mechanisms and machinery across metazoans is reflected by Grim-mediated degradation of XIAP via ubiquitination (Silke *et al*., 2004).

Unlike mammals, the fly is highly sensitive to loss of its primary IAP, Diap1. Diap1 null animals die from massive caspase activation and developmental defects during embryogenesis (Wang *et al*., 1998; Goyal *et al*., 2000). Loss of function mutants in *Diap2* and *dBruce* are homozygous viable but have a compromised immune response or exhibit male sterility, respectively (Vernooy *et al*., 2002; Arama *et al*., 2003; Huh *et al*., 2006).

Mammals contain IAP antagonists similar to *RHG*, Smac/DIABLO, Omi/Htr2A, and ARTS which oppose the proapoptotic actions of XIAP, cIAP1, and cIAP2 (Verhagen *et al*., 2000; Du *et al*., 2000; Wu *et al*., 2000; Huang *et al*., 2003; Shiozaki and Shi, 2004; Hegde *et al*., 2002; Gottfried *et al*., 2004). Smac/DIABLO is localized in the mitochondria in unstressed cells and translocates to the cytosol upon apoptotic stimulus. Cytosolic Smac/DIABLO has an exposed IBM motif which allows it to physically bind to and inhibit XIAP, cIAP1, and cIAP2 subsequently promoting caspase activation much like RHG (Verhagen *et al*., 2000; Du *et al*., 2000; Wu *et al*., 2000; Huang *et al*., 2003; Shiozaki and Shi, 2004). Omi/Htr2A is a mitochondrial IBM-containing serine protease which translocates to the cytosol to effect cell killing via IAP binding to XIAP, cIAP1, and cIAP2 (Hegde *et al*., 2002). The mitochondrial Septin protein ARTS is another IAP-antagonist which facilitates apoptosis by inhibition and degradation of XIAP (Gottfried *et al*., 2004; Garcia-Fernandez *et al*., 2010; Edison *et al*., 2012).

Chapter 2

Introduction to Endoplasmic Reticulum (ER) Stress

2.1 Endoplasmic reticulum stress

Secretory and membrane proteins attain their tertiary and quaternary conformations in the endoplasmic reticulum (ER). Chaperones and foldases ensure proteins reach their native state by modifying and folding proteins in the ER (Meunier *et al*., 2002; reviewed in: Cox *et al*., 1997; Helenius *et al*., 1992; Gething and Sambrook, 1992). The ER is the location where signaling cascade building blocks such as receptors and ligands are produced and it stores signaling molecules such as calcium which enable a cell to communicate messages within it or to neighboring cells. The ER is also the site of lipid biosynthesis and its proper functioning is necessary for eukaryotic cell survival. The ER must be able to regulate its output contingent upon cues from the within the cell and its surroundings. The folding process in the ER is dynamic, subject to error, and susceptible to perturbations in homeostasis within the cell or the extracellular environment. If the ER becomes overwhelmed by the accumulation of unfolded or misfolded proteins, components necessary for cell survival will become compromised, leading to the eventual demise of the cell.

ER stress is a state of inefficient protein folding within the ER due to the accumulation of unfolded or misfolded proteins (Marciniak and Ron, 2006). Eukaryotes utilize evolutionarily conserved mechanisms to protect cells from the toxic effects of accumulated proteins in the ER and to restore homeostasis: the unfolded protein response (UPR) and ER associated degradation (ERAD) (Casagrande *et al*., 2000; Foti *et al*., 1999; Lippincott-Schwartz *et al*., 1988; Amara *et al*., 1989). The UPR increases protein-folding capacity by translation attenuation, transcriptional induction of chaperones, and/or physical expansion of the ER, depending on the complexity of the organism (Shi *et al*.,

1998; Kozutsumi *et al*., 1988; Lee *et al*., 2003; Adachi *et al*., 2008; reviewed in: Marciniak and Ron, 2006; Mori, 2009; Ron and Walter, 2007; Rutkowski and Hegde, 2010; Walter and Ron, 2011). Translation attenuation reduces the load of client proteins entering the ER allowing the organelle to catch-up with protein folding. UPR transcriptional induction increases the production of chaperones that actively participate in folding proteins into their native conformation (Scheuner *et al*., 2001). During ERAD, terminally misfolded proteins are identified and retrotranslocated into the cytosol where they are ubiquitinated and undergo proteasomal degradation (Kaneko *et al*., 2002; Hampton *et al*., 1996; reviewed in: Vembar and Brodsky, 2008). The UPR and ERAD are interdependent; cells defective in ERAD activate the UPR to fold excess proteins in the ER and the UPR alleviates ER stress by inducing ERAD gene transcription to increase the rate of protein degradation (Lee *et al*., 2003; Adachi *et al*., 2008; Friedlander *et al*., 2000; Travers *et al*., 2000). If ER stress is prolonged and the UPR and/or ERAD cannot restore homeostasis, the ER becomes severely damaged by the inability to synthesize necessary proteins and the apoptotic program is activated (Woehlbier and Hetz, 2011).

The accumulation of excess unfolded or misfolded proteins during ER stress is sensed in the lumen of the ER by transmembrane proteins which activate the UPR to reconstitute equilibrium. The number of transmembrane proteins and the complexity of their function have increased throughout evolution. In the yeast *S. cerevisiae*, *inositol requiring enzyme 1* (*IRE1*) is the sole ER stress sensor and transducer (Mori *et al*., 1993; Cox *et al*., 1993). *C. elegans*, *D. melanogaster*, and mammals contain three transmembrane proteins which sense ER stress: IRE1, [double-stranded RNA-activated protein kinase (PKR)-like ER kinase] (PERK), and activating transcription factor-6

(ATF6). *IRE1*, *PERK*, and *ATF6* are present as single copies in the fly and worm genomes, but *IRE1* is the principal ER stress sensor and UPR activator (Hollien *et al.,* 2006; Calfon *et al*., 2002; Shen *et al*., 2001; Shen *et al*., 2005). Mammals have one copy of *PERK* and two copies of *IRE1* (*IRE1*α/β) and *ATF6* (*ATF6*α/β). Unlike worms and flies, *IRE1*, *PERK*, and *ATF6* are fully utilized to elicit the mammalian UPR UPR (Harding *et al*., 1999; Tirasophon *et al*., 1998; Wang *et al*., 1998; Haze *et al*., 1999; Figure 2.1; reviewed in: Mori, 2009; Walter and Ron, 2011).

ERAD encompasses the recognition, removal, and proteasomal degradation of terminally misfolded proteins (Fernandez *et al*., 1996; Knop *et al*., 1996; reviewed in: Vembar and Brodsky, 2008; Smith *et al*., 2011). ERAD is a quality control mechanism used to remove non-native proteins which aggregate within or disrupt ER and/or proteasome function. ERAD is often divided into a series of steps involving the recognition of misfolded substrates, transport across the membrane, and ubiquitination followed by delivery to the proteasome for degradation (Carvalho *et al*., 2006). ERAD is conserved from yeast to humans, but it is best defined in yeast. The components used to remove proteins are based on the location of lesions on misfolded proteins; ERAD-C, ERAD-L, and ERAD-M are used for proteins with cytosolic, luminal, and transmembrane domain lesions, respectively (reviewed in: Vashist and Ng, 2004; Denic *et al*., 2006). In addition to the location of a lesion, the state of glycosylation of luminal proteins provides cues as to whether a protein requires additional rounds of folding or should be eliminated by ERAD (Liu *et al*., 1999; Quan *et al*., 2008). Misfolded glycoproteins interact with ER degradation enhancing α-mannosidase-like protein (EDEM) in mammals or htm1 in yeast which facilitates their targeting and degradation in

Figure 2.1: The UPR is conserved from yeast to mammals

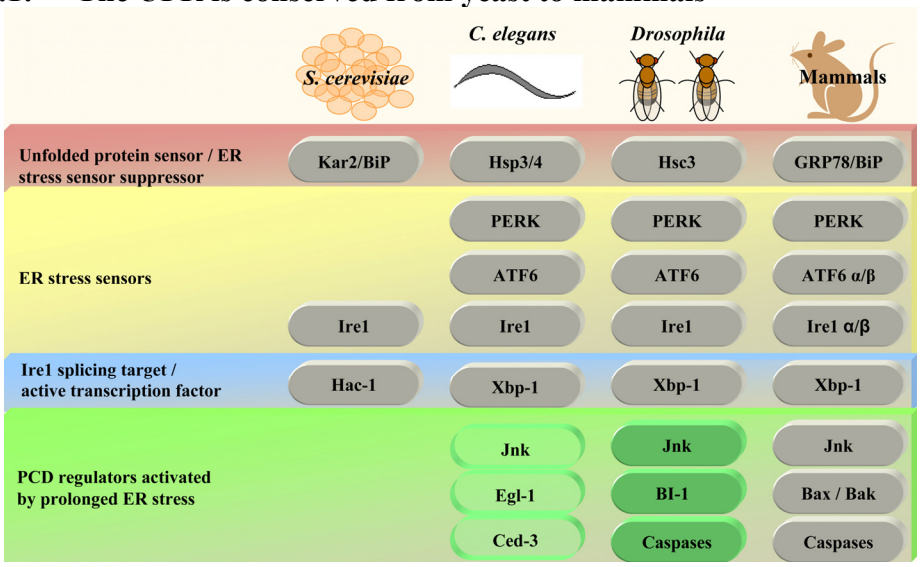

Figure 2.1: Each column details the major proteins used to convey ER stress signals in *S. cerevisiae*, *C. elegans*, *Drosophila* melanogaster, and mammals. The rows list the ER stress sensor suppressor, ER stress sensor, IRE1 splicing target, and ER stress-induced PCD regulators in the aforementioned organisms. Yeast have a single ER stress sensor IRE1 which is held in an inactive state by KAR2/BiP. Once unfolded proteins accumulate in the ER, IRE1 splices *HAC1* to alleviate ER stress. HAC1 activates the transcription of chaperones to increase protein folding capacity in the ER. *C. elegans* and *Drosophila* encode one copy of *IRE1*, *ATF6*, and *PERK*, whose activities are suppressed by the *KAR2/BiP* homologues *HSP*3/4 and *Hsc3*, respectively. Worms, flies, and mammals use IRE1 to splice their HAC1 homologue, XBP1, in order to activate transcription of chaperones and restore ERAD components. Mammals also utilize IRE1, PERK, and ATF6 to sense unfolded proteins and activate the UPR after they dissociate from BiP. Mammals encode two forms of *ATF6* and *IRE1* owing to the increased complexity of the genome. If ER stress persists and the UPR cannot restore homeostasis, the apoptotic pathway is activated to eliminate irreparably damaged cells.

the proteasome (Hosokawa *et al*., 2001; Oda *et al*., 2003; Molinari *et al*., 2003; Clerc *et al*., 2009). Once terminally misfolded proteins are identified and tagged for destruction, p97, a cytosolic ATPase promotes the removal and subsequent degradation of ERAD substrates (Kopayashi *et al*., 2003; Ye *et al*., 2004).

The accumulation of proteins can be detrimental to an organism and it is implicated in the pathology of several diseases including retinitis pigmentosa, diabetes, Alzheimer's disease, and Parkinson's disease. Retinitis pigmentosa (RP) is a retinal degenerative disease caused by ER stress-induced apoptosis of photoreceptors (Davidson and Steller, 1998; Mendes *et al*., 2005; Ryoo *et al*., 2007; Kang and Ryoo, 2009). Missense mutations in the visual protein rhodopsin can cause it to become trapped in the ER, aggregate in the cytoplasm, mislocalize in the cell, or improperly function causing the death of photoreceptor cells and blindness in individuals (Mendes *et al*., 2005). Experiments conducted by Ryoo *et al*. using *Drosophila* demonstrated ER stress contributes to RP pathology and that the loss of functional ER stress components or ectopic expression of ERAD modules can exacerbate or suppress the severity of RP, respectively (Ryoo *et al*., 2007; Kang and Ryoo, 2009). The inability of the pancreas to produce sufficient amounts of insulin or the failure of cells to respond to insulin levels leads to diabetes. In the pancreas, beta cells secrete insulin and regulate glucose levels. PERK is highly expressed in the pancreas and its targeted deletion in mice revealed ER dysfunction contributes to diabetes pathology. *PERK*$^{-/-}$ pancreatic beta cells are unable to cope with the voluminous secretory demands of the organ and eventually die by apoptosis. Beta cell depletion leads to reduced insulin levels and hyperglycemia (Harding *et al*., 2001; Zhang *et al*., 2002). Alzheimer's disease (AD) is a neurodegenerative disease

that causes memory and cognitive impairment. The accumulation of hyperphosphorylated tau, amyloid-β aggregates, neuron loss, and neurofibrillary tangles constitute characteristic features of AD. Evidence of UPR activation is present in AD brain histological samples and AD tissues have increased PERK and BiP protein expression which is absent in non-demented controls (Hoozemans *et al*., 2009). Sustained PERK activation can lead to the transcription of proapoptotic genes such as *CHOP* and may account for neuronal cell loss in AD patients (Zinszner *et al*., 1998; Marciniak *et al*., 2004; Prasanthi *et al*., 2011). Cell culture experiments and analysis of AD brains revealed splice-variant mutations in presinilin-2 promoted amyloid-β aggregate production which decreases the activation of ER stress effectors, and increases susceptibility to exogenous ER stress (Hoozemans *et al*., 2009; Sato *et al*., 2001). Parkinson's disease (PD) is a neurodegenerative disease resulting in the loss of dopaminergic neurons. PD dopaminergic neuron loss is mimicked in mice and neuronal cell culture (PC12 cells) by the administration of 6-hydroxydopamine (6-OHDA). PC12 cells exposed to 6-OHDA have elevated IRE1 and PERK phosphorylation and increased expression of UPR genes such as *BiP*, *calreticulin*, and *CHOP* (Ryu *et al*., 2002). UPR activation may have protective or destructive consequences on the progression of AD and PD depending on the duration of its activity. PERK immunoreactivity is detected in tissue samples from patients with Alzheimer's and Parkinson's disease, but not in the tissues of unaffected individuals (Hoozemans *et al*., 2007; Hoozemans *et al*., 2009; Ryu *et al*., 2002). The UPR has a role in the pathology of several neurodegenerative diseases and learning how to manipulate this pathway will be critical to addressing health concerns of a booming aging population.

2.2 Initial insights into the unfolded protein response

Early studies into the UPR stemmed from observations of chick embryo fibroblasts (CEFs) transformed with Rous sarcoma virus (Shiu *et al*., 1977). Transformed CEFs had elevated levels of 78kDa and 95kDa proteins which were absent from non-transformed CEFs. Investigators sought to distinguish between the appearance of the proteins as a direct consequence of transformation or as an indirect result of nutrient deprivation. Continuous supplementation of transformed CEF media with glucose prevented the appearance of the 78kDa and 95kDa proteins leading to the conclusion the proteins are induced by glucose depletion. The proteins were subsequently called GRP78 and GRP95, where GRP stands for glucose regulated protein (Shiu *et al*., 1977). GRP78 and GRP95 were later identified as ER-resident proteins upregulated by and physically associated with misfolded and/or aggregated proteins in the ER (Kozutsumi *et al*., 1988; Hurtley *et al*., 1989). The realization that cells elicit a stereotypic response to counter the effects of compromised proteins in the ER prompted the search for additional regulators of ER function.

2.3 The unfolded protein response in yeast

The basic mechanisms governing the UPR were elucidated in *S. cerevisiae* from studies to identify upstream regulators of the ER stress responsive protein KAR2/BiP. By the early 1990s, ER stress was known to induce the upregulation of the ER chaperones KAR2 and protein disulfide isomerase (PDI) (Mori et al., 1992). KAR2 resides in the ER and physically associates with unfolded proteins to ensure they reach their native state (Normington *et al*., 1989). *KAR2* and *PDI* contain a minimal ER stress responsive element in their promoters which is called the unfolded protein response element

(UPRE). The UPRE fused to LacZ drives the expression of LacZ in an ER stress-induced manner and UPRE reporters were used in several screens to identify mutants unable to elicit the UPR (Mori *et al*., 1992; Mori *et al*., 1998).

ER stress is sensed by the transmembrane protein Ire1 (also called ERN1). IRE1 was identified as a regulator of ER stress and UPR transduction in independent screens for yeast mutants which failed to activate UPRE reporters and KAR2/BiP during ER stress (Cox *et al*., 1993; Mori *et al*., 1993). Yeast cells lacking Ire1 function are unable to activate the UPRE reporter and are highly susceptible to ER stress-inducing conditions such as growth on media containing the glycosylation inhibitor tunicamycin. Despite the necessity for Ire1 to activate the UPR, *Ire1* mRNA levels are not increased upon ER stress, indicating its activity depends on posttranslational modification (Mori *et al*., 1993). Additionally, *Ire1* mutants are auxotrophic for inositol and require growth on rich media or media supplemented with inositol (Nikawa and Yamashita, 1992).

Ire1 is a type I transmembrane protein composed of an N-terminal luminal domain, a transmembrane region, a cytoplasmic kinase domain, and C-terminal endoribonuclease. It was initially postulated that the Ire1 luminal domain is physically associated with KAR2/BiP and that binding to KAR2/BiP keeps Ire1 in an inactive state in unstressed cells. During ER stress, KAR2 dissociates from Ire1 to assist in protein folding thereby enabling Ire1 to oligomerize, trans-autophosphorylate, and activate downstream signaling targets (Okamura *et al*., 2000). The generation of *Ire1* mutants unable to bind KAR2, yet capable of transducing ER stress signaling necessitated the modification of the KAR2/BiP association/dissociation model (Oikawa *et al*., 2007). Structural analysis of the Ire1 luminal domain revealed Ire1 has a groove capable of

accommodating peptide binding. Based on the additional structural information, KAR2/BiP dissociation and/or peptide binding were determined to be contributing factors for Ire1 activation and oligomerization (Credle *et al*., 2005). Ire1 activation also requires a functional kinase and ribonuclease domain (Shamu and Walter, 1996). After Ire1 dissociates from BiP and/or interacts with misfolded proteins, Ire1 is free to oligomerize. Once Ire1 oligomerizes, the kinase domains of adjacent Ire1 monomers *trans*-autophosphorylate each other in a face-to-face orientation, which enables binding of ADP, and re-orientation of the Ire1 dimer into a back-to-back conformation able to engage in ribonuclease function and to elicit the UPR (Shamu and Walter, 1996; Lee *et al*., 2008; Korennykh *et al*., 2009).

After the identification of Ire1, additional UPRE reporter screens were conducted to find ER stress-specific regulators of *KAR2* transcription. A screen for genes which restore UPRE activation when ectopically expressed in *Ire1* mutants led to the discovery of *HAC1* (*homologue of the mammalian activating transcription factor/cAMP-responsive element (CRE)-binding protein, ER to nucleus 4* (*ERN4*)) (Cox and Walter, 1996). HAC1 was also selected in a separate screen for proteins capable of UPRE binding and activation (Mori *et al*., 1996). HAC1 is a transcription factor composed of a basic region domain and leucine zipper region and it upregulates BiP/KAR2 in response to ER stress. HAC1 is required for the activation of the UPR and *hac1* mutants fail to activate KAR2/BiP, PDI, and other chaperones during ER stress. In addition, *hac1* mutants are inositol auxotrophs like *Ire1* mutants (Cox and Walter, 1996; Mori *et al*., 1996).

HAC1 is transcribed as two species; one when yeast are unstressed ($HAC1^u$) and another produced by the excision of 252 nucleotides during ER stress ($HAC1^i$). $HAC1^i$ is translated during the UPR, but $HAC1^u$ protein is not expressed due translational attenuation by the intron (Chapman and Walter, 1997). If both $HAC1^u$ and $HAC1^i$ mRNAs were translated, they would encode proteins with a common 220 amino acid N-terminus and differing C-termini. The excision of 252 nucleotides from $HAC1^u$ mRNA induces a shift in the *HAC1* reading frame producing an ER stress-specific protein with a unique C-terminus of 18 amino acids, while the unstressed protein would have an alternate 10 amino acid C-terminus (Cox and Walter, 1996; Kawahara *et al*., 1997).

Ire1 is necessary for *HAC1* splicing and *Ire1* mutants consequently fail to produce HAC1 protein during ER stress. Ectopic expression of $HAC1^i$ elicits the UPR in an *Ire1* mutant background (Cox and Walter, 1996; Kawahara *et al*., 1997). With the connection between *Ire1* and *HAC1* set, the significance of and the mechanism for Ire1 mediated cleavage of *HAC1* was investigated. Transcription activation assays led to the discovery that the unique eighteen amino acids generated by *Ire1* splicing, affixes an activation domain onto the HAC1 C-terminus producing a potent transcription factor (Mori *et al*., 2000). Localization studies showed that Ire1 is diffusely expressed in the ER under non-ER stress conditions and that it forms foci during ER stress, due to oligomerization. *HAC1* mRNA is diffusely spread in the cytoplasm of unstressed cells and co-localizes with Ire1 at foci during ER stress. *HAC1* mRNA localization at foci is Ire1 dependent and requires a highly conserved region in the 3'UTR (Aragón *et al*., 2009).

In addition to *Ire1* and *HAC1*, *Rlg1* was identified in a screen as a critical component of the yeast UPR (Sidrauski *et al*., 1996). *Rlg1* encodes a tRNA ligase and complete loss of function for Rlg1 causes lethality. The allele generated in the screen to identify ER stress regulators is specifically compromised in UPR activation and is capable of all other functions. Rlg1 is necessary to ligate the ends of *HAC1* produced by ER stress-induced Ire1 splicing. Ire1 splicing of *HAC1* occurs normally in *Rlg1* mutants; however, *HAC1* mRNA becomes degraded and $HAC1^{i}$ protein translation does not take place. Later experiments demonstrated Rlg1 facilitates $HAC1^{i}$ protein production by associating with $HAC1^{u}$ before Ire1 recognition, ensuring the $HAC1^{u}$ intron is displaced after Ire1 splicing and then initiating the translation of $Hac1^{i}$ (Mori *et al*., 2010).

During ER stress, Ire1 senses the accumulation of unfolded proteins and activates the UPR by cleaving $HAC1^{u}$ mRNA into $HAC1^{i}$. $HAC1^{i}$ encodes a transcription factor which activates the transcription of chaperone and ERAD genes. The increased production of chaperones and ERAD components enables the restoration of ER function.

2.4 The mammalian unfolded protein response

The mammalian UPR is biphasic. Initially, the ER responds to the accumulation of unfolded or misfolded proteins by translation attenuation and then transcriptional induction. Translation attenuation is mediated by PERK and transcriptional activation is brought about by ATF6 and IRE1 signaling to downstream targets (Hetz and Glimcher, 2009). In unstressed cells, the luminal domains of IRE1, PERK, and ATF6 are kept in an inactive state by their physical association with the chaperone BiP. When proteins accumulate in the ER, BiP is sequestered to facilitate protein folding and PERK, ATF6, and IRE1 are free to activate their downstream targets (Figure 2.2; Bertolotti *et al*., 2000;

Figure 2.2: PERK, ATF6, and IRE1 sense ER stress and activate the UPR

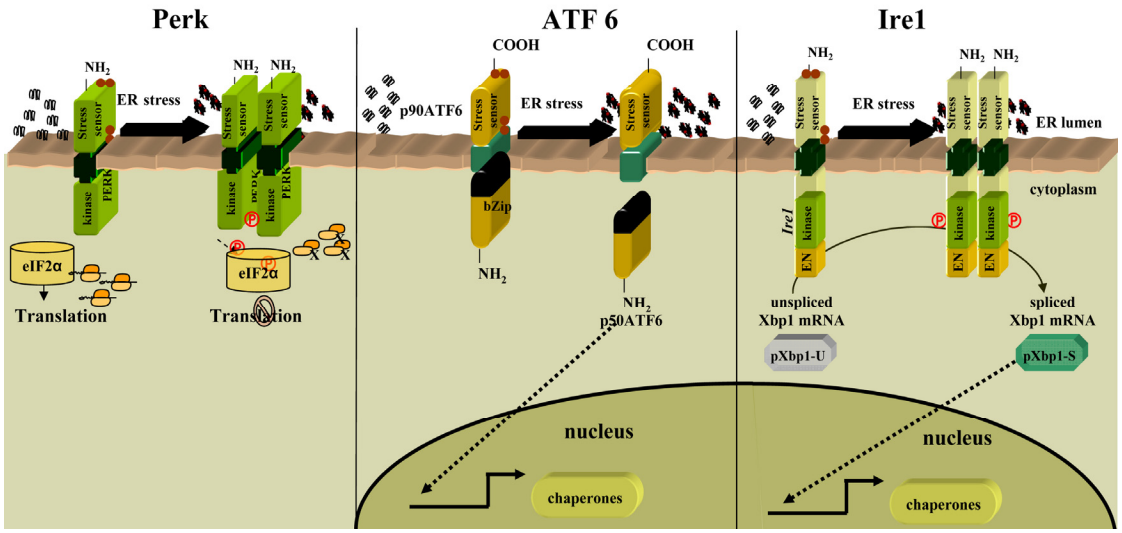

Figure 2.2: During ER stress, BiP (red dots) helps to fold accumulating proteins (squiggles) and dissociates from PERK, ATF6, and IRE1 enabling them to activate downstream targets. PERK reduces the influx of proteins entering the ER by attenuating translation. During ER stress, PERK becomes fully activated after it dimerizes and autophosphorylates. Once activated, PERK disrupts the formation of translation initiation complexes by phosphorylating eIF2α. If ER stress persists, ATF6 (p90ATF6) translocates from the ER to the Golgi, where it is cleaved by site-1 and site-2 proteases into p50ATF6 (not depicted). p50ATF6 is a transcription factor that activates the transcription of chaperones. Upon ER stress, IRE1 oligomerizes and trans-autophosphorylates, becoming an active endoribonuclease. IRE1 cleaves *XBP1* mRNA producing *XBP1S*, a potent transcription factor. XBP1S increases the production of secretory proteins that enable physical expansion of the ER and boosts the transcription of chaperones and ERAD genes.

Ma *et al*., 2002; Shen *et al*., 2002; Tirasophon *et al*., 2000).

IRE1 is conserved from yeast to mammals and is increased copy number from one to two isoforms, *IRE1*α and *IRE1β* in mammals. IRE1α is ubiquitously expressed and IRE1β is limited to the gut. IRE1 is a type-I transmembrane ER-resident protein kinase and RNase with an N-terminal luminal domain, transmembrane domain, linker, kinase domain, and endoribonuclease domain structure. IRE1 senses ER stress and increases the expression of chaperones and ERAD components during the UPR. The ectopic expression of IRE1 is sufficient to drive expression of BiP/GRP78 and conversely, loss of IRE1 prevents the upregulation of ERAD genes such as EDEM (Wang *et al*., 1998; Tirasophon *et al*., 1998; Bertolotti *et al*., 2000; Yoshida *et al*., 2003).

Mammalian IRE1 activity relies on its oligomerization, kinase activation, and RNase activity to propagate ER stress signaling. The regulation of IRE1 activity by BiP in mammals is thought to be mechanistically similar to yeast. BiP is assumed to modulate the duration and the amplitude of ER stress signaling by physically interacting with IRE1α. BiP insures IRE1 does not become precociously activated due to low levels of stress and it also dampens the ER stress signaling after UPR activation (Pincus *et al*., 2010).

After BiP dissociates from IRE1, the luminal domains dimerize allowing the continuation of IRE1 higher-order assembly. During higher order assembly of IRE1, ATP binds to a pocket in the IRE1 cytoplasmic kinase domain and IRE1 dimers attain a face-to-face orientation allowing *trans*-autophosphorylation. Once the kinase domains are phosphorylated, the IRE1 dimer attains an RNase-'active' back-to-back orientation and becomes competent to splice downstream targets (Ali *et al.*, 2011). IRE1

autophosphorylation and subsequent RNase activation requires the binding of ATP in the kinase domain, if ADP or ATP competitive inhibitors bind to kinase domain, the RNase activity of IRE1 is inhibited (Ali *et al.*, 2011). The importance of having functional RNase and kinase domains was demonstrated by transcomplementation experiments with RNase-defective and kinase-defective *IRE1* mutants. The RNase-defective protein is capable of phosphorylating the kinase-defective mutant; however, chimeric dimers containing a defective RNase fail to activate the UPR (Tirasophon *et al*., 2000).

IRE1 RNase activity is utilized for the decay of ER-localized mRNAs, itself, and splicing *XBP1*, the mammalian homologue of yeast HAC1 (Tirasophon *et al*., 2000; Hollien *et al*, 2009; Yoshida *et al*., 2001). Regulated IRE1-dependent decay (RIDD) describes the degradation of ER-localized mRNAs during prolonged periods of ER stress. The decay of ER mRNAs increases ER protein folding capacity by reducing the influx of proteins entering the organelle. RIDD requires both an intact kinase and RNase domain and its prolonged activation can correlate with increased apoptosis (Hollien *et al*., 2009; Han *et al*., 2009). Many of the RIDD targets encode secretory pathway proteins and their extended destruction can negatively impact membrane integrity. Degradation of *IRE1* mRNA during ER stress may used to tame the UPR. Assuming BiP significantly limits IRE1 activity by physical association, IRE1 induced production of BiP protein and coincident RIDD of IRE1 mRNA could retard the UPR by increasing the frequency and efficiency of IRE1 binding by BiP.

XBP1 is the mammalian homologue of yeast *HAC1* and it is spliced by IRE1 to activate the transcription of chaperones. *XBP1* was initially identified in a yeast one-hybrid screen of a human cDNA library for ER stress response element (ERSE) binding

proteins (Yoshida *et al*., 1998; Yoshida *et al*., 2001). The ERSE is a consensus sequence CCAAT-N_9-CCACG found in the promoter region of mammalian ER stress responsive genes such as *BiP*, *calreticulin*, *GRP94*, and *protein disulfide isomerase* (*PDI*) (Yoshida *et al*., 1998). Cells expressing reporter constructs containing tandem ERSE repeats fused to LacZ or luciferase are activated upon ER stress stimulus. Like *HAC1*, *XBP1* is transcribed as two species, one form is predominantly found in unstressed cells and a second is produced during ER stress. The unspliced form of XBP1 (XBP1U) is translated both in unstressed and stressed cells, while the spliced form of XBP1 (XBP1S) is generated by a 26nt ER stress-induced excision of *XBP1* mRNA by IRE1. Similar to *HAC1*, the splicing event of *XBP1* to produce *XBP1S* leads to the formation of a potent transcription factor (Mori *et al*., 2000; Yoshida *et al*., 2001; Shinya *et al*., 2011). XBP1 target genes have been identified by microarray analysis of *XBP1*$^{-/-}$ mouse embryonic fibroblasts (MEFs) and MEFs expressing ectopic XBP1S. XBP1 induces UPR target genes such as *BiP*, *PDI*, *EDEM*, *p58*^{IPK}, and *PDI-P5* (Lee *et al*., 2003). *p58*^{IPK} is an inhibitor of PERK and its induction by *XBP1* indicates XBP1 can negatively regulate PERK signaling. XBP1 upregulation of $p58^{IPK}$ could facilitate switching the cell from translation attenuation to transcription and increased protein production (Yan *et al*., 2002). Additional microarray studies of *XBP1*$^{-/-}$ mutants revealed XBP1 is required for activating protein biosynthesis and apoptosis/cell survival genes (Acosta-Alvear *et al*., 2007). In yeast, HAC1 and IRE1 expression is required for full induction of lipid synthesis and membrane expansion to assuage ER stress (Schuck *et al*., 2009). Similarly, mammals utilize IRE1 splicing of *XBP1* to facilitate membrane expansion during ER stress (Sriburi *et al*., 2007).

In yeast, the 252nt intron in *HAC1* prevents the formation of unspliced and spliced HAC1 proteins (Cox and Walter 1996; Chapman and Walter 1997). In mammals, the 26nt intron is too small to attenuate translation of XBP1U resulting in its constitutive expression. The continuous expression of XBP1U allows it to regulate the expression of XBP1S and ATF6 (Yoshida *et al*., 2006; Yoshida *et al*., 2009). XBP1U protein contains a nuclear localization signal (NLS), a nuclear exclusion signal (NES), and a C-terminal degradation domain. The NLS and NES in XBP1U protein enables it shuttle between the nucleus and cytoplasm where it can interact with XBP1S and ATF6 during ER stress. XBP1U physically associates with XBP1S and ATF6 and promotes their proteasomal degradation via its degradation domain. By degrading XBP1S and ATF6, XBP1U assists to turn off the UPR. Accordingly, as the level of XBP1U increases during the recovery period of ER stress, the levels of XBP1S and ATF6 begin to decline (Yoshida *et al*., 2006; Yoshida *et al*., 2009). XBP1U is also responsible for transporting its mRNA to the surfaces of membranes for splicing by IRE1. XBP1U contains a hydrophobic region thought to target in its mRNA to membranes as part of an mRNA-ribosome-nascent chain complex. At the membrane, *XBP1* mRNA can be spliced by IRE1 and *XBP1S* mRNA is released into the cytosol for translation (Yanagitani *et al*., 2009).

IRE1 interacts with many components of the cell death pathway. IRE1 physically associates with TNF-receptor-associated factor 2 (TRAF2) and activates c-Jun NH_2-terminal kinases (JNK) under ER stress conditions. The kinase domain *of* IRE1 is required for binding to TRAF2 and kinase-dead IRE1 mutants fail to activate JNK during ER stress (Urano *et al*., 2000). ER stress triggered by the aggregation of polyglutamine containing proteins leads to the formation of an apoptosis signal-regulating kinase-1

(ASK1)-TRAF2-IRE1 complex and signaling cascade. *ASK1* is essential for IRE1 signaling during ER stress induced apoptosis in MEFs and *ASK1*$^{-/-}$ mice fail to activate JNK upon ectopic IRE1 expression (Nishitoh *et al*., 2002). ASK1 interacting protein-1 (AIP1) induces ASK1 activation by displacing the ASK1 inhibitor 14-3-3. AIP1 permits the formation of the ASK1-TRAF2-IRE1 complex by promoting IRE1 dimerization. *AIP1*$^{-/-}$ MEFs have blunted XBP1 signaling and are resistant to ER stress-induced cell death (Luo *et al*., 2008). IRE1 is also regulated by protein-tyrosine phosphatase 1B (PTP-1B). *PTP-1B*$^{-/-}$ MEFs, have reduced *XBP1* splicing and fail to induce EDEM and JNK activation during ER stress (Gu *et al*., 2004). In addition to modulating the JNK pathway, IRE1 interacts with Bcl-2 family members such as Bak, Bax, Bim, and Puma (Hetz *et al*., 2006; Klee *et al*., 2009; Lisbona *et al*., 2009; Puthalakath *et al*., 2007). Bax and Bak are proapoptotic members of the Bcl-2 family and contribute to IRE1 signaling. *Bax* and *Bak* double knock-out cells have reduced *XBP1* splicing, JNK activation, and susceptibility to ER stress induced apoptosis (Hetz *et al*., 2006). IRE1α physically associates Bak, indicating IRE1 could be directly regulated by Bcl-2 family activity. *Bim*$^{-/-}$ thymocytes are refractory to ER stress induced apoptosis and reticular localization of Bim and Puma in *Bak/Bax* double knock-out cells restores IRE1 signaling and JNK/TRAF2 mediated apoptosis (Klee *et al*., 2009; Puthalakath *et al*., 2007). Bax inhibitor 1 (BI-1) is an anti-apoptotic protein and it negatively regulates IRE1. *BI-1*$^{-/-}$ cells have increased levels of *XBP1* splicing and mRNA expression of XBP1 targets (Lisbona *et al*., 2009). BI-1 physically associates with IRE1 preventing IRE1/Bax association and the suppression of IRE1-dependent-ER stress induced autophagy and cell death (Castillo *et al*., 2011; Bailly-Maitre *et al*., 2006). IRE1 can exhibit pro-survival

properties when the *XBP1* splicing activity of IRE1 is artificially introduced and RIDD is eliminated. Kinase-dead IRE1 mutants with an enlarged ATP-binding site bound to the ATP-analog INM-PP1 and a functional RNase domain can activate *XBP1* splicing in the absence of RIDD and promote survival during prolonged periods of ER stress (Lin *et al*., 2007).

PERK is a type-I transmembrane ER-resident protein kinase and specifically phosphorylates eukaryotic translational initiation factor 2α (eIF2α) in response to ER stress (Harding *et al*., 1999; Sood *et al*., 2000). eIF2 is a trimeric protein necessary for the binding of the initiator methionine to ribosomal initiation complexes and eIF2B. The γ subunit of eIF2 binds Met-tRNA$_i$, while the eIF2 α- and β- subunit engage in guanine nucleotide binding/exchange. The translation initiation complex is inactive when eIF2 is bound to GDP (eIF2:GDP) and activated when bound to GTP (eIF2:GTP) via guanine nucleotide exchange by eIF2B. Phosphorylated eIF2α bound to GDP has a higher affinity for eIF2B and acts as an eIF2B sink preventing the formation of eIF2:GTP thereby inhibiting protein translation. eIF2B is produced in lower quantities compared to eIF2 and translation initiation can be easily inhibited by preventing restoration of eIF2:GTP by eIF2B (Safer *et al*., 1983; Prostko *et al*., 1992). Delaying protein synthesis allows the ER to cope with the excess demands its experiencing without the additional burden of having to produce unnecessary proteins. However, prolonged delay of protein synthesis can be detrimental to the cell since proteins necessary for cellular function would not be produced. If translation attenuation is insufficient to restore ER homeostasis, PERK activates transcription of growth arrest and DNA damage-34 (GADD34) which dephosphorylates eIF2α (Novoa *et al*., 2001).

GADD34 aids in restoring translation by forming a complex with protein phosphatase 1 (PP1) which can dephosphorylate eIF2α, thereby generating a negative feedback loop of eIF2α activation. GADD34 expression complements that of phosphorylated eIF2α, as levels of phosphorylated eIF2α increase, GADD34 protein increases to counter the effects of translation attenuation. *PERK*$^{-/-}$ cells fail to induce phosphorylated eIF2α and consequently do not exhibit increased GADD34 protein under ER stress conditions. GADD34 is necessary for restoration of transcription and *GADD34* mutant cells fail to efficiently counter the effects of translation attenuation and do not have upregulated ER stress induced BiP/GRP78 expression and *XBP1* splicing (Novoa *et al*., 2001; Novoa *et al*., 2003).

PERK activation of GADD34 allows for the transcription of *activating transcription factor-4* (*ATF4*) and *CCAAT/enhancer binding protein* (*C/EBP*) *homologous binding protein* (*CHOP, GADD153*). ATF4 is necessary for the activation of genes functioning in amino acid import, metabolism, and oxidative stress (Harding *et al*., 2000; Harding *et al*., 2003). PERK activation of ATF4 suggests PERK may actively try to counter oxidative stress which occurs during ER stress. ATF4 also activates the transcription of CHOP, which activates GADD34, which ultimately leads to the lifting of translation attenuation (Bartlett *et al*., 1992; Harding *et al*., 2000; Marciniak *et al*., 2004). *CHOP*$^{-/-}$ mice fail to activate GADD34 and do not dephosphorylate eIF2α in response to ER stress. In addition, analysis of *CHOP* mutant mice revealed CHOP contributes to ER stress induced apoptosis. Wild-type mice injected with tunicamycin display renal cell death, however, *CHOP*$^{-/-}$ mice display less death than wild-type animals (Marciniak *et al*., 2004; Zinszner *et al*., 1998). PERK also counters its translation attenuation by

maintaining ATF6α expression during prolonged periods of ER stress. ATF6α is a transcription factor which advances the switch to translation initiation by promoting the activation of CHOP during ER stress (Yoshida *et al*., 2000).

Activating transcription factor 6 (ATF6) is the third transmembrane ER stress sensor in mammals and is found in two forms ATF6α and ATF6β (Haze *et al*., 1999; Haze *et al*., 2001). ATF6α/β are type II transmembrane glycoproteins comprised of a C-terminal luminal domain, basic leucine zipper, transmembrane domain, and cytosolic N-terminal domain. ATF6α/β were identified as proteins capable of binding to the *cis*-acting ER stress response element (ERSE) in the promoter of mammalian UPR responsive genes such as *GRP78*/*BiP*, *calreticulin*, and *GRP94* (Yoshida *et al*., 1998; Yoshida *et al*., 2000; Yamamoto *et al.*, 2004). ATF6α is constitutively expressed as a 90kDa protein (p90ATF6α) which is converted into a 50kDa protein (p50ATF6α) during periods of ER stress. ATF6β is continuously expressed as a 110kDa protein *(*p110ATF6β*)* and is converted into a 60kDa (p60ATF6β) protein during periods of ER stress (Yoshida *et al*., 1998; Haze *et al*., 1999; Haze *et al*., 2001). During ER stress, ATF6 dissociates from BiP and then it is transported to the Golgi in COPII vesicles where it becomes cleaved is by Site-1 protease (S1P) and Site-2 protease (S2P). Once ATF6 is cleaved, it translocates to the nucleus where it acts as a transcription factor inducing the production of chaperones, XBP1, and CHOP. Disruption of S1P, S2P, or COPII vesicle formation function prevents ATF6 processing at the Golgi leading to a diminished UPR (Ye *et al*., 2000; Nadanaka *et al*., 2004; Schindler and Schekman, 2009; Wu *et al*., 2007; Okada *et al*., 2002). Although two ER stress inducible isoforms of ATF6 exist, p50ATF6α is considered the primary ATF6 effector of ER stress transduction. Ectopic ATF6α expression stimulates increased

BiP/GRP78 protein and siRNA knock-down or site-directed abolition of ATF6α function inhibits ERSE responsive gene activation upon ER stress stimulus. In contrast, ectopic expression of *ATF6β* or its deletion has a miniscule effect on ERSE target gene induction (Thuerauf *et al*., 2004; Yamamoto *et al*., 2007). ATF6α binding and activation of the ERSE can account for the induction of BiP seen in *IRE1*/*XBP1*$^{-/-}$ MEFs (Lee *et al*., 2003).

Insight into ATF6 signaling and its contribution to the UPR were greatly benefitted by the generation of *ATF6*$^{-/-}$ mice and functional genomic analysis of these animals exposed to ER stress stimulus. *ATF6α*$^{-/-}$ and *ATF6β*$^{-/-}$ mice are viable and fertile, but *ATF6α*/*ATF6β* double knock-out mice die during embryogenesis. *ATF6α*$^{-/-}$ MEFs are highly susceptible to ER stress induced apoptosis and inefficiently process proteins compared to wild-type MEFs. The previous results demonstrate ATF6 is necessary for optimized protein folding, secretion, and cell survival when the ER is beyond its folding capacity (Yamamoto *et al*., 2007; Wu *et al*., 2007). Upon ER stress conditions, *ATF6α*$^{-/-}$ MEFs had diminished upregulation of BiP, XBP1, and ERAD components such as EDEM1 and Hrd1. Based on the finding that *XBP1* expression is reduced in *ATF6α*$^{-/-}$ MEFs, ATF6α was assayed for its ability to bind the *XBP1* consensus sequence (TGACGTGG/A) also known as the unfolded protein response element (UPRE) and to the ER stress response element-II (ERSE-II, ATTGG-N_1-CCACG) (Yamamoto *et al*., 2004; Yamamoto *et al*., 2007*). ATF6* was found to heterodimerize with *XBP1* to effect the transcription of ERAD proteins and UPRE binding sites. In the absence of ATF6, cells are unable to fully engage ERAD. The failure to induce ERAD is consequence *ATF6α*$^{-/-}$cells of not increasing *XBP1* mRNA in response to ER stress stimulus (Lee *et al*., 2002). Microarray analysis of untreated and ER stressed *ATF6α*$^{-/-}$ MEFs resulted in the

identification of thirty genes specifically requiring ATF6α during ER stress (Adachi *et al*., 2008). In accordance with previously obtained reporter and binding affinity assay data, BiP, a portion of ERAD components, and genes necessary for ER homeostasis, biosynthesis, trafficking, and to a lesser degree protein transport were identified in the microarray screens for ATF6α target genes (Adachi *et al*., 2008; Wu *et al*., 2007). In addition to upregulating chaperones and ER factors, ATF6α expression drives ER expansion by increasing lipid abundance and secretory pathway components (Bommiasamy *et al*., 2009).

The generation of conditional knock-outs for key UPR genes has provided insight into many human maladies. *PERK*$^{-/-}$, *ATF6*$^{-/-}$, *IRE1*$^{-/-}$, *XBP1*$^{-/-}$, and *BiP*$^{-/-}$ cells and mice have varying defects which reflect their necessity to organismal survival. Most *PERK*$^{-/-}$ animals die during embryonic development and those that survive have defects in pancreatic, skeletal, mammary gland, and adipocyte differentiation function (Zhang *et al*., 2002; Bobrovnikova-Marjon *et al*., 2008). PERK is normally highly expressed in the pancreas and its loss causes the death of insulin secreting beta cells, hyperglycemia, and diabetes and eventually death. The level of PERK expression in bone tissues is similar to the pancreas and it is necessary for collagen production. Not surprisingly, bone tissue is highly dependent upon PERK function for development. *PERK*$^{-/-}$ mice exhibited skeletal deformities such as diminished bone mineralization, reduced bone density, asymmetric vertebrae, and a hunchback (Zhang *et al*., 2002). *ATF6α*$^{-/-}$ animals in contrast to *PERK*, *IRE1*, and *XBP1* nulls do not exhibit overt developmental defects unless specifically challenged with environmental ER stress (Wu *et al*., 2007). *IRE1α*$^{-/-}$ animals die during early embryogenesis due to defects in placenta and liver formation (Iwawaki *et al*., 2009;

Zhang *et al*., 2005). IRE1α is also required for B lymphopoiesis and B cell differentiation into plasma cells (Zhang *et al*., 2005). The defect in plasma cell differentiation and liver formation in *IRE1*$^{-/-}$ mutants is expected since XBP1 is necessary for plasma cell differentiation and liver development (Reimold *et al*., 2000; Reimold *et al*., 2001; Shaffer *et al*., 2004). Microarray analysis of *XBP1*$^{-/-}$ mouse splenic B cells revealed XBP1 targets include genes necessary for ERAD and the secretory pathway. XBP1 induces components for heavy chain processing and the physical expansion of the ER both of which are necessary to cope with the secretory demands of immunoglobulin production. *XBP1*$^{-/-}$ mice die during early embryogenesis from retarded growth and hypoplastic livers due to reduced growth rates and increased apoptosis of hepatocytes (Reimold *et al*., 2001; Shaffer *et al*., 2004). *BiP* is upregulated by and works to counter the deleterious effects of a variety of stresses such as nutrient deprivation, disrupted calcium homeostasis, and ER stress (Morris *et al*., 1997). BiP expression is detected during early embryogenesis in the trophectoderm and inner cell mass of blastocysts. *BiP*$^{-/-}$ mice exhibit severe defects due to its pivotal role during early embryonic development. BiP function is crucial for the support of life. *BiP*$^{-/-}$ mice fail to develop past E7.5 and E3.5 embryos grown in culture have reduced rates of proliferation and increased apoptosis (Luo *et al*., 2005).

2.5 The UPR in *C. elegans*

Three transmembrane ER stress sensing proteins *IRE1* (IRE-1), ATF6 (ATF-6), and PERK (Pek-1) are present in *C. elegans*, but IRE-1 is considered the primary transducer of the UPR in this organism (Shen *et al*., 2001). *ire-1*, *xbp-1*, *pek-1*, and *atf-6* null worm strains exist and allowed genomic array analysis to identify the contributions of those genes in unstressed or ER-stressed animals (Shen *et al*., 2001; Shen *et al*., 2005).

Studies of the UPR in *C. elegans* took advantage of the powerful genetic techniques available in this system and the presence of single copy genes encoding the main UPR transducers. In particular, *C. elegans* was used to verify IRE-1 splices a substrate in response to ER stress and that the substrate is *XBP-1*. In nematodes, *HSP-3* and *HSP-4* are the ER stress-inducible homologues of *KAR2*/*BiP*. GFP-tagged HSP-4 becomes upregulated when worms are treated with the N-glycosylation inhibitor tunicamycin or exposed other ER stress inducing conditions (Shen *et al*., 2001; Calfon *et al*., 2002). One group utilized worms expressing HSP-4-GFP to isolate *XBP-1* as a loss-of-function suppressor of HSP-4-GFP activity and identified it as a target of IRE-1-mediated cleavage (Calfon *et al*., 2002). A second group identified an *ire-1* null mutant and confirmed *HSP-3*, *HSP-4*, and *XBP-1* require IRE-1 for their expression during the UPR. *pek-1*$^{-/-}$ animals up-regulated UPR signaling similarly to wild-type animals indicating PEK-1 has a minor in the UPR. In contrast, RNAi for *XBP-1* demonstrated it was necessary for induction of the UPR (Shen *et al*., 2001). Single mutants for *ire-1*, *xbp-1*, *pek-1*, and *atf-6* are viable; however, double mutants for *ire-1*/*pek-1*, *ire-1*/*atf-6*, and *xbp-1*/*atf-6* are synthetic lethal, indicating IRE-1 and XBP-1 play pivotal roles in worm UPR regulation. PEK-1 and ATF-6 are not essential for ER stress induced signaling, but can moderately substitute for IRE-1/XBP-1 provided the animals are not challenged with additional stresses (Shen *et al*., 2001; Shen *et al*., 2005).

In the worm, the UPR is necessary to meet increased secretory demands during larval development and countering the effects of environmental ER stress and as such it is termed the constitutive-UPR (c-UPR) and inducible-UPR (i-UPR), respectively (Shen *et al*., 2005). The c-UPR genes encode proteins for metabolism, protein synthesis,

membrane transporters, protein degradation, cell architecture, chaperones, and cell growth. The c-UPR genes are thought to be necessary during stages of high protein synthesis during larval development such as growth and molting. Microarray analysis of *ire-1*, *atf-6*, and *xbp-1* mutants and *atf-6* RNAi treated larvae resulted in the identification of genes necessary for c-UPR and i-UPR. Three hundred and twenty-four c-UPR genes were identified and over seventy percent of the genes depended on XBP-1 function, while roughly twenty percents of the genes required IRE-1. The large contribution of genes specifically requiring XBP-1 suggests unspliced XBP-1 protein may have a role in development (Shen *et al*., 2005). Microarray analysis of worms expressing ectopic *XBP-1U* or *XBP-1S* may identify specific genes regulated by the different *XBP-1* isoforms. Two hundred and two i-UPR genes were identified and their expression depended upon individual or combinatorial activation of *IRE-1*, *XBP-1*, *ATF-6*, and *PEK-1*. The vast majority of genes (84%) required IRE-1 and XBP-1; this is expected since IRE-1 endoribonuclease activity generates active XBP-1. Protein folding, ERAD, protein trafficking, cell death and metabolic genes were highly reliant on IRE-1 and XBP-1 function for the i-UPR. The *IRE-1*/*XBP-1* genes are pivotal to an effective UPR; they signal to targets which induce the expression of lipids and other metabolic genes thereby increasing the physical capacity of ER. In contrast to IRE-1/XBP-1, ATF-6 expression only affected six genes and none of them were directly linked to ERAD, protein folding, or secretion. The minor contribution of ATF-6 indicates evolutionary selection for this pathway occurred after worms. PEK-1 was required for full induction of roughly 23% of the i-UPR genes and its functions overlapped genes regulated by either Ire-1, ATF-6, and/or XBP-1. PEK-1 expression contributed to upregulation of metabolism, secretory,

and protein degradation genes, but not ERAD, cell death, or protein folding genes indicating it too does not have a primary role in the UPR. However, PEK-1 dependent activation of secretory and protein degradation genes indicates it could act in parallel with the IRE-1/XBP-1 branch during the UPR. Like ATF-6, a significant role for PEK-1 in the UPR evolved after worms. *C. elegans* PEK-1 can phosphorylate eIF2α when it is expressed in yeast, but it does not have the role of activating cell death regulators under prolonged UPR signaling like its mammalian homologue PERK.

A screen by a second group identified 19 genes which are upregulated in *xbp-1* mutants, but not in wild-type animals during the UPR. The screen led to the identification of a family of genes which encode activated in blocked UPR (ABU) proteins. ABU proteins have a hydrophobic N-terminus, a transmembrane domain, and short cytoplasmic C-terminus. GFP tagged abu-1 has a punctate expression pattern in the intestine indicating ABU proteins may suppress the UPR in the gut during development. Loss of *abu-1* function leads to increased ER stress in the larval gut and *abu-1*/*xbp-1* mutant worms were highly sensitive to developmental ER stress (Urano *et al*., 2002). The activation of genes specifically in UPR compromised animals demonstrates the critical nature of ER functionality during ontogeny.

In addition to regulating i-UPR and c-UPR, *C. elegans* IRE-1, XBP-1, and PEK-1 also have a role in host defense. During larval *C. elegans* development, animals fed the pathogenic bacteria *Pseudomonas aeruginosa* require a functional IRE-1/XBP-1 branch. *P. aeruginosa* activates the innate immune response which triggers ER stress in the intestines of larvae and XBP-1 is necessary to elicit the UPR and promote survival (Richardson *et al*., 2010; Richardson *et al*., 2011). *xbp-1* null animals exposed to *P.*

aeruginosa have increased PEK-1 activity in order to cope with the innate immune response induced ER stress and they can survive to adulthood when grown at 16^{o}C. In contrast, *xbp-1*/*pek-1* null animals do not survive, demonstrating PEK-1 has some capacity to regulate the UPR in worms and it can partially substitute for IRE-1/XBP-1 activities during ER stress.

In worms, the IRE-1/XBP-1 branch plays a primary role in the regulation of the UPR during development and as a consequence of environmental stresses. PEK-1 and ATF6-1 make a minor contribution in the UPR, but they can modestly substitute for the IRE-1/XBP-1 branch if it is not functional. ABU genes may provide additional assistance to PEK-1 and ATF6 when the IRE-1/XBP-1 pathway of UPR induction is compromised.

2.6 The unfolded protein response in flies

Three transmembrane ER stress sensing proteins Ire1, ATF6, and PERK (Pek) are present in *D. melanogaster*; however, Ire1 is considered the primary transducer of UPR in this system. The methods used to dissect the UPR in the fly include microarray analysis of *xbp1* and *ire1* RNAi treated *Drosophila* S2 cells, characterization of wild-type *xbp1* and *PERK* gene products, limited mutant analysis, and over-expression studies. Although the details of UPR regulation in fly have not been dissected, the fly lends itself as a tool for analyzing the effects of the UPR in disease models (Hollien and Weissman, 2006; Sood *et al*., 2000; Plongthongkum *et al*., 2007; Souid *et al*., 2007; Pomar *et al*., 2003; Ryoo *et al*., 2007; Malzer *et al*., 2010).

In *Drosophila*, the *BiP* homologue is *heat shock cognate 3* (*hsc3*) and like its yeast, worm, and mammalian counterparts it is upregulated by ER stress. The *xbp1* splicing activity of Ire1 during ER stress is conserved in the fly and several groups have

used an Xbp1_EGFP reporter as the primary read-out of ER stress activity in this system (Plongthongkum *et al*., 2007; Ryoo *et al*., 2007; Souid *et al*., 2007; Mendes *et al*., 2009; Kang and Ryoo, 2009; Tinto *et al*., 2011). The Xbp1_EGFP reporter consists of the Xbp1U sequence which includes the Ire1 splice site and an out-of-frame EGFP; only when *xbp1* is spliced by Ire1 is EGFP expressed (Ryoo *et al*., 2007). *xbp1U* and *xbp1S* mRNA are expressed throughout embryonic, larval, and adult stages; however, the majority of the mRNA corresponds to *xbp1U*. *xbp1S* mRNA is elevated during larval stages, in salivary glands, and in the adult testis (Souid *et al*., 2007). The regulation of Xbp1U and Xbp1S protein in the fly during development using specific antibodies has not been extensively conducted. Hsc3/BiP upregulation during ER stress is Ire1 and Xbp1 dependent. $xbp1^{-/-}$ clonal tissues from imaginal discs incubated under ER stress conditions have lower levels of Hsc3 compared to neighboring wild-type and heterozygous tissue indicating Xbp1 is necessary for ER stress-induced expression of Hsc3. In a complementary experiment, ectopic expression of Xbp1S increased *hsc3* mRNA levels (Ryoo *et al*., 2007). *xbp1* RNAi in S2 cells revealed that in addition to upregulating *hsc3*/*BiP* in response to ER stress, Xbp1 is necessary for the upregulation of secretory, folding, metabolic, and trafficking genes (Hollien and Weissman, 2006).

Functional characterization of wild-type *D. melanogaster* PERK (Pek) in flies, yeast, and mammalian cell culture was conducted by the de Haro group (Pomar *et al*., 2003). They found *pek* mRNA is expressed throughout development and is enriched during the embryonic and adult stages. *Drosophila* Pek protein structure is similar to mammals and is capable of autophosphorylation and phosphorylating eIF2α in response to ER stress in S2 cells and nutrient deprivation when expressed in yeast. Deletion

constructs of *pek* were analyzed for their localization in 293T human fibroblasts and activity in yeast deficient for the eIF2α kinase GCN2. Wild-type Pek localized to the ER and regulatory domain deleted Pek exhibited cytoplasmic distribution and both were sufficient to rescue GCN2 deficient yeast. In contrast, *pek* constructs with signal peptide or transmembrane domain deletions associated with low-density membrane fractions such as the Golgi and failed to rescue growth defects of *GCN2* mutant yeast. The results of the deletion construct analysis indicate Pek exerts its function in regions with higher concentrations of ribosomes where translation is actively occurring (Pomar *et al*., 2003).

pek RNAi experiments in S2 cells indicate that Pek is necessary for the formation of translationally silenced mRNAs in cytoplasmic complexes (stress granules) upon exposure to arsenite (Farny *et al*., 2009). Translation suppression requires the disassembly of polysomes which is mediated by phosphorylated eIF2α and Pek is necessary for phosphorylation of eIF2α when cells are exposed to arsenite. Pek expression can affect cell cycle progression and ectopic expression of *pek* in the adult eye induces cell cycle arrest at G2-S (Malzer *et al*., 2010). However, a thorough analysis of the ER stress response in *pek* mutants remains to be conducted.

The contributions of Ire1 during the UPR were dissected with a microarray screen of DTT treated S2 cells cultured with *ire1* RNAi or left untreated. Ire1 was found to be necessary for the up regulation of secretory, trafficking, metabolic, and folding genes. Ire1 as also found to specifically degrade ER-localized mRNAs encoding membrane signal sequences during ER stress (Hollien and Weissman, 2006). The susceptibility of mRNAs to Ire1 degradation during ER stress likely serves as a means to reduce the protein load of unnecessary or difficult to fold proteins. Ire1 expression during

ER stress induces *hsc3* and consequently *ire1* RNAi treated S2 cells fail to upregulate Hsc3 protein in culture media containing the reducing agent DTT (Ryoo *et al*., 2007). Similar to mammals, Ire1 in the fly is negatively regulated by Bax inhibitor-1 (BI-1). Wild-type larvae exposed to ER stress conditions exhibited increased *xbp1* splicing, while BI-1 over-expressing larvae had significantly less spliced *xbp1* mRNA (Lisbona *et al*., 2009). The increased suppression of Ire1 signaling in BI-1 over-expressing larvae mitigated UPR activation and consequently reduced *xbp1* mRNA levels. Autophagy may function as a means of eliminating accumulated proteins *en masse* during prolonged UPR (Yorimitsu *et al*., 2006). BI-1 disrupts Ire1 and Jnk signaling and is necessary for suppressing ER stress induced autophagy. *bI-1* RNAi larvae over-activate the autophagy program and exhibit increased mortality when grown on media containing the N-glycosylation inhibitor tunicamycin compared to wild-type larvae grown on ER stress-inducing media or untreated *bI-1* RNAi animals (Castillo *et al*., 2011).

Detailed analysis of *atf6* function in the wild-type and or mutant conditions await further testing. Preliminary RNAi screening for *ATF6* function in S2 cells reveals it has a minor role in the UPR (Hollien *et al.,* 2006).

Although the molecular characterization of the UPR components in the fly is in its relative infancy, many studies modeling human diseases with UPR underpinnings have been investigated in the fly. Retinitis pigmentosa, a retinal disease stemming from misfolded rhodopsin proteins causing ER stress has been studied in the fly with mutant alleles of rhodopsin and rhodopsin chaperones (Ryoo *et al*., 2007; Mendes *et al*., 2009; Kang and Ryoo, 2009). The $nina^{G69D}$ mutation is a *D. melanogaster* model of autosomal dominant retinitis pigmentosa. ER stress actively occurs in $ninaE^{G69D}$ photoreceptors and

loss of Xbp1 function increases the severity of adult photoreceptor degeneration in the *ninaE*^{G69D} rhodopsin mutant (Ryoo *et al*., 2007). Expression of ERAD components such as Hrd1, EDEM1, and EDEM2 is sufficient to enhance protein folding of ectopic mutant and wild-type rhodopsin 1 (Kang and Ryoo, 2009). Diminished Xbp1 activity also increased photoreceptor cell susceptibly to the toxic effect of ectopic amyloid-β in Alzheimer's disease modeling in the fly eye. The accumulation of cytoplasmic calcium is suggested to contribute to amyloid-β cytotoxicity and ectopic expression of amyloid-β causes a rough eye appearance in the adult animal. Ectopic expression of murine Xbp1S counters the toxic effects of amyloid-β by inhibiting ryanodine calcium channels and thus prevents increased cytosolic calcium release by amyloid-β (Casas-Tinto *et al*., 2011).

ER stress is caused by the accumulation of unfolded or misfolded proteins. Ire1, PERK, and ATF6 sense ER stress and activate the unfolded protein response to reconstitute ER homeostasis. If the cell cannot cope with the proteins trapped in the ER it will activate the apoptotic pathway. The ER is a complex organelle with a host of responses to perturbations affecting its function. The tools at its disposal to ward off ER stress have yet to be fully elucidated and are actively being pursued.

Chapter 3

A Genetic Screen to Identify Novel Regulators of ER Stress Induced Apoptosis

3.1 Introduction

The endoplasmic reticulum (ER) is the site of protein folding and lipid biosynthesis in the cell. Chaperones and foldases interact with proteins in the ER to ensure proteins reach their native tertiary and quaternary configurations. Membrane and secretory proteins generated in the ER maintain cellular integrity as well as propagate messages both inside and outside of the cell. If ER function becomes compromised by the accumulation of misfolded or unfolded proteins it enters a state of ER stress. In order to combat ER stress, the organelle has devised a series of responses to enhance protein folding capabilities; ER associated degradation (ERAD) and the unfolded protein response (UPR) (Mori, 2009; Ron and Walter, 2007; Walter and Ron, 2011; Ellgaard and Helenius, 2003; Vembar and Brodsky, 2008; Smith *et al*., 2011). ERAD involves the targeting, retro-translocation, and proteasomal degradation of terminally misfolded proteins. Proteins with cytoplasmic, luminal, or membrane domain missense mutations are eliminated by components of the ERAD-C, ERAD-L, and ERAD-M pathways, respectively (Vashist and Ng, 2004; Denic *et al*., 2006). The UPR increases protein folding capacity by translation attenuation and/or increased transcription of chaperones, foldases, and ERAD components (Vembar and Brodsky, 2008). If ER stress is prolonged and the cell is severely damaged, the apoptotic program is activated to eliminate the defective cell (Zinszner *et al*., 1998; Hetz *et al*., 2006; Woehlbier and Hetz, 2011).

The UPR is conserved from yeast to mammals. In mammals, the UPR is activated by the ER stress sensors PERK, IRE1, and ATF6 (Mori, 2009). PERK attenuates translation enabling the ER catch-up with protein folding during the early phase of the UPR, whilst Ire1 and ATF6 activate the transcription of chaperones and

ERAD genes to increase protein folding capacity when translation attenuation is insufficient to restore ER homeostasis (Ron and Walter, 2007; Walter and Ron, 2011). If the UPR does not regenerate normal ER function, PERK activates the proapoptotic gene *CHOP* and Ire1 activates the JNK signaling pathway or Bcl-2 family members to induce cell death (Zinszner *et al*., 1998; Marciniak *et al*., 2004; Hetz *et al*., 2006).

Several studies have shown that the Ire1/Xbp1 pathway of the UPR is utilized to alleviate ER stress in the fly. However, the contributions of ATF6 and Pek have yet to be fully addressed (Hollien and Weissman, 2006; Ryoo *et al*., 2007; Kang and Ryoo, 2009; Mendes *et al*., 2009; Casas-Tinto *et al*., 2011). Ire1 senses unfolded and/or misfolded proteins and splices *xbp1* mRNA into Xbp1S, a powerful transcription factor. Xbp1S promotes the transcription of chaperones and ERAD components to facilitate protein folding (Ryoo *et al*., 2007; Kang and Ryoo, 2009). Unlike mammals, the fly does not have a *CHOP* homologue to initiate ER stress-induced apoptosis (ERSIA) during prolonged ER stress. The fly has JNK and Bcl-2 family homologues which may be activated by the Ire1/Xbp1 pathway to remove damaged cells (Lisbona *et al*., 2009).

The canonical cell death pathway in the fly includes the proximal cell death activators rpr, hid, and grim (RHG proteins), the *APAF-1* homologue *dark,* and caspases (Figure 1.1). Homozygous-mutant *H99* (RHG-deficient) embryos and tissues are devoid of developmental cell death and are refractory to ectopic apoptosis induced by stress and injury (reviewed in Fuchs and Steller, 2011). Caspases are cysteine aspartyl proteases which execute cell death by cleaving cellular targets to induce nuclear condensation, cell shrinkage, and the destruction of the cell (Hengartner, 2000). Caspases are initially synthesized as inactive zymogens and are divided into two groups, “initiator” caspases

and “effector” caspases. Initiator caspases have long prodomains that contain CARD or DED domains which are capable of protein-protein interactions and they become activated by induced-proximity oligomerization (Shi, 2002). Effector caspases have short prodomains and are activated by initiator caspase-mediated proteolytic cleavage (Reed *et al*., 2004). The fly has two initiator caspases Dronc and Dredd and five effector caspases, Drice, Damm, Decay, Strica, and Dcp-1 (Bergmann, 2010).

Ryoo *et al*. showed that a compromised UPR can lead to increased cell death of photoreceptors in a *Drosophila* model of autosomal dominant retinitis pigmentosa ($ninaE^{G69D}$) (Ryoo *et al*., 2007). $ninaE^{G69D}$ heterozygous flies express a mutant form of rhodopsin 1 which accumulates in the ER and causes ERSIA of photoreceptor cells. Animals doubly heterozygous for the $ninaE^{G69D}$ and *xbp1* mutations have markedly increased photoreceptor cell death due to inefficient UPR signaling. The authors also demonstrated that imaginal discs incubated in culture media containing the reducing agent DTT undergo ER stress and have increased *hsc3*/*BiP* expression and *xbp1* splicing.

It is currently unknown which genes from the canonical programmed cell death pathway regulate ERSIA and whether mutations affecting *xbp1* and *ire1* impact ERSIA activation. This study was undertaken to determine which of the conical apoptotic and UPR genes modulate ERSIA and to identify novel regulators of the ER stress and apoptotic pathway in *D. melanogaster*. In order to identify regulators of ERSIA, a screen was conducted using 452 FRT p-element lethal stocks derived from the UCLA Undergraduate Consortium in Functional Genomics (Call *et al*., 2007). The lines were tested for loss-of-function activation or suppression of caspase activity using an *ex vivo* ER stress culture technique.

3.2 Results

3.2.1 Establishing a reproducible technique to identify regulators of ERSIA

Ryoo *et al*. demonstrated that imaginal discs incubated in S2 media containing DTT undergo ER stress. However, the authors did not investigate in detail the consequences of prolonged periods of ER stress in discs (Ryoo *et al*., 2007). In order to conduct a screen of ERSIA regulators, optimal conditions had to be determined to reproducibly elicit ERSIA in eye-antennal imaginal discs.

yw larvae were grown on standard media containing 0.05% bromophenol blue (blue food) and staged as either early or late third instar larvae. Blue food permits the staging of wandering third instar larvae on the basis of the amount of food remaining in the gut. As larvae approach pupation, the contents of the gut are gradually excreted out of the animal until the gut is essentially free of solid material. The guts of early third instar larvae grown on blue food appear filled with blue/violet material and the innards of late third instar larvae contain little to no blue matter (Figure 3.1: A, B). Eye-antennal discs, the brain, and assorted imaginal discs attached during the initial gross dissection (eye-brain complexes) from early and late third instar larvae were dissected in S2 media and cultured for 16-18 hours at 25^{o}C in wells filled with S2 media or S2 media containing DTT (S2 DTT). The discs were then stained with cleaved caspase 3 and analyzed for cleaved caspase 3 activity. The cleaved caspase 3 antibody primarily recognizes an epitope of dronc and to a lesser degree other effector caspases (Fan and Bergmann, 2010). Eye-antennal discs from *yw* early third instar larvae were refractory to ERSIA and do not exhibit cleaved caspase 3 activity (Figure 3.1: A’’). In contrast, discs from *yw* late third instar larvae had significant ERSIA and caspase activity (Figure 3.1: B’’).

Figure 3.1: Larval tissue sensitivity to ERSIA is age dependent

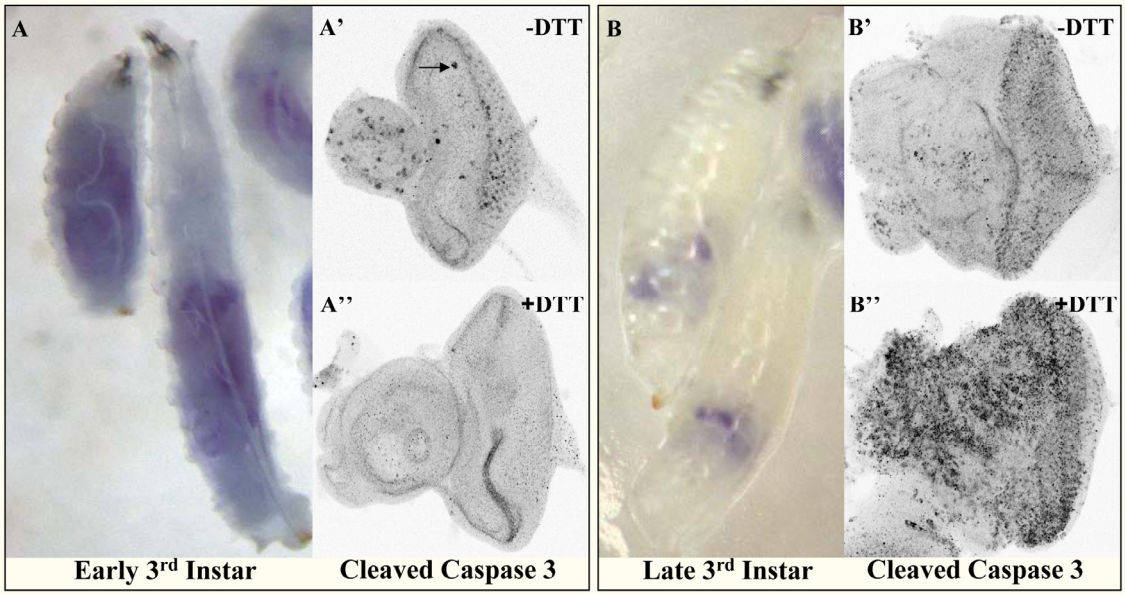

Figure 3.1: [A] *yw* early third instar larvae grown on blue food are identified by their guts filled with blue material. **[A']** *yw* eye-antennal disc from an early third instar larva mock incubated in S2 media and stained for cleaved caspase 3 activity (arrow, black dots). The eye-antennal disc had little caspase activation. **[A'']** The eye-antennal disc of a *yw* early third instar larva incubated in S2 DTT and stained for cleaved caspase 3 activity was devoid of cleaved caspase 3 activity and exhibited no ERSIA. **[B]** *yw* late third instar larvae contained little blue food in their guts. **[B']** The eye-antennal disc from a *yw* late third instar larva mock incubated in S2 media and stained for cleaved caspase 3 activity (black). Mock incubated late third instar larvae had some evidence of developmental cell death in eye-antennal discs. **[B'']** The eye-antennal disc of a *yw* late third instar larva incubated in S2 DTT and stained for cleaved caspase 3. Late third instar larvae incubated in S2 DTT exhibited substantial caspase activity and ERSIA (black dots).

Optimization experiments indicated that the staging of third instar larvae is critical for inducing ERSIA. Early third instar larvae are resistant to ERSIA and are unsuitable for screening, while late third instar larvae are highly susceptible to ERSIA. In addition, a culture period of 16-18 hours is required for favorable ERSIA induction.

After prime conditions for culturing imaginal discs to induce ERSIA were determined, screening for modifiers of this cell death paradigm was initiated in two phases. The first phase involved testing mutants of known cell death and ER stress pathway regulators for their effect on ERSIA. For example, loss-of-function mutations in proapoptotic genes such as *H99* (*RHG*), *dronc*, and *drice* were expected to suppress ERSIA. The second phase consisted of analyzing the 452 p-element lethal FRT lines from the UCLA Undergraduate Consortium in Functional Genomics (Call *et al*., 2007).

The analysis of mutant PCD and UPR genes was conducted using the flippase/ flippase recognition target (FLP/FRT) technique whenever possible. The FLP/FRT technique generates mitotic clones in a heterozygous animal in specific tissues and stages (Golic *et al*., 1997). The FLP/FRT technique can yield mosaic wild-type, heterozygous, and homozygous mutant tissues in a specific location of an animal heterozygous for a wild-type and mutant allele. If a mutation is homozygous-lethal at an early stage, it is not possible to assess its role during later development in -/- animals, hampering insight into its functions. The advantage of the FLP/FRT method is the possibility of analyzing homozygous-mutant clonal tissues in non-essential organs such the eye in heterozygous animals. If an FRT allele of a mutation were not available, eye-brain complexes from homozygous-mutant animals cultured in S2 or S2 DTT were analyzed.

Whenever possible, mosaic late third instar larval eye-brain complexes from *eyeless flippase* expressing females with wild-type, GFP marked-FRT chromosomes crossed to males with mutations on unmarked FRT chromosomes were mock-incubated or cultured under ER stress conditions and assayed for differential cleaved caspase 3 activity. Wild-type, heterozygous, and homozygous mutant tissues from the cultured discs were scored for differences in caspase activation (Figure 3.2). Mutations were scored as loss-of-function non-regulators, enhancers, or suppressors of ERSIA if homozygous-mutant clones, when compared to wild-type and heterozygous clones demonstrated uniform, increased, or decreased caspase activity, respectively.

3.2.2 *H99*, *dronc*, *drice*, and *dark* affect ERSIA

In order to determine which canonical PCD regulators have a role in ERSIA, mosaic eye-antennal discs from *H99* (*RHG*), $dronc^{I24}$, $drice^{17}$, $dark^{L46}$, and $cyt\text{-}c\text{-}d^{Z2\text{-}1091}$ heterozygotes were incubated in S2 or S2 DTT and analyzed for differential caspase activation. Eye-antennal discs of late third instar $dredd^{B118}$ and $dcp\text{-}1^{Prev1}$ homozygous mutant animals were assayed for caspase activation since FRT alleles of those stocks were unavailable. Mutations in *cyt-c-d*, *dredd*, and *dcp-1* did not affect ERSIA (Figure 3.3).

$cyt\text{-}c\text{-}d^{Z2\text{-}1091\text{-}/\text{-}}$ clones in DTT treated discs did not show differential caspase activation compared to wild-type and heterozygous tissues indicating *cyt-c-d* was not utilized for ERSIA (Figure 3.3: B-B''). $Dredd^{-/-}$ and $dcp\text{-}1^{-/-}$ eye-antennal discs exhibited significant caspase activation after culture in S2 DTT and at this time there is no evidence that these caspases significantly contribute to ERISA (Figure 3.3: C', D'). However, the absence of a *dcp-1* FRT allele limits definitive conclusions regarding a role of *dcp-1* in

Figure 3.2: Experimental procedures for the FRT ERSIA screen (DTT assay)

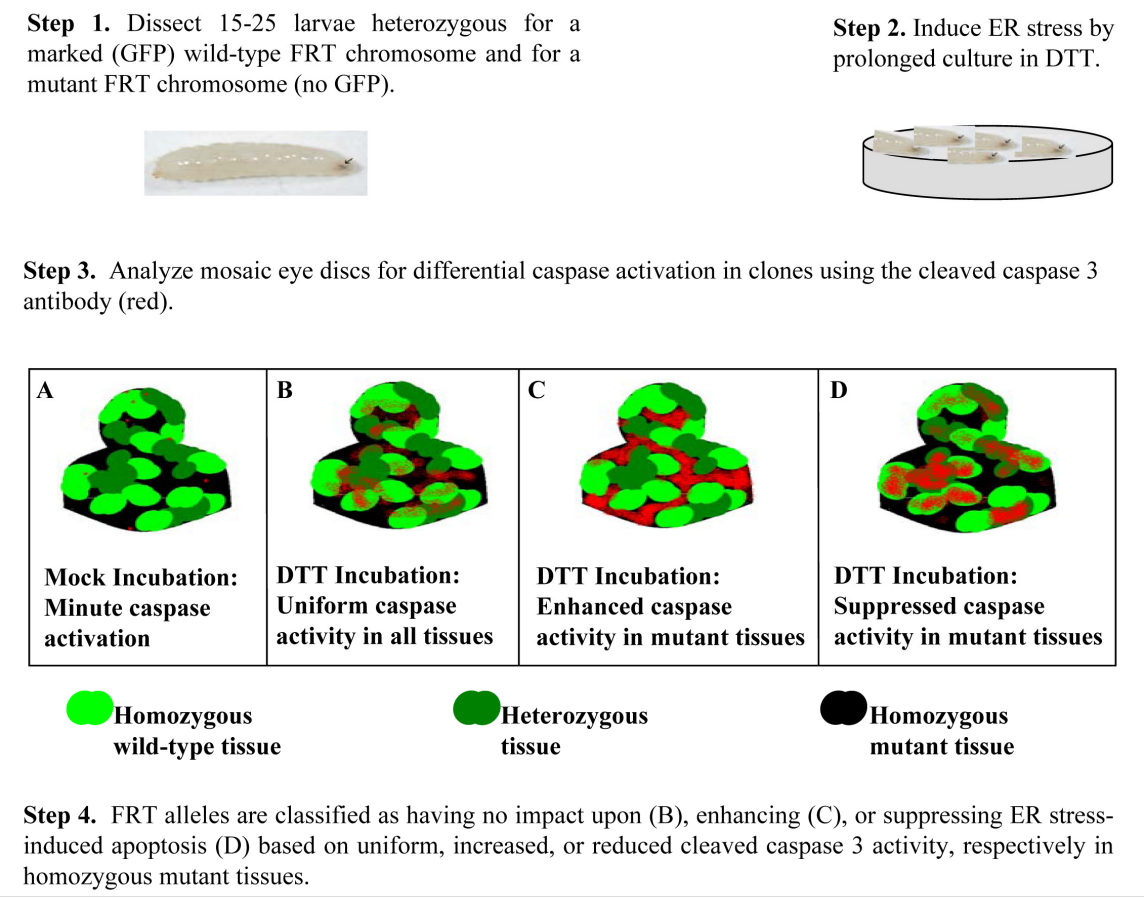

Figure 3.2: The above is a schematic of the technique to assess caspase activation in the p-element lethal FRT screen (DTT assay). Eye-antennal discs from larvae heterozygous for a marked, wild-type FRT and unmarked FRT mutant chromosome are dissected, cultured in S2 or S2 DTT, stained for cleaved caspase 3 activity (red), and analyzed for differential caspase activation in clonal tissues. **[A]** Mock incubated tissues have little caspase activity throughout the disc. **[B]** Non-regulators of ERSIA have uniform caspase activity in clones. **[C]** Enhancers of ERSIA have increased caspase activity in homozygous-mutant tissues. **[D]** Suppressors of ERSIA have reduced caspase activity in homozygous-mutant tissues.

ERSIA. In contrast, *RHG*, *dronc*, *drice*, and *dark* are required for ERSIA (Figure 3.4). *H99*$^{-/-}$, *dronc*$^{-/-}$, *dark*$^{-/-}$, and *drice*$^{-/-}$ clones did not exhibit cleaved caspase 3 activity in eye-antennal discs incubated in S2 DTT (Figure 3.4: B-B'', D-D'', F-F'', H-H'', respectively). Cell death as a consequence of prolonged culture under non-ideal conditions, i.e. lack of nutrients and poor oxygenation, can be eliminated since mock incubated discs did not have elevated caspase activity (Figure 3.3: A-A'', C, D; Figure 3.4: A-A'', C-C'', E-E'', G-G''). The pilot screen of canonical apoptosis regulators revealed *H99*, *dronc*, *drice* and *dark* activate ERSIA. On the other hand, *cyt-c-d*, *dredd*, and *dcp-1* were not further pursued in the absence of overt effects of mutations in these genes on ERSIA.

3.2.3 Ire1 plays a role in ERSIA

Once reproducible conditions to induce ERISA in cultured imaginal discs were established, mutants for *xbp1* and *ire1* were tested for an effect on ERSIA (Figure 3.5). *xbp1*$^{-/-}$ clones did not have reduced ERSIA compared to neighboring wild-type and heterozygous tissues (Figure 3.5: B-B'', C-C''). However, *ire1*$^{-/-}$ clones occasionally exhibited a small reduction in ERSIA (Figure 3.5: E-E'', F-F''). In particular, *ire1*$^{-/-}$ clones occasionally showed a mild reduction in cleaved caspase 3 activity at the apical surface of discs (Figure 3.5: E-E'', arrows and clone outlined in gray). In Figure 3.5, all the discs are arranged with the anterior to the left and posterior to the right. The apical layer of DTT treated discs tended to exhibit less ERSIA compared to basal layers (Figure 3.5: E-F''). The clone outlined in Figure 3.5: E, E'' had noticeably less caspase activation compared to wild-type and heterozygous clonal tissues dorsal and ventral to the clone. Caspase activation was much more intense in the basal layer of the eye-antennal disc and

Figure 3.3: *cyt-c-d*, *dcp-1*, and *dredd* are not required for ERSIA

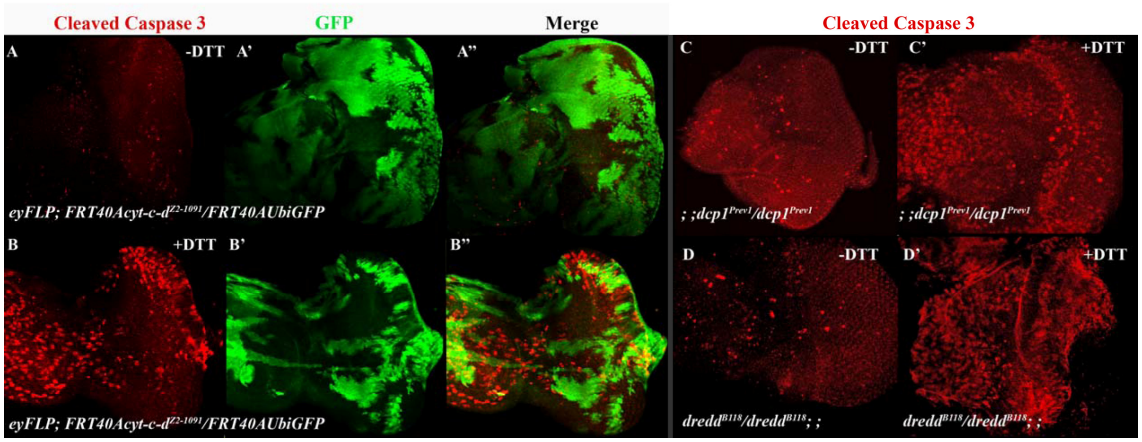

Figure 3.3: [A-D'] *cyt-c-d*, *dcp-1*, and *dredd* mutants failed to suppress ERSIA. **[A-D']** Late third instar eye-antennal discs cultured in S2 (A-A'', C, D) or S2 DTT (B-B'', C', D'). Apoptotic cells were labeled with the cleaved caspase 3 antibody (red). UbiGFP expression (green) marks wild-type or heterozygous tissues, areas without GFP were homozygous mutant. **[A-A'']** Mock incubated *cyt-c-d*$^{Z2\text{-}1091}$*/UbiGFP* disc. **[B-B'']** DTT treated *cyt-c-d*$^{Z2\text{-}1091}$*/UbiGFP* disc. **[C]** *dcp1*^{Prev1} eye-antennal disc incubated in S2 media. **[C']** *dcp1*^{Prev1} eye-antennal disc incubated in S2 DTT. **[D]** Mock incubated *dredd*^{B118} eye-antennal disc. **[D']** DTT treated *dredd*^{B118} eye-antennal disc.

consequently *ire1*$^{-/-}$ suppression of ERSIA is less pronounced. Basal *ire1*$^{-/-}$ clones had a minute reduction in the intensity of cleaved caspase 3 activity (Figure 3.5: F-F'', arrows and clones bracketed in gray). *H99*$^{-/-}$, *dronc*$^{-/-}$, and *drice*$^{-/-}$ basal layer clones displayed strong ERSIA suppression (data not shown). Caspase induction and cell death are separable events. Therefore, cell death assessed by TUNEL was conducted on discs dissected from *xbp1/UbiGFP* and *ire1/UbiGFP* larvae (Figure 3.5: G-G'', H-H''). Homozygous-mutant *xbp1* clones had TUNEL labeling similar to wild-type and heterozygous tissues. *ire1*$^{-/-}$ clones had reduced TUNEL labeling compared to adjacent wild-type and heterozygous tissues (Figure 3.5: H-H'', arrows point to outlined clones with reduced ERSIA). Therefore, loss of Xbp1 function appears not to inhibit ERSIA, but Ire1 seems to be required for normal ERSIA.

The *xbp1*^{k13803} allele used in this study was generated by a p-element insertion into the *xbp1* 5' UTR and is considered a strong hypomorph and possible null-allele. *xbp1*^{k13803} flies have been shown to have defective ER stress signaling (Ryoo *et al*., 2007; www.flybase.org). The *ire1*^{f02170} allele was generated by a p-element insertion into the *ire1* coding sequence; it is homozygous lethal, considered a strong hypomorph, and is defective in *xbp1* splicing (personal communication P. Domingos; www.flybase.org).

3.2.4 A screen to identify novel regulators of ER stress induced apoptosis

In order to identify regulators of ERSIA, a screen was conducted with 452 FRT p-element lethal stocks derived from the UCLA Undergraduate Consortium in Functional Genomics using the DTT assay (Call *et al*., 2007; Table 1). Eye-antennal discs were scored as shown in Figure 3.2. The screen led to the identification of five loss-of-function enhancers and seven loss-of-function suppressors of ERSIA.

Figure 3.4: *RHG* (*H99*), *dronc*, *dark*, and *drice* are required for ERSIA

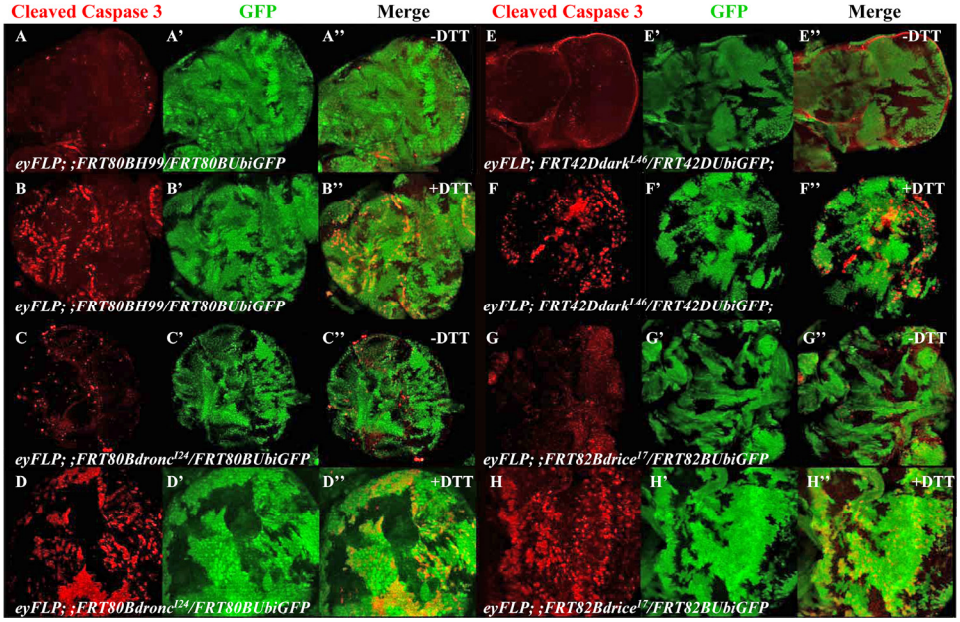

Figure 3.4: [A-H''] ERSIA was inhibited in *H99*, *dronc*, *dark*, and *drice* mutant clones. **[A-H'']** Late third instar eye-antennal discs with mosaic clones generated with *eyeless flippase* cultured in S2 media (A-A'', C-C'', E-E'', G-G'') or S2 DTT (B-B'', D-D'', F-F'', H-H''). Apoptotic cells were labeled by cleaved caspase 3 antibody activity (red). Wild-type or heterozygous clonal tissues were marked by UbiGFP expression (green), regions devoid of UbiGFP expression were homozygous-mutant clones. Each set of three images depicts a single eye disc, where the first, second, and third panels reveal cleaved caspase 3, GFP, and merged channels, respectively. **[A-A'']** Mock incubated *H99/UbiGFP* mosaic eye-antennal disc. **[B-B'']** DTT treated *H99/UbiGFP* eye-antennal disc. **[C-C'']** Mock incubated $dronc^{I24}$*/UbiGFP* imaginal disc. **[D-D'']** DTT treated $dronc^{I24}$*/UbiGFP* eye-antennal disc. **[E-E'']** Mock incubated $dark^{L46}$*/UbiGFP* eye-antennal disc. **[F-F'']** S2 DTT incubated $dark^{L46}$*/UbiGFP* eye-antennal disc. **[G-G'']** Mock incubated $drice^{17}$*/UbiGFP* eye-antennal disc. **[H-H'']** DTT treated $drice^{17}$*/UbiGFP* eye-antennal disc. -/- tissues for all lines incubated in S2 DTT had little or no ERSIA.

Diminished Nuclear fallout and Sac1/CG9187 greatly increased ERISA, while CG17090, kinesin heavy chain, and CG30496/CG30493 weakly increased ERSIA (images not shown). *CG8108* was the strongest loss-of-function ERSIA suppressor and Darkener of apricot, CG31012, CG14867, Walrus, Heat shock protein cognate 5, and Ken and Barbie/Thiolase loss weakly suppressed ERSIA (Figure 3.6; images not shown).

CG8108$^{-/-}$ tissues suppressed ER stress induced cell death resulting from prolonged culture in DTT (Figure 3.6: B-B'', C-C''). *CG8108*$^{-/-}$ clones tended to be smaller, largely absent from the antennal portion of the disc, and found primarily towards the mid to posterior regions of the disc (Figure 3.6). *CG8108*$^{-/-}$ clones have reduced caspase activation and TUNEL labeling in DTT treated discs (Figure 3.6: arrows B, B'', C, C'', D, D''). Based on the reduced cleaved caspase 3 activity and TUNEL labeling of *CG8108*$^{-/-}$ clones, *CG8108* was scored as a loss-of-function ERSIA suppressor.

3.3 Discussion

In this chapter, a technique to identify regulators of ER stress induced apoptosis (DTT assay) was described and its application was used to isolate genes affecting cell viability in tissues undergoing prolonged ER stress in culture (Figure 3.2). The success of the DTT assay is dependent on two factors; the age of the larvae dissected and the duration of the incubation at 25^{o}C. The growth of larvae on blue food enables the animals to be staged and increases the frequency of discs obtained by an investigator exhibiting ERSIA. Early third instar larvae are refractory to the effects of DTT, whilst late third instar larvae are susceptible to prolonged culture in DTT (Figure 3.1: compare caspase activation {black dots} in panel A'' to B''). The expression of ecdysone during the mid-third instar may contribute to larval competency for ERSIA. *dronc* expression is

Figure 3.5: Ire1, but not Xbp1 may be necessary for full activation of ERSIA

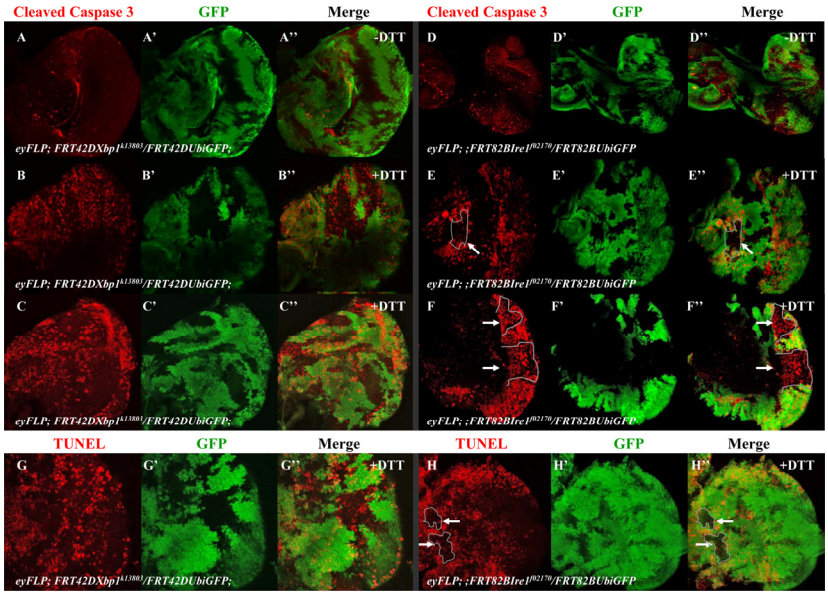

Figure 3.5: [A-H''] ERSIA was not strongly suppressed in *xbp1*$^{-/-}$ and *ire1*$^{-/-}$ clones. **[A-H'']** Late third instar eye-antennal discs with *eyeless flippase* generated clones cultured in S2 (A-A'', D-D'') or S2 DTT (B-B'', C-C'', E-E'', F-F'', G-G'', H-H'') media for 18 hours. Apoptotic cells were labeled by cleaved caspase 3 antibody activity or TUNEL (red). Wild-type or heterozygous clonal tissues were marked by UbiGFP (green), regions without UbiGFP expression were homozygous-mutant clones. **[A-A'']** Mock incubated *xbp1*^{k13803}*/UbiGFP* disc. **[B-B'', C-C'', G-G'']** DTT treated *xbp1*^{k13803}*/UbiGFP* discs. *xbp1*$^{-/-}$ clones did not show reduced caspase activation or TUNEL compared to adjacent tissues. **[D-D'']** Mock-incubated *ire1*^{f02170}*/UbiGFP* disc. **[E-E'', F-F'']** Apical and basal images of the same DTT treated *ire1*^{f02170}*/UbiGFP* disc. *ire1*$^{-/-}$ clones exhibited reduced caspase activation compared to adjacent wild-type and heterozygous tissues at apical surfaces of the disc (E-E'') and to a lesser degree at basal layers (F-F''; white arrows and areas within the gray outlines). **[H-H'']** DTT treated *ire1*^{f02170}*/UbiGFP* disc. Arrows and gray boundaries highlight *ire1*$^{-/-}$ clones with reduced TUNEL labeling.

upregulated by ecdysone and was necessary for caspase activation during ERSIA (Dorstyn *et al*., 1999; Figure 3.4: D-D''). Eye-brain complexes from late third instar larvae may have higher levels of *dronc* throughout the course of the S2 DTT incubation leading to increased cell death. The duration of the DTT incubation is also a key factor in effectively utilizing the DTT assay. Culture in S2 DTT for 16-18 hours at 25^{o}C is the most advantageous time and temperature for ERSIA induction. Incubation periods less than 16 hours will cause ER stress, but will not elicit cell death. Incubations at temperatures below 25^{o}C retards ERSIA induction, extends the duration of DTT incubation, and increases the likelihood unfavorable culture conditions. The mass screening of eye-antennal discs for ERSIA using the DTT assay requires the incubation of late third instar larval eye-brain complexes for 16-18 hours in S2 DTT at 25^{o}C in a humid chamber.

The DTT assay was utilized with the intention of discovering novel regulators of ERSIA. Mosaic eye-antennal discs derived from crosses of *eyeless flippase*; *FRTUbiGFP* females crossed to males from 452 p-element lethal FRT lines generated by UCLA Undergraduate Consortium were tested for modulating ERSIA (Call *et al*., 2007; Table 1). Eye-brain complexes from larvae expressing *eyeless flippase*, heterozygous for a wild-type GFP-labeled FRT chromosome and an unmarked mutant FRT chromosome were incubated in S2 DTT to invoke ER stress-induced cell death. The eye-brain complexes were stained for caspase activity using the cleaved caspase 3 antibody. Eye-antennal discs were analyzed for differential caspase activation in wild-type, heterozygous, and homozygous-mutant clones. Whether a gene was scored as an activator or suppressor of ERSIA depended on the extent of cell death in a homozygous

Table 1: Results of cleaved caspase 3 activity screen for regulators of ERISA

Late third instar larvae with the indicated disrupted gene(s) were analyzed for differential cleaved caspase 3 activity after prolonged ER stress in culture media containing DTT. UCLA FRT lines obtained from the Kyoto DGRC Stock center have their stock numbers listed in the first column. UCLA FRT lines obtained directly from Dr. Utpal Banerjee begin with the letter UB and are sequentially numbered. P-element lethal lines without a specific gene assigned to the p-element insertion are labeled NG (no gene). Cell lethal lines or lines that produced clones too small for analysis are labeled (CL). Stock numbers of mutations which led to increased ERSIA are in bold and highlighted in peach and stock numbers of mutations which led to reduced ERSIA are in bold and highlighted in turquoise.

ERISA loss-of-function-mutant phenotypes were scored as follows:

Strong ERSIA increase	+++	Strong ERSIA suppression	---
Moderate ERSIA increase	++	Moderate ERSIA suppression	--
M ERSIA increase	+	Minute ERSIA suppression	-
Does not modify ERSIA	N/A		

Table 1: Results of the cleaved caspase 3 activity screen for regulators of ERISA

3L FRT80B UCLA FRT Lines			
Kyoto Stock No.	Disrupted Gene 1	Disrupted Gene 2	ERSIA phenotype
UB-1	NG	-	N/A
UB-2	sallimus	-	N/A
UB-3	bantam	-	N/A
UB-4	**CG9187**	***Sac1***	**+++**
UB-5	Ribosomal protein L8	Misshapen	N/A
UB-6	CG14821	-	N/A
UB-7	Cdc27	-	N/A
UB-8	tonalli	-	N/A
UB-9	capricious	-	N/A
UB-10	26-29kD-proteinase	-	N/A
111021	fringe connection	CG32174	N/A
111024	schizo	-	N/A
111261	mirror	-	N/A
111372	NG	-	N/A
111378	mitochondrial acyl carrier protein 1	-	N/A
111379	Heat shock protein 83	-	N/A
111382	smallminded	-	N/A
111384	CG32030	-	N/A
111386	SHC-adaptor protein	CG3967	N/A
111392	Trithorax-like	-	N/A
111394	CG7427	-	N/A
111395	RhoGAP71E	-	N/A
111399	mitochondrial ribosomal protein S34	-	N/A
111400	CG33158	CG32159	N/A
111403	MYPT-75D	-	N/A
111404	CG3902	-	N/A
111481	Organic anion transporting polypeptide 74D	-	N/A
111488	**CG17090**	**-**	**+**
111490	sugarless	-	N/A
111491	Ral guanine nucleotide exchange factor 2	-	N/A
111495	seven in absentia	Rhodopsin 4	N/A
111497	Mediator complex subunit 24	-	N/A
111499	CG7728	CG6664	N/A
111518	ftz transcription factor 1	-	N/A
111519	CG17090	-	N/A
111526	tribbles	-	N/A
111536	**nuclear fallout**	**-**	**+++**
111537	JIL-1	-	N/A
111539	Nedd2-like caspase	CG6685	N/A
111541	Neurptactin	-	N/A
111542	sallimus	-	N/A
111544	Sunday driver	CG8268	N/A
111545	Transferrin 2	-	N/A
111548	sticky	-	N/A
111554	Protein on ecdysone puffs	-	N/A
111556	Peptidoglycan recognition protein LF	CG4347	N/A
111559	Cip4	-	N/A
111561	Guanylyl cyclase at 76C	-	N/A
111567	CG10630	-	N/A
111570	polo	-	N/A
111572	Cbl	-	N/A
111579	armitage	-	N/A

Table 1: Results of the cleaved caspase 3 activity screen for regulators of ERISA			
3L FRT80B UCLA FRT Lines			
Kyoto Stock No.	Disrupted Gene 1	Disrupted Gene 2	ERSIA Phenotype
111583	Tonally	-	N/A
111589	Vihar	-	N/A
111591	chromosome bows	-	N/A
111593	CG9004	-	N/A
111607	CG3911	-	N/A
111608	mitochondrial ribosomal protein L17	-	N/A
111611	***CG8108* [*p{SuporP}CG8108*]**	**-**	**– – –**
111613	Pathetic		N/A
111614	Trio	CG9205	N/A
111619	CG12734	-	N/A
111620	Glued	-	N/A
111631	nuclear fallout	-	N/A
111635	nuclear fallout	nanchung	N/A
3R FRT 82B UCLA FRT Lines			
Kyoto Stock No.	Disrupted Gene 1	Disrupted Gene 2	ERSIA Phenotype
111026	elongation initiation factor 5C	-	N/A
111027	Another transcription unit	-	N/A
111028	CG1965	-	N/A
111030	Dihydroorotate dehydrogenase	-	N/A
111031	CG8036	-	N/A
111032	CG33936	-	N/A
111033	mitochondrial transcription factor B2	CG11722	N/A
111035	C-terminal Src kinase	-	N/A
111036	CG8630	-	N/A
111038	B52	-	N/A
111039	trithorax	-	N/A
111041	MRG15	-	N/A
111042	CG14867	-	N/A
111043	sarah	-	N/A
111044	COP9 complex homolog subunit 5	-	N/A
111046	Daughters against dpp	-	N/A
111047	vibrator	-	N/A
111048	modifier of mdg4	-	N/A
111050	Glutamate-cysteine ligase modifier	-	N/A
111051	crumbs	CG5715	N/A
111052	CG5746	-	N/A
111053	CycB3	-	N/A
111054	Oligosaccharyl transferase 3	-	N/A
111055	NG	-	N/A
111056	**Darkener of apricot**	**-**	**–**
111057	string	-	N/A
111058	ND	-	N/A
111059	prolyl-4-hydroxylase-alpha EFB	-	N/A
111060	**CG31012**	**-**	**–**
111061	hephaestus	-	N/A
111232	ND	-	N/A
111264	NG	-	N/A
111268	NG	-	N/A
111405	**CG14867**	**-**	**–**
111406	Alhambra	-	N/A
111407	neuralized	-	N/A

Table 1: Results of the cleaved caspase 3 activity screen for regulators of ERISA			
3R FRT82B UCLA FRT Lines			
Kyoto Stock No.	Disrupted Gene 1	Disrupted Gene 2	ERSIA Phenotype
111409	NG	-	N/A
111410	CG8863	-	N/A
111411	squid	-	N/A
111413	CG9924	-	N/A
111414	trithorax	-	N/A
111416	14-3-3epsilon	-	N/A
111417	CG11779	nanos	N/A
111418	vibrator	-	N/A
111419	Na pump α subunit	-	N/A
111420	Rab-protein 11	-	N/A
111421	held out wings	-	N/A
111422	scribbled	-	N/A
111423	CG10011	-	N/A
111425	similar	-	N/A
111459	NG	-	N/A
111479	headcase	-	N/A
111496	couch potato	-	N/A
111505	Heat shock RNA ω	-	N/A
111511	branchless	-	N/A
111535	NG	-	N/A
111546	CG5802	-	N/A
111568	CG1746	-	N/A
111582	crumbs	-	N/A
111588	polychaetoid	-	N/A
111594	CG14713	-	N/A
111595	γ-coatomer protein	-	N/A
111599	CG17838	-	N/A
111617	similar	-	N/A
111625	NG	.	
2L FRT 40A UCLA FRT Lines			
Kyoto Stock No.	Disrupted Gene 1	Disrupted Gene 2	ERSIA Phenotype
111062	NG	-	N/A
111064	escargot	-	N/A
111066	cropped	-	N/A
111067	raw	-	N/A
111068	capulet	-	N/A
111072	Heterogeneous nuclear ribonucleoprotein at 27C	-	N/A
111079	crooked legs	-	N/A
111080	lilliputian	-	N/A
111083	nebbish	-	N/A
111088	little imaginal discs	-	N/A
111097	no mitochondrial derivative	-	N/A
111101	kismet	-	N/A
111102	Rab-protein 6	-	N/A
111104	U2 small nuclear riboprotein auxiliary factor 38	-	N/A
111106	turtle	-	N/A
111108	taiman	-	N/A
111111	overgrown hematopoietic organs at 23B	-	N/A
111122	Collagen type IV	viking	N/A
111123	Mothers against dpp	-	N/A
111125	KDEL receptor	-	N/A
111127	Collagen type IV	viking	N/A
111128	Thor	-	N/A

Table 1: Results of the cleaved caspase 3 activity screen for regulators of ERISA			
2L FRT40A UCLA FRT Lines			
Kyoto Stock No.	Disrupted Gene 1	Disrupted Gene 2	ERSIA Phenotype
111130	Hsp70/Hsp90 organizing protein homolog	-	N/A
111134	echinoid	-	N/A
111143	Eukaryotic initiation factor 4a	-	N/A
111145	Dopa decarboxylase	-	N/A
111147	CG31680	-	N/A
111159	Sec61α	-	N/A
111165	Threonyl-tRNA synthetase	-	N/A
111169	milton	-	N/A
111173	Sec61α	-	N/A
111174	porin	-	N/A
111177	NG	-	N/A
111181	CG5776	CG12292	N/A
111185	piwi	-	N/A
111186	v(2)k05816	-	N/A
111187	vrille	-	N/A
111192	Pendulin	-	N/A
111196	Bekka	CG5924	N/A
111199	expanded	-	N/A
111201	maternal expression at 31B	-	N/A
111202	Ribonucleoside diphosphate reductase	-	N/A
111203	Aac11	-	N/A
111204	split ends	-	N/A
111206	expanded	-	N/A
111207	NG	-	N/A
111209	A kinase anchor protein 200	-	N/A
111213	CG7364	-	N/A
111214	kekkon-1	-	N/A
111218	CG9523	-	N/A
111221	Angiotensin-converting enzyme-related	-	N/A
111222	CENP-ana	-	N/A
111225	Nnp-1	-	N/A
111228	NG	-	N/A
111230	Glycogen phosphorylase	-	N/A
111234	ND	-	N/A
111243	brother of odd with entrails limited	-	N/A
111252	Trehalose-6-phosphate synthase 1	-	N/A
111257	Myosin 31DF	-	N/A
111260	CG8678	-	N/A
111265	Ribosomal protein S13	-	N/A
111266	CG17646	-	N/A
111267	rickets	-	N/A
111275	CG31672	-	N/A
111278	Pdsw	-	N/A
111281	mir-275	-	N/A
111282	CG31917	-	N/A
111284	CG3036	-	N/A
111285	kismet	-	N/A
111286	CG33316	-	N/A
111287	Fatty acid (long chain) transport protein	-	N/A
111290	Myosin heavy chain	-	N/A
111291	NG	-	N/A
111292	Coproporphyrinogen oxidase	-	N/A
111296	dorsal	-	N/A
111298	CG9523	-	N/A

Table 1: Results of the cleaved caspase 3 activity screen for regulators of ERISA			
2L FRT 40A UCLA FRT Lines			
Kyoto Stock No.	Disrupted Gene 1	Disrupted Gene 2	ERSIA Phenotype
111300	polypeptide GalNAc transferase 5	CG5828	N/A
111304	kismet	-	N/A
111305	NG	-	N/A
111306	heixuedian	-	N/A
111311	Rieske iron-sulfur protein	-	N/A
111316	expanded	-	N/A
111318	Ubiquitin conjugating enzyme 2	-	N/A
111324	Thor	-	N/A
111325	CG3645	-	N/A
111327	Basigin	-	N/A
111328	Sema-1a	-	N/A
111330	CG2807	-	N/A
111332	NG	-	N/A
111333	Replication factor C 38kD subunit	-	N/A
111334	Cytochrome c proximal	CG31782	N/A
111337	NG	-	N/A
111338	CG11098	-	N/A
111343	CSN8	CG7627	N/A
111344	grapes	-	N/A
111349	CG14914	-	N/A
111352	CG10641	CG15168	N/A
111356	ebi	-	N/A
111357	CG5953	-	N/A
111359	RNA polymerase I 135kD subunit	-	N/A
111360	thickveins	-	N/A
111366	lethal (2) k16918	-	N/A
111367	Basigin	-	N/A
111369	Target of rapamycin	-	N/A
111373	NG	-	N/A
111374	rolling stone	-	N/A
111430	lethal (2) s5379	CG15387	N/A
111431	ND	-	N/A
111433	heixuedian	-	N/A
111434	PRL-1	-	N/A
111435	mitochondrial ribosomal protein L4	-	N/A
111461	NG	-	N/A
111462	NG	-	N/A
111463	NG	-	N/A
111470	NG	-	N/A
111471	NG	-	N/A
111472	NG	-	N/A
111474	NG	-	N/A
111485	kismet	-	N/A
111486	cAMP-dependent protein kinase 1	-	N/A
111494	lethal (2) 35Di	-	N/A
111502	CG17259	-	N/A
111507	polypeptide GalNAc transferase 5	-	N/A
111512	Gliotactin	CG3793	N/A
111514	spire	-	N/A
111515	CG7337	-	N/A
111516	Kruppel homolog 1	-	N/A
111520	chiffon	-	N/A
111524	glial cells missing	-	N/A
111558	CG6509	-	N/A

Table 1: Results of the cleaved caspase 3 activity screen for regulators of ERISA			
2L FRT 40A UCLA FRT Lines			
Kyoto Stock No.	Disrupted Gene 1	Disrupted Gene 2	ERSIA Phenotype
111562	NG	-	N/A
111563	CG9535	-	N/A
111564	Leukocyte-antigen-related-like	-	N/A
111571	second mitotic wave missing	CG10189	N/A
111573	Laminin B1	-	N/A
111574	CG7277	CG31989	N/A
111575	CG31900	CG8552	N/A
111577	CG31694	-	N/A
111578	Arc-p34	-	N/A
111584	NG	-	N/A
111585	out at first	-	N/A
111586	abrupt	-	N/A
111590	Inositol 1,4,5-triphosphate kinase 1	-	N/A
111592	decapentaplegic	-	N/A
111596	infertile crescent	-	N/A
111597	NG	-	N/A
111598	CG9140	-	N/A
111600	CG9328	-	N/A
111601	Rab-protein 5	-	N/A
111602	CG15141	-	N/A
111603	Kruppel homolog 2	-	N/A
111604	CG5446	CG6388	N/A
111606	CLIP-190	-	N/A
111610	CG31666	-	N/A
111612	CG18397	-	N/A
111615	anterior open	-	N/A
111621	transfer RNA:tyr1:22Fb	transferRNA:tyr1:22Fa	N/A
111622	cropped	-	N/A
111623	Tetratricopeptide repeat protein 2	-	N/A
111624	CG3347	-	N/A
111630	Sensitized chromosome inheritance	-	N/A
111634	vasa	-	N/A
111636	NG	-	N/A
2R FRT 42D UCLA FRT Lines			
Kyoto Stock No.	Disrupted Gene 1	Disrupted Gene 2	ERSIA Phenotype
111020	Misexpression suppressor of KSR 2	-	N/A
111025	overgrown hematopoietic organs 55DE	-	N/A
111063	Matrix metalloproteinase 2	-	N/A
111069	mastermind	-	N/A
111071	NG	-	N/A
111073	Sec61beta	-	N/A
111074	shotgun	-	N/A
111076	charlatan	-	N/A
111082	Death caspase-1	-	N/A
111084	Kruppel	-	N/A
111089	dacapo	-	N/A
111090	blistered	-	N/A
111092	**ken and barbie**	**Thiolase**	**–**
111094	Syndecan	-	CL
111095	lethal(2)44DEa	-	N/A
111096	**CG30496**	**CG30493**	**+**
111099	Sema-2a	-	N/A

Table 1: Results of the cleaved caspase 3 activity screen for regulators of ERISA			
2R FRT 42D UCLA FRT Lines			
Kyoto Stock No.	Disrupted Gene 1	Disrupted Gene 2	ERSIA Phenotype
111103	**walrus**	**-**	**–**
111107	Valyl-tRNA synthetase	-	N/A
111110	apontic	-	N/A
111112	grainy head	-	N/A
111115	Proteasome p44.5 subunit	-	N/A
111116	Cyt-b5	-	N/A
111117	CG8078	-	N/A
111119	Argonaute 1	-	N/A
111126	schnurri	-	N/A
111129	jelly belly	-	N/A
111132	β-Tubulin at 56D	-	N/A
111133	ND	-	N/A
111135	Calmodulin	-	N/A
111137	lin-19-like	-	N/A
111138	muscleblind	-	N/A
111140	mir-14	-	N/A
111146	NG	-	N/A
111150	lola like	-	N/A
111154	ND	-	N/A
111157	deadpan	-	N/A
111158	CG1648	-	N/A
111166	muscleblind	-	N/A
111167	gemini	-	N/A
111168	Aspartyl-tRNA synthetase	-	N/A
111170	CG30118	-	N/A
111171	**Heat shock protein cognate 5**	**-**	**–**
111172	Ryanodine receptor 44F	-	N/A
111175	midlife-crisis	-	N/A
111178	NG	-	N/A
111179	CG12924	CG1665	N/A
111180	CG6426	-	N/A
111182	meiotic W68	-	N/A
111184	lethal(2)k05713	-	N/A
111190	CG1472	-	N/A
111191	par-1	-	N/A
111193	Suppressor of zeste 2	-	N/A
111194	atypical protein kinase C	CG30475	N/A
111198	Cyclin-dependent kinase 4	-	N/A
111200	NG	-	N/A
111211	CG33455	vegetable	N/A
111212	Vha36	-	N/A
111215	CG14480	-	N/A
111216	CG6796	-	N/A
111217	lethal (2) k07433	-	N/A
111219	CG6424	-	N/A
111220	ribonuclease H1	drosha	N/A
111223	three rows	-	N/A
111226	Posterior sex combs	-	N/A
111229	rigor mortis	-	N/A
111231	18 wheeler	-	N/A
111235	G protein γ 1	CG13746	N/A
111236	COP9 complex homolog subunit 4	-	N/A
111238	Argonaute 1	CG33184	N/A
111241	Nup44A	-	N/A

Table 1: Results of the cleaved caspase 3 activity screen for regulators of ERISA			
2R FRT 42D UCLA FRT Lines			
Kyoto Stock No.	Disrupted Gene 1	Disrupted Gene 2	ERSIA Phenotype
111244	CG6543	-	N/A
111245	coracle	-	N/A
111246	Glutathione S transferase S1	-	N/A
111250	CG12744	-	N/A
111253	NG	-	N/A
111259	NG	-	N/A
111262	CG1814	-	N/A
111269	spinster	-	N/A
111270	Dek	-	N/A
111272	lethal(2)05510	-	N/A
111274	CG6424	-	N/A
111283	mir-14	-	N/A
111288	Hormone receptor-like in 46	-	N/A
111289	Misexpression suppressor of KSR 2	-	N/A
111293	bicaudal	-	N/A
111294	Ate1	-	N/A
111295	Glutathione S transferase S1	-	N/A
111297	methuselah-like 3	CG10764	N/A
111299	wunen-2	wunen	N/A
111302	NG	-	N/A
111303	CG6424	-	N/A
111308	Apaf-1-related-killer	-	N/A
111309	olf186-F	-	N/A
111312	tout-velu	-	N/A
111313	Glycogen phosphorylase	-	N/A
111314	preli-like	-	N/A
111315	NG	-	N/A
111319	Lissencephaly-1	-	N/A
111320	CG13506	-	N/A
111321	**Kinesin heavy chain**	**-**	**+**
111322	Kinesin heavy chain	-	N/A
111323	CG8026	-	N/A
111326	Dek	-	N/A
111329	Prosap	-	N/A
111331	X box binding protein-1	-	N/A
111339	tripeptidyl-peptidase II	Cap-G	N/A
111341	NG	-	N/A
111342	lethal (2) k14708	-	N/A
111345	unchained	-	N/A
111346	Cysteine proteinase-1	-	N/A
111347	Dystroglycan	-	N/A
111350	fat-spondin	teflon	N/A
111351	costa	-	N/A
111353	Dynamitin	-	N/A
111355	bancal	-	N/A
111362	visceral mesodermal armadillo-repeats	-	N/A
111363	cleavage and polyadenylation specificity factor	-	N/A
111364	baboon	-	N/A
111365	Ribosomal protein L11	-	N/A
111368	CG13512	-	N/A
111371	fused lobes	-	N/A
111376	Cyclin-dependent kinase 4	-	N/A
111377	bancal	-	N/A
111436	NG	-	N/A

Table 1: Results of the cleaved caspase 3 activity screen for regulators of ERISA			
2R FRT 42D UCLA FRT Lines			
Kyoto Stock No.	Disrupted Gene 1	Disrupted Gene 2	ERSIA Phenotype
111437	NG	-	N/A
111438	CG8479	-	N/A
111439	scruin like at the midline	-	N/A
111440	lethal (2) k09913	-	N/A
111442	NG	-	N/A
111444	Peptidylglycine-α-hydroxylating	-	N/A
111445	Zinc finger protein RP-8	-	N/A
111446	spaghetti	-	N/A
111447	twinstar	-	N/A
111450	CG4589	-	N/A
111451	Matrix metalloproteinase 1	-	N/A
111452	Nucleosome remodeling factor – 38kD	-	N/A
111454	CG9047	-	N/A
111468	mastermind	-	N/A
111469	wunen	-	N/A
111473	NG	-	N/A
111475	Calcium ATPase at 60A	-	N/A
111476	NG	-	N/A
111478	NG	-	N/A
111482	Ubiquitin conjugating enzyme 10	-	N/A
111483	jitterbug	-	N/A
111487	Proteasome α subunit	-	N/A
111498	tripeptidyl-peptidase II	Cap-G	N/A
111500	pipsqueak	-	N/A
111503	CG11107	-	N/A
111523	Tyrosine kinase-related protein	-	N/A
111527	Pabp2	-	N/A
111530	Aspartyl-tRNA synthetase	-	N/A
111531	conserved membrane protein at 44E	-	N/A
111533	combgap	-	N/A
111538	cul-4	-	N/A
111551	Tim10	-	N/A
111555	Matrix metalloproteinase 1	-	N/A

mutant clone compared to immediately adjacent wild-type and heterozygous clones (Figure 3.2). A mosaic eye-antennal disc allows the simultaneous assessment of all three mutant genotypes (+/+; +/-; -/-) in a single tissue sample, thereby allowing the evaluation of subtleties in a gene's contribution to ERSIA. For example, an eye disc dissected from an *ire1*$^{-/-}$ larva that exhibits considerable caspase activation might indicate that Ire1 plays no role in ERSIA, whereas a mosaic disc revealing subtle but significant differences between mutant and control tissues could reveal a role of this gene for full activation of ERSIA (Figure 3.5)

Before conducting a screen to identify genes involved in ERSIA, the feasibility of such an approach was determined. For this purpose, the effect of several mutant alleles of programmed cell death genes on ERSIA was tested. The DTT assay was used to screen seven components of the canonical PCD pathway and identified *RHG* genes, *drice*, *dronc*, and *dark* as important for ERSIA (Figure 3.4). Individual loss-of-function mutations for *rpr*, *hid*, and *grim* on FRTs were not available and prohibited testing of each *RHG* gene for a direct effect on ERSIA. In contrast, mutations in *cyt-c-d*, *dredd*, and *dcp-1* did not significantly affect ERSIA as homozygous-mutant tissues derived from animals with null alleles of the aforementioned genes had substantial cleaved caspase-3 activity (Figure 3.3). The *H99* deletion potently suppresses apoptosis and its strong inhibition of ERSIA was expected (White *et al*., 1994). The requirement for *dronc*, *drice*, and *dark* to elicit ERSIA was also anticipated due to their well-established role in propagating apoptosis. Dronc is the initiator caspase utilized for activating executioner caspases in the fly, Drice functions as the primary executor caspase during stress-induced cell death and Dark is essential for apoptosome formation in the fly (Dorstyn *et al*., 1999;

Figure 3.6: ***CG8108*** **is a loss-of-function regulator of ERISA**

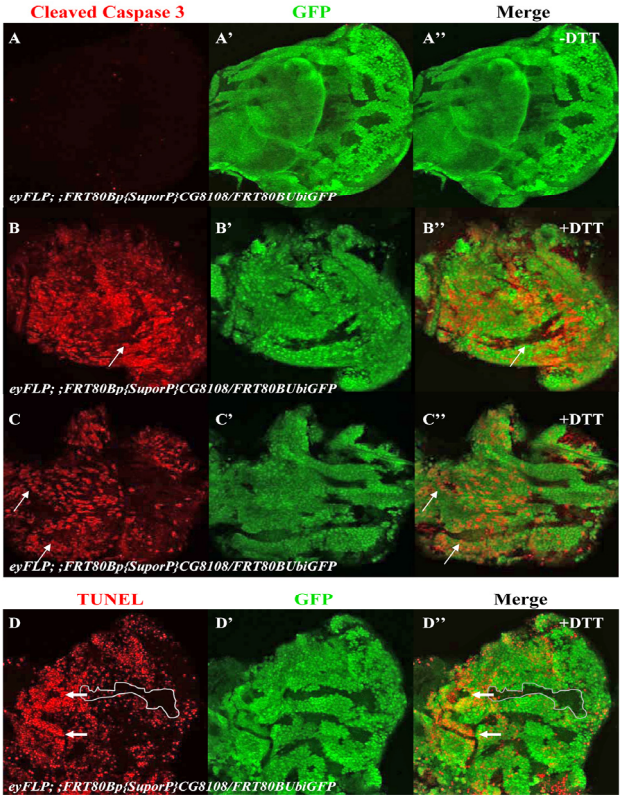

Figure 3.6: [A-D''] ERSIA was suppressed in *p{SuporP}CG8108* clones. **[A-D'']** Late third instar eye-antennal discs cultured in S2 (A-A'') or S2 DTT for 18 hours (B-B'', C-C'', D-D''). Apoptotic cells were labeled by cleaved caspase 3 antibody activity or TUNEL (red). Wild-type or heterozygous clonal tissues were marked by UbiGFP (green), regions without UbiGFP expression were homozygous-mutant clones. **[A-A'']** Mock incubated *p{SuporP}CG8108/UbiGFP* eye-antennal disc. **[B-B'', C-C'', D-D'']** DTT treated *p{SuporP}CG8108/UbiGFP* eye-antennal discs. The arrows in B-B'' and C-C'' point to $CG8108^{-/-}$ clones with reduced cleaved caspase 3 activity compared to neighboring tissues. The arrows and outlined area in D, D'' point to $CG8108^{-/-}$ clones with reduced TUNEL labeling compared to neighboring wild-type and heterozygous tissues. Loss of *CG8108* function suppressed ERSIA.

Muro *et al*., 2006; Zhou *et al*., 1999; Rodriguez *et al*., 1999). Although *cyt-c-d* is required for spermatid differentiation and the timing of interommatidial cell death in the adult fly, it was not expected to have a pivotal role in ERSIA since it is not the dominant isoform of cytochrome-c in somatic cells (Arama *et al*., 2003; Arama *et al*., 2006; Mendes *et al*, 2006). Dredd functions primarily in immunity and it is subsequently not projected to have a vital role in ERSIA (Leulier *et al*., 2000). Dcp-1 functions during oogenesis and can cooperate with Drice to induce cell death (Laundrie *et al.*, 2003; Xu *et al*., 2006). It is possible *dcp-1* has an effect on the kinetics and intensity of ERSIA, but the lack of a *dcp-1*^{Prev1}-FRT allele prevented rigorous testing using the DTT assay. In summary, the pilot screen of canonical PCD regulators did not reveal any role of *cyt-c-d*, *dredd*, and *dcp-1* for ERSIA. However, it demonstrated that *RHG* genes, *drice*, *dronc*, and *dark* are all required to induce ERSIA in late third instar tissues incubated in S2 DTT.

xbp1 and *ire1* were tested for an effect on ERSIA and Xbp1 was eliminated as a regulator of ERSIA (Figure 3.5: B-B'', C-C'', G-G''). In contrast, Ire1 may be required for full activation of ER stress induced cell death (Figure 3.5: E-E'', F-F'', H-H''). Cleaved caspase 3 activity in *xbp1*$^{k13803-/-}$ clones was indistinguishable from adjacent heterozygous and wild-type tissues in DTT treated discs (Figure 3.5: B-B'', C-C''). *ire1*^{f02170} mutants were tested using the DTT assay and occasional suppression of ERSIA was seen in *ire1*$^{-/-}$ tissues on the apical surface of imaginal discs (compare Figure 3.5: E-E'', apical layer to F-F'', basal layer). The suppression of ERSIA in the basal layer of *ire1*$^{-/-}$ tissues was minute compared to apical surfaces. Since caspase activation and actual cell death are separable events, mosaic eye-antennal discs from *xbp1*^{k13803}*/UbiGFP* and *ire1*^{f02170}*/UbiGFP* larvae were DTT treated and processed for TUNEL. The conclusions

regarding Xbp1 and Ire1 regulation of ERSIA stemming from TUNEL labeling of *xbp1*$^{-/-}$ and *ire1*$^{-/-}$ tissues mirrored the assertions based on the cleaved caspase 3 activity results (Figure 3.5: G-G'', H-H''). *xbp1*$^{-/-}$ clones exhibited TUNEL staining indistinguishable from adjacent tissues and apical *ire1*$^{-/-}$ clones had fewer TUNEL positive cells compared to neighboring wild-type and heterozygous tissues. With the fly stocks that are currently available, the results of the DTT assay suggest Xbp1 does not play a significant role in ERSIA and that Ire1 contributes to ER stress induced cell death in the fly.

The amount of ER stress in DTT treated discs is probably above physiological levels of ER stress experienced in discs. The DTT assay may be too "harsh" to detect substantial suppression of ERSIA in *xbp1*$^{k13803-/-}$ and *ire1*$^{f02170-/-}$ tissues. A possible means to test the *xbp1* and *ire1* alleles under less-extreme conditions would involve ectopic expression of proteins that induce ER stress such as Rhodopsin 1 (Kang and Ryoo, 2009). For example, proteins capable of inducing ERSIA during larval stages could be overexpressed in discs with mosaic *xbp1* and *ire1* tissues and their respective homozygous-mutant tissues could be assayed for altered cell death.

The *xbp1*^{k13803} allele is a strong hypomorph and was demonstrated to exacerbate ERSIA in the context of the *nina*^{EG69D} photoreceptor degeneration (Ryoo *et al*., 2007). In yeast and worms the loss of HAC1/XBP-1 function increases an organism's sensitivity to ER stress-induced stimuli (Mori *et al*., 1996; Richardson *et al*., 2011). Based on previous findings that the loss of *xbp1* function can adversely affect an organisms' response to ER stress, the results of this study indicating Xbp1 does not affect ERSIA is likely an accurate assertion. In order to definitively exclude Xbp1 as an ERSIA regulator, an (FRT) Xbp1 protein-null imprecise-excision line would need to be generated and tested.

IRE1 activates the JNK pathway or Bcl-2 family members when cells endure prolonged ER stress in mammalian cell culture (Urano *et al*., 2000; Nishitoh *et al*, 2002; Hetz *et al*., 2006; Hetz and Glimcher, 2009). In the fly, ER stress induced splicing of *xbp1* by Ire1 can be suppressed by ectopic expression of *Drosophila Bax inhibitor 1* (Lisbona *et al*., 2009). However, the $ire1^{f02170}$ allele remains to be tested for differential Jnk or Bcl-2 family member activation. The $ire1^{f02170}$ allele used in this study is thought to be a strong hypomorph and is defective in *xbp1* splicing (personal communication, P. Domingos). The caspase activation seen in the basal layers of $ire1^{f02170\text{-}/\text{-}}$ clones may be due to residual Ire1 protein expression. Numerous efforts have been made to generate an imprecise excision line by hopping the p-element disrupting $ire1^{f02170}$, but all efforts have failed. Only an *ire1* null-allele tested with the DTT assay would permit a declarative statement regarding Ire1's impact on ERSIA.

The cleaved caspase 3 activity seen in $ire1^{-/-}$ clones could reflect caspase activation by the Pek and ATF6 branches of the UPR. Loss-of-function analysis of *pek* and *atf6* flies has yet to take place and they may activate the cell death pathway. In mammalian cell culture, prolonged ER stress mediated PERK activation of the apoptotic protein CHOP (Zinszner *et al*., 1998; Marciniak *et al*., 2004). Although the fly does not have a *CHOP* homologue, it is plausible a protein with an analogous function exists and that it is active in $ire1^{-/-}$ clones.

Mosaic eye-antennal discs derived from crosses to 452 p-element lethal FRT lines generated by UCLA Undergraduate Consortium in Functional Genomics were tested for modulating ERSIA. Twelve novel genes/gene-pairs were discovered in the screen as loss-of-function enhancers or suppressors of ERSIA (Table 1). Diminished

nuclear fallout, *sac1/CG9187*, *CG17090*, *CG30496/CG30493*, and *kinesin heavy chain* increased ERSIA and *CG8108*, *Darkener of apricot*, *CG31012*, *CG14867*, *walrus*, *heat shock protein cognate 5*, and *ken and karbie/thiolase* suppressed ERSIA. *CG8108*$^{-/-}$ clones of DTT treated discs exhibited significantly reduced caspase activity and TUNEL labeling relative to neighboring tissues (Figure 3.6: B, B'' and C, C'' arrows, D-D'' arrows and region outlined in gray). *CG8108* was the strongest ERSIA suppressor identified in the screen and was selected for further studies (Figure 3.6).

3.4 Materials and Methods

3.4.1 *Drosophila* stocks

The 452 p-element lethal FRT stocks screened for novel regulators of ERSIA were initially generated by the UCLA Undergraduate Consortium and obtained from the Kyoto Stock Center and Dr. Utpal Banerjee (Call *et al*., 2007; and Table 1). The $Xbp1^{k13803}$, $Ire1^{f02170}$, and *FRTUbiGFP* stocks were received from the Bloomington Stock center. The $drice^{17}$, $dronc^{I24}$, $dcp1^{prev1}$, $dark^{L46}$, and $dredd^{B118}$ mutant stocks were gifts from Drs. Andreas Bergmann ($drice^{17}$, $dronc^{I24}$, and $dark^{L46}$), Kimberly McCall ($dcp1^{prev1}$), and Bruno Lemaitre ($dredd^{B118}$) (Xu *et al*., 2005; Xu *et al*., 2006; Laundrie *et al*., 2003; Srivastava *et al*., 2007; Leulier *et al*., 2000). The $drice^{17}$ and $dark^{L46}$ mutant stocks were recombined onto FRTs by Cesar Mendes. The *H99* stock was recombined onto an FRT by Jose Rodriguez.

Fly stocks were maintained on standard medium and grown at 18°C, 21°C, or 25°C. Crosses for the DTT assay were maintained on blue food (see below) at 25°C and then shifted to 21°C once wandering third instar larvae began to emerge from the food.

3.4.2 DTT assay

Fly crosses for ERSIA screening were made on blue food to enable staging of larval progeny. Blue food was made by removing and melting standard fly food media from vials, thoroughly mixing in 0.05% bromophenol blue, and replacing the blue food media into the vials. Larvae with very little or no blue staining in the gut were characterized and selected as late third instar larvae (Figure 3.1). Late third instar larvae used for mosaic eye-antennal disc analysis were generated by crossing twenty to thirty *FRT40AUbiGFP*, *FRT42DUbiGFP*, *FRT80BUbiGFP*, or *FRT82BUbiGFP* virgin

females to ten to fifteen males with mutations on the corresponding FRT chromosome. Equivalent numbers of females and males were used for crosses of homozygous viable stocks such as *yw*, $dcp1^{prev1}$, and $dredd^{B118}$.

For each cross, fifteen to twenty five eye-brain complexes from late third instar larvae were dissected in room temperature S2 media and placed into a single well of a glass nine-well plate containing 400 µl S2 media. Eye-brain complex collection was limited to a maximum of two-and-a-half hours. Once the desired numbers of larvae were collected, a fresh batch of room temperature S2 + 2 mM DTT (S2 DTT) was prepared and the 400 µl of S2 media was replaced with a 250 µl of S2 DTT for experimental cultures. Eye-brain complexes were incubated in 250 µl DTT-free S2 media for mock incubations. The nine-well plate was covered with parafilm and placed in a humid chamber to prevent desiccation and the eye-brain complexes were incubated for 16-18 hours at 25^{o}C. Eye-brain complexes were used for incubations since isolated eye-antennal discs become misshapen during prolonged culture and to avoid mechanical stress of eye discs. At the end of the incubation, the S2 (S2 DTT) media was removed and the discs were fixed in 300 µl 4% paraformaldehyde (PFA, 4% paraformaldehyde in 1X PBS) for 1-2 hours at room temperature or overnight at 4^{o}C and processed for antibody staining.

3.4.3 Antibody staining

Rinses were defined as the removal and replacement of solutions from samples. Washes were defined as the removal and replacement of solutions from samples followed by rocking on an orbital shaker for a period greater than three minutes.

Eye-brain complexes, associated discs, and/or salivary glands of late third instar larvae were dissected in S2 media, incubated 16-18 hours in S2 (S2 DTT) media, and

fixed in 300 µl 4% PFA for 1-2 hours at room temperature and/or overnight at 4°C. Fixed tissues were washed for 5-15 minutes in 400 µl PBS, rinsed twice with PBTr (1X PBS + 0.3% Triton-X-100), and then blocked for one hour in 400 µl PBTrN (1X PBS + 0.3% Triton + 5% normal goat serum). Tissues were incubated in primary antibody solution diluted in PBTrN for 1-2 hours at room temperature and/or overnight at 4°C. Larval tissues were rinsed twice, washed once for 10-15 minutes in PBTr after primary antibody staining, and then incubated in secondary antibody diluted in PBTrN for two hours at room temperature. After secondary antibody incubation, tissues were rinsed twice, washed once for 10-15 minutes, fine dissected on a microscope slide to isolate desired larval tissues in PBTr, and mounted with VectaShield mounting medium containing DAPI (Vector Laboratories). Cleaved caspase 3 antibody staining was conducted using a rabbit polyclonal antibody anti-cleaved caspase 3 (Asp175) (Cell Signaling Technology) diluted 1:200. GFP antibody staining was performed using a chicken anti-GFP antibody (Aves Labs) diluted 1:500. Secondary anti-rabbit and anti-chicken antibodies were obtained from Jackson Laboratories and diluted 1:200.

Mounted larval tissues were stored at 4°C in the dark for a maximum of one week before imaging and were analyzed using a Zeiss confocal microscope.

3.4.4 TUNEL staining

Rinses were defined as the removal and replacement of solutions from samples. Washes were defined as the removal and replacement of solutions from samples followed by rocking on an orbital shaker for a period greater than three minutes. The TUNEL staining protocol of testis described in Arama and Steller was modified for its application

to imaginal discs (Arama and Steller, 2006). The ApopTag peroxidase *in situ* apoptosis detection kit (Millipore) was used to identify apoptotic cells.

Eye-brain complexes, associated discs, and salivary glands of late third instar larvae were dissected in S2 media, incubated 16-18 hours in S2 (S2 DTT) media, and fixed in 300 µl 4% PFA for 1-2 hours at room temperature and/or overnight at 4^{o}C. After fixation, the larval tissues were rinsed with 400 µl PBS. Next, the tissues were rinsed twice, and washed once for 10-15 minutes in 1X BSS (5-fold dilution of 5X BSS – 270 mM NaCl, 200 mM KCl, 37 mM $MgSO_4$, 12 mM $CaCl_2 \bullet 2H_2O$, 24 mM Tricine, 1.8% (wt/vol) Glucose and 8.5% (wt/vol) Sucrose). After the BSS wash, tissues were incubated for one hour at room temperature in 75-100 µl equilibration buffer. The equilibration buffer was replaced with 75-100 µl working strength TdT enzyme (reaction buffer + TdT enzyme, diluted 3:7) and tissues were incubated at 37^{o}C for three hours in a humid chamber placed on an orbital shaker. The TdT reaction was stopped by incubating larval tissues in 200 µl stop/wash buffer (1:34 dilution stock stop solution to dH_2O) for three hours at 37^{o}C. The stop/wash reaction was followed by two rinses, a 5-15 minute wash with 400 µl PBTw (PBS + 0.3% Tween20), and a one hour block in BTN (1X BSS + 0.3% Triton-X-100 + 5% normal goat serum). After the one hour block, tissues were incubated overnight in the dark at 4^{o}C in BTN containing Anti-Digoxigenin-Rhodamine (Roche) diluted 1:200. Tissues were rinsed twice, washed once for 10-15 minutes, fine dissected in PBTr (PBS + 0.3% Triton-X-100) and mounted in VectaShield mounting medium containing DAPI (Vector Laboratories). If additional antibody staining were desired, primary was added to the BTN Anti-Dig solution and samples were incubated overnight at 4^{o}C. Samples were rinsed and washed as described above and followed by

secondary antibody staining with fluorescent antibodies. The GFP primary antibody used was chicken anti-GFP (Aves Labs) diluted 1:200 in BTN and the secondary antibody diluted 1:200 in PBTrN was obtained from Jackson Laboratories.

Mounted larval tissues were stored at 4^{o}C in the dark for a maximum of one week before imaging and were analyzed using a Zeiss confocal microscope.

Chapter 4

CG8108 Regulates Proximal and Distal ERSIA Events

4.1 Introduction

It is well established that Ire1 senses ER stress and induces *xbp1* splicing during the UPR in flies. Once *xbp1* is spliced, it activates the transcription of the chaperone Hsc3 (BiP) to facilitate protein folding. Previous studies have demonstrated that Hsc3 upregulation during the UPR is inhibited in $xbp1^{-/-}$ tissues and that loss of Xbp1 function sensitizes cells to the deleterious effects of ER stress (Ryoo *et al*., 2007). Since antibodies for most of the *Drosophila* regulators of ER stress are currently unavailable, one commonly used tool for assessing ER stress in the fly is an *Xbp1_EGFP* reporter (Ryoo *et al*., 2007). The reporter consists of a truncated *xbp1U* coding sequence which includes the Ire1 splice site fused to *EGFP*. The EGFP tag is out-of-frame when cells are unstressed and it is pulled into frame when Ire1 splices the *Xbp1_EGFP* reporter. The reporter has been used to show ER stress is an underlying cause of neuronal degeneration in fly models of retinitis pigmentosa and Alzheimer's disease (Ryoo *et al*., 2007; Kang and Ryoo, 2009; Casas-Tinto *et al*., 2011).

In the fly, ER stress can have both protective and negative effects on cell survival. Previous research has shown that mild ER stress over prolonged periods can protect cells from exogenous secondary stresses. For example, mutations in the ER chaperone *NinaA* suppress photoreceptor cell apoptosis in animals expressing ectopic *dp53* in the eye. Additionally, S2 cells pre-treated with ER stress inducing agents were found to have decreased caspase activation when subsequently challenged with a second stress such as cyclohexamide or UV (Mendes *et al*., 2009). In contrast, extended periods of strong ER stress such as the ectopic expression of Rhodopsin 1 or amyloid-β leads to photoreceptor degeneration (Ryoo *et al*., 2007; Casas-Tinto *et al*., 2011).

In the previous chapter, the DTT assay was introduced as a means of identifying novel regulators of ER stressed induced apoptosis (ERSIA). Gross-dissected eye-brain complexes from late third instar larvae expressing *eyeless flippase* and heterozygous for a mutant-FRT allele and a wild-type GFP-marked FRT chromosome were cultured in S2 DTT to induce ER stress and subsequently stained for cleaved caspase 3 activity. Mosaic eye-antennal discs from 452 p-element lethal FRT stocks were assayed for differential caspase activation and mutant lines were classified for their effect on ERSIA (Figures 3.2, 3.6; Table 1). *CG8108* was isolated as a strong loss-of-function ERSIA suppressor and selected for further studies.

The function of *CG8108* is largely unknown and the publically available data on this gene and its protein is limited to sequence analysis or studies from genome-wide and proteome-wide screens. High throughput RNA profiling revealed *CG8108* is expressed throughout development (www.flybase.org). Sequence analysis indicated CG8108 has two C2H2 zinc-fingers and that it may be an ortholog of Ciz1 in humans (www.flybase.org). Ciz1 is a protein required for cell cycle progression and it is a component of the nuclear matrix; however, its role in ER stress has not been investigated (Coverley *et al*., 2005; Ainscough *et al*., 2007). *CG8108* was identified as a potential JAK/STAT pathway activator in an S2 cell screen using fluorescent JAK/STAT reporters. RNAi knock-down of *CG8108* in S2 cells suppressed a JAK/STAT reporter line, indicating CG8108 may activate the JAK/STAT pathway (Müller *et al*., 2005). CG8108 was recently identified as a component of the nuclear matrix in an embryo and S2 cell nuclear matrix proteome screen (Kallappagoudar *et al*., 2010). *CG8108* was isolated in an S2 screen for regulators of small RNA pathways and was scored as a gene

necessary for activation of multiple branches of the small RNA pathway (Zhou *et al*., 2008). *CG8108* was also found to be highly activated by *GAL4* in a screen for *Gal4* responsive genes (Liu and Lehmann, 2008). CG8108 was identified as an Xbp1 and Cpr92F binding protein in a yeast-two-hybrid screen to elucidate the *Drosophila* protein interaction map (Giot *et al*., 2003). Cpr92F is a component of chitin and it is necessary for cuticle formation (www.flybase.org).

The yeast-two-hybrid data indicating CG8108 physically binds to Xbp1 opened the possibility that CG8108 acts at proximal and distal events during ER stress and ERSIA. Therefore, CG8108 was tested for a role in the regulation of *xbp1* splicing using the Xbp1_EGFP reporter in imaginal discs. In addition, experiments were conducted to determine if CG8108 physically interacts with Xbp1U and/or Xbp1S in fly tissues and S2 cells. Radiation has been shown to activate members of the UPR and CG8108 was subsequently examined for cell death suppression in the paradigm of radiation-induced apoptosis. Since the CG8108 expression profile is currently limited to high-throughput RNA screening, efforts were made to generate tagged CG8108 lines to determine its protein expression pattern during development.

4.2 Results

4.2.1 Diminished CG8108 function suppresses *xbp1* splicing

During ER stress, Ire1 splices Xbp1 into a potent transcription factor which activates chaperones and ERAD components (Yoshida *et al*., 2001; Lee *et al*., 2003; Yoshida *et al*., 2003). An *xbp1* splicing reporter (*Xbp1_EGFP*) for use in the fly was generated to enable the identification of cells undergoing ER stress (Ryoo *et al*., 2007). The construct consists of truncated *xbp1U* sequence which includes the Ire1 splice site fused to *EGFP*. The reporter remains unspliced and *EGFP* is not expressed when cells are unstressed; however, *EGFP* is brought into frame and expressed during ER stress.

One prominent step during the initial activation of the UPR is the splicing of *Xbp1* by Ire1 to generate Xbp1S (Yoshida *et al*., 2001; Lee *et al*., 2003; Yoshida *et al*., 2003). Since CG8108 suppresses ERSIA and can bind to Xbp1, CG8108 was tested for its regulation of proximal events during the UPR (Figure 3.6; Giot *et al*., 2003). In order to determine if CG8108 function has an effect upon *xbp1* splicing, a *p{SuporP}CG8108* stock which carried the *xbp1_EGFP* transgene was generated. The activation of the *xbp1_EGFP* reporter was analyzed in *p{SuporP}CG8108*$^{-/-}$ clones and in whole *p{SuporP}CG8108*$^{-/-}$ tissues (Figure 4.1). The loss of *CG8108* function did not induce promiscuous *xbp1* splicing in *CG8108*$^{-/-}$ clones in mock incubated discs (Figure 4.1: A-A''). *CG8108*$^{-/-}$ clones exhibited delayed *xbp1* splicing during early stages of ER stress, but eventually, all clones displayed uniform *xbp1* splicing at later periods of ER stress (Figure 4.1: compare B-B'' to C-C''). When whole eye discs were analyzed, wild-type *xbp1_EGFP* reporter animals had substantial *xbp1* splicing after 18 hours in S2 DTT; whereas, *p{SuporP}CG8108*$^{-/-}$ discs had less *xbp1* splicing (Figure 4.1: compare D-D' to

Figure 4.1: Loss of *CG8108* function affects *xbp1_EGFP* reporter splicing

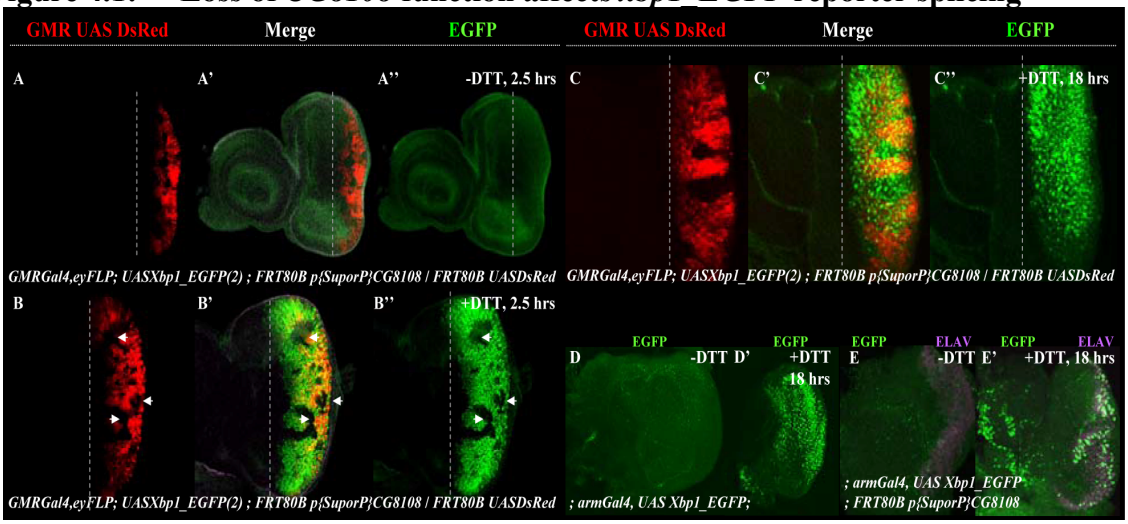

Figure 4.1: [A-E''] Late third instar eye-antennal discs from animals expressing the *xbp1_EGFP* reporter cultured in S2 (A-A'', D, E) or S2 DTT (B-B'', C-C'', D', E') for the indicated amount of time. Cells undergoing ER stress were labeled by EGFP (green). **[A-C'']** Clones were generated by *eyFLP*. Wild-type and heterozygous tissues were labeled by GMRGal4 UASDsRed, regions devoid of UASDsRed in the *GMR* region were $CG8108^{-/-}$ tissues (the *GMR* region is to the right of the gray dotted line). **[A-A'']** Loss of *CG8108* function did not activate the Xbp1 reporter in mock incubated discs. **[B-B'', C-C'']** S2 DTT incubated discs. $CG8108^{-/-}$ clones in discs incubated in S2 DTT for 2.5 hours had delayed *xbp1* splicing compared to neighboring wild-type and heterozygous tissues (B-B'', white arrows). $CG8108^{-/-}$ clones in discs DTT treated for 18 hours had *xbp1* splicing comparable to wild-type and heterozygous clones (C-C'). **[D-D'']** Discs from *armGal4;UASXbp1_EGFP* larvae. **[D]** Mock incubated disc lacks *xbp1* splicing. **[D']** 18 hour DTT treated disc has extensive *xbp1* splicing. **[E-E'']** $p\{SuporP\}CG8108^{-/-}$ discs. **[E]** S2 incubated disc did not have *xbp1* splicing. **[E'']** $CG8108^{-/-}$ disc cultured in S2 DTT for 18 hours had less *xbp1* splicing compared to wild-type reporter animals.

E-E'). CG8108 suppression of Xbp1 reporter splicing was not limited to the eye; salivary glands and imaginal discs from *p{SuporP}CG8108*$^{-/-}$ animals incubated in S2 DTT for 18 hours had reduced *xbp1* splicing, while those of wild-type animals expressing the reporter had strong nuclear Xbp1_EGFP activity (data not shown). The loss of *CG8108* function delays or suppresses Xbp1 reporter splicing in clonal or whole tissues, respectively.

The *p{SuporP}CG8108* allele of *CG8108* was generated by a *p{SuporP}* p-element insertion into the *CG8108* 5'UTR which disrupts *CG8108* function and induces pupal lethality (www.flybase.org; Figure 4.2: A; data not shown). In order to confirm the p-element disruption in *p{SuporP}CG8108* was responsible for the suppression of ERSIA and *xbp1* splicing in *CG8108*$^{-/-}$ clones, p-element mobilization was used to generate *p{SuporP}CG8108* excision lines. Precise excision events were expected to restore *CG8108* function and tissue sensitivity to ERSIA and *xbp1* reporter splicing. Putative precise excision lines were identified by PCR amplification of genomic DNA from *yw*, *p{SuporP}CG8108*$^{-/-}$, and homozygous excision line larvae using four primer pairs spanning the *CG8108* coding region. Candidate precise-excision lines had identically sized and sequenced PCR products for primer pairs several hundred bp before and after the *p{SuporP}* p-element insertion site compared to *yw* controls and for regions flanking the p-element (Figure 4.2: A; A''', A'''' lanes 1, 3, and lanes 2, 4, respectively). Precise excision lines had PCR products which were absent due to the p-element insertion in *p{SuporP}CG8108*$^{-/-}$ animals (Figure 4.2: A; A'', A'''' lanes 2, 4). Candidate lines were recombined onto FRTs and tested for reversion of *CG8108*$^{-/-}$ phenotypes. Precise excision of the p-element in *p{SuporP}CG8108* heterozygotes restored tissue sensitivity to ERSIA and *xbp1* splicing (Figure 4.2: B-B'', C-C'' and D-D'', E-E'', respectively).

Figure 4.2: Precise excision of the *p{SuporP}* p-element restores *CG8108* function

[A] Top panel, partial gene span of the region encompassing *CG8108* and the neighboring gene *CG6718*. P-element insertion sites in the *CG8108* 5'UTR and first protein coding exon are indicated (red and violet triangle glyphs). **[A'-A'''']** PCRs using four specific primers on genomic DNA prepared from *yw*, *p{SuporP}CG8108*$^{-/-}$, and the precise *p{SuporP}CG8108* excision 69 (Ex69) larvae. Animals with precise excision events had PCR products identical to *yw* animals and produced bands which are normally absent due to the *p{SuporP}* insertion in *p{SuporP}CG8108*$^{-/-}$ animals (compare A''', A'''' and A', A'', A'''' respectively). **[B-E'']** Eye-antennal discs from third instar larvae incubated in S2 DTT with *eyFLP* generated clones. **[B-C'']** Apoptotic cells were labeled by cleaved caspase 3 antibody (red). Wild-type or heterozygous clonal tissues were marked by UbiGFP (green), regions without UbiGFP expression were homozygous-mutant (B-B'') or excision clones (C-C''). **[B-B'']** *p{SuporP}CG8108*$^{-/-}$ clones have reduced cleaved caspase 3 activity during prolonged ER stress. **[C-C'']** DTT treated *p{SuporP}CG8108Ex69-14/UbiGFP* disc. Precise excision of the *p{SuporP}* p-element disrupting *CG8108* restored tissue sensitivity to ERSIA resulting in caspase activation in non-GFP clones. **[D-E'']** Eye-antennal discs from animals expressing the Xbp1 reporter. ER stressed cells were labeled by EGFP (green). Wild-type or heterozygous clonal tissues were marked by GMRUASDsRed (red), regions without GMRUASDsRed expression were homozygous-mutant (D-D'') or excision clones (E-E''). **[D-D'']** *p{SuporP}CG8108*$^{-/-}$ clones had delayed *xbp1* splicing during short periods of ER stress. **[E-E'']** DTT treated *p{SuporP}CG8108Ex69-14/UASDsRed* disc. Precise excision of the *p{SuporP}* p-element disrupting *CG8108* restored *xbp1* splicing in excision clones.

Figure 4.2: Precise excision of the *p{SuporP}* p-element restores *CG8108* function

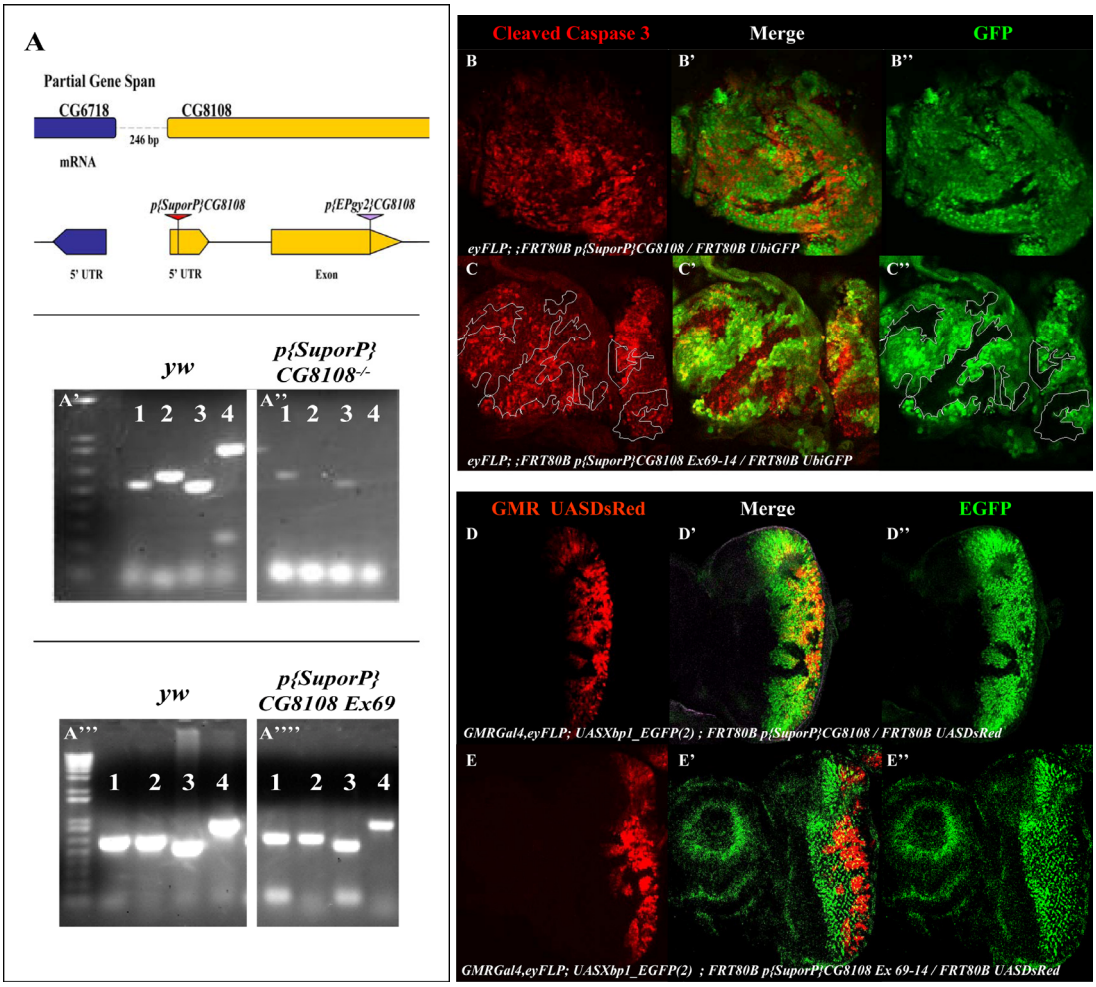

Although the precise excision of the p-element disrupting *p{SuporP}CG8108* reverted the phenotypes seen in *CG8108*$^{-/-}$ tissues, there was a concern that the *p{SuporP}* p-element disrupting *CG8108* affected the neighboring gene *CG6718* (*iPLA2-VIA*) (Figure 4.3: A). The 5'UTRs of the two genes are separated by 246bp and qRT-PCR was used to determine if the transcription of *CG8108* and *CG6718* was affected by the *p{SuporP}* p-element. A second p-element allele of *CG8108*, *p{EPgy2}CG8108* which has a *p{EPgy2}* p-element insertion into the first protein coding exon of *CG8108* was also tested for an effect on *CG6718* transcription (Figure 4.3: A). *p{SuporP}CG8108*$^{-/-}$ animals had a 42% and 27% transcriptional reduction in *CG8108* and *CG6718*, respectively. In contrast, *CG8108* transcription was exclusively reduced in *p{EPgy2}CG8108*$^{-/-}$ animals (Figure 4.3: A).

Based on the qRT-PCR data indicating the *p{SuporP}* p-element inserted in *p{SuporP}CG8108* line affected two genes, three methods were used to verify the suppression of ERSIA and *xbp1* splicing is due to reduced *CG8108* function. First, a null allele of *CG6718* was acquired, recombined onto an FRT, and tested for suppression of ERSIA and *xbp1* splicing. Second, a null allele of *CG8108* was generated by imprecise excision of the *p{EPgy2}* p-element in *p{EPgy2}CG8108* animals. Third, *CG8108* and *CG6718* genomic rescue transgenes were generated, transformed into flies, and analyzed for the ability to rescue ERSIA and lethality attributed to *CG8108*.

4.2.2 Loss of *CG6718* function cannot explain the *p{SuporP}CG8108*$^{-/-}$ phenotypes

In order to confirm the suppression of ERSIA and *xbp1* splicing obtained with the *p{SuporP}CG8108* allele was due to diminished *CG8108* function, a null allele of *CG6718* (*p{EPgy2}CG6718*) was acquired from the Bloomington Stock Center. The

Figure 4.3: Loss of *CG6718* function affects neither ERSIA nor *xbp1* splicing

[A] Partial gene span of *CG6718* and *CG8108* including the insertion sites of three p-elements used to generate the p-element and p-element excision alleles tested in this study. qRT-PCR data from *yw*, *p{SuporP}CG8108*$^{-/-}$, and *p{EPgy2}CG8108*$^{-/-}$ larval total RNA preparations is contained in the chart below the partial gene span diagram. qRT-PCR data indicated the *p{SuporP}* p-element insertion in *p{SuporP}CG8108* affected both *CG6718* and *CG8108*. In contrast, the *p{EPgy2}* p-element insertion in *p{EPgy2}CG8108* specifically affected *CG8108* (asterisk). **[B-E'']** Late third instar eye-antennal discs with *eyFLP* generated clones cultured in S2 (B-B'', D-D'') or S2 DTT (C-C'', E-E'') for the indicated amount of time. **[B-C'']** Apoptotic cells were labeled by TUNEL (red). Wild-type or heterozygous tissues were marked by UbiGFP (green), areas without UbiGFP were *CG6718*$^{-/-}$ clones. **[B-B]** S2 incubated *p{EPgy2}CG6718/UbiGFP* disc. **[C-C]** S2 DTT incubated *p{EPgy2}CG6718/UbiGFP* disc. *CG6718*$^{-/-}$ clones did not have reduced TUNEL compared to neighboring tissues. The white outlined area highlights a *CG6718*$^{-/-}$ clone with strong TUNEL activity. The turquoise outlined area encloses a *CG6718*$^{-/-}$ clone with intense TUNEL activity in one section of the clone. *CG6718* does not regulate ERSIA. **[D-E'']** Eye-antennal discs from animals expressing the *xbp1* reporter transgene. ER stressed cells were labeled with EGFP (green). Wild-type or heterozygous clonal tissues were marked by GMRUASDsRed (red), regions without GMRUASDsRed expression are homozygous-mutant clones. **[D-D'']** S2 incubated *p{EPgy2}CG6718/UASDsRed* disc. *CG6718*$^{-/-}$ clones did not splice the *xbp1_EGFP* reporter in the absence of ER stress. **[E-E'']** DTT treated *p{EPgy2}CG6718/UASDsRed* disc. *CG6718*$^{-/-}$ tissues did not delay *xbp1* splicing during short periods of ER stress.

Figure 4.3: Loss of *CG6718* function affects neither ERSIA nor *xbp1* splicing

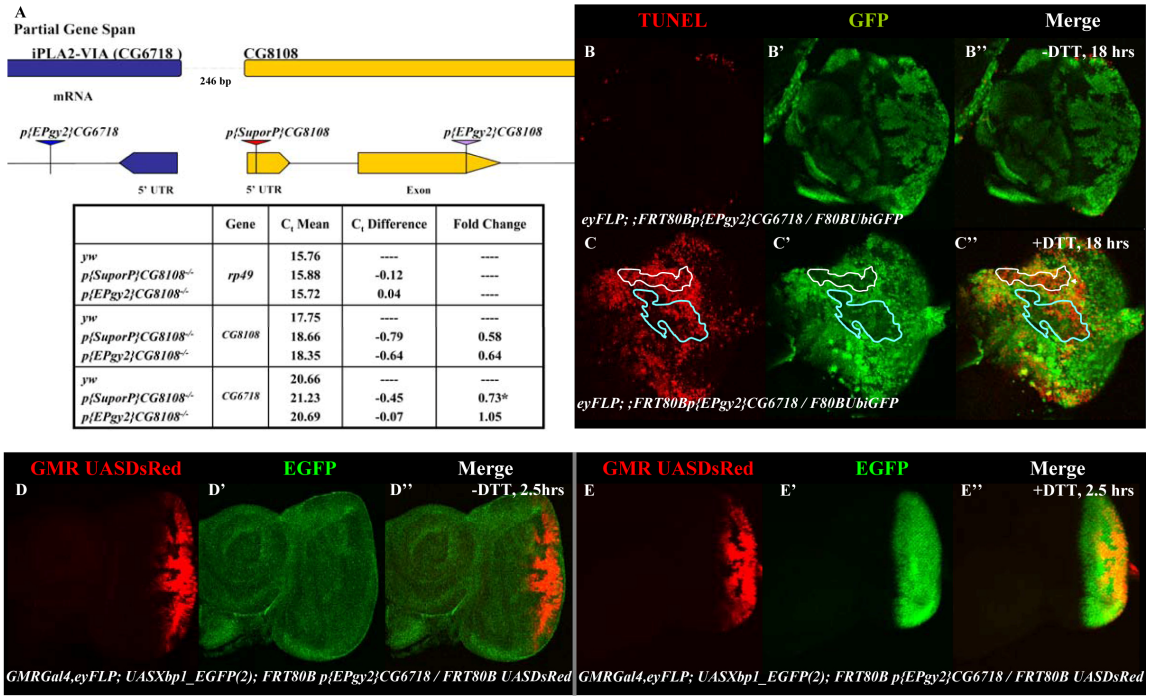

	Gene	C_t Mean	C_t Difference	Fold Change
yw	*rp49*	15.76	----	----
p{SuporP}CG8108$^{-/-}$		15.88	-0.12	----
p{EPgy2}CG8108$^{-/-}$		15.72	0.04	----
yw	*CG8108*	17.75	----	----
p{SuporP}CG8108$^{-/-}$		18.66	-0.79	0.58
p{EPgy2}CG8108$^{-/-}$		18.35	-0.64	0.64
yw	*CG6718*	20.66	----	----
p{SuporP}CG8108$^{-/-}$		21.23	-0.45	0.73*
p{EPgy2}CG8108$^{-/-}$		20.69	-0.07	1.05

p{EPgy2}CG6718 allele is an RNA null, homozygous viable, and was shown to impact cardiolipin biosynthesis in a *Drosophila* model of Barth syndrome (Xu *et al*., 2006; Malhotra *et al*., 2009). Barth syndrome is caused by mutations in the *tafazzin* (*taz*) gene which leads to dysregulated cardiolipin homeostasis. Cardiolipin is a component of the mitochondria in eukaryotes and it is necessary for mitochondrial function. $taz^{-/-}$ flies have abnormal cardiolipin production and $taz^{-/-}$ males have defects in sperm individualization which results in sterility. Loss of *CG6718* function restores fertility and increases cardiolipin levels in $taz^{-/-};CG6718^{-/-}$ animals; however, $taz^{+/+};CG6718^{-/-}$ animals have unaltered cardiolipin function (Malhotra *et al*., 2009).

The *p{EPgy2}CG6718* allele was recombined onto an FRT and multiple recombinants were tested for an effect on ERSIA and *xbp1* splicing (Figure 4.3: B-E''). Late third instar eye-antennal discs from *eyFLP*;;*CG6718/UbiGFP* animals incubated S2 media did not have TUNEL activity after prolonged culture (Figure 4.3: B-B''). S2 DTT incubation of *eyFLP*;;*CG6718/UbiGFP* discs led to increased TUNEL (Figure 4.3: C-C'', red immunofluorescence). $CG6718^{-/-}$ clones had significant TUNEL activity when incubated for 18 hours in S2 DTT (Figure 4.3: C-C'', white and turquoise outlined areas). *GMRGal4*,*eyFLP*; *UASXbp1_EGFP*; *p{EPgy2}CG6718/UASDsRed* eye-antennal discs mock incubated in S2 media did not exhibit spontaneous *xbp1* splicing (Figure 4.3: D-D''). $CG6718^{-/-}$ clones from *eyFLP*; *UASXbp1_EGFP*; *p{EPgy2}CG6718/UASDsRed* larvae did not have delayed *xbp1* splicing compared to neighboring wild-type and heterozygous tissues. The loss of *CG6718* function did not recapitulate the ER stress and cell death phenotypes seen in $p\{SuporP\}CG8108^{-/-}$ tissues. *CG8108*, not *CG6718* is necessary for efficient ERSIA and *xbp1* splicing.

4.2.3 *CG8108* deletion mutants weakly suppress ERSIA and *xbp1* splicing

Despite the data indicating the loss of *CG6718* affects neither ERSIA nor *Xbp1* splicing and that the suppression of ERSIA and *xbp1* reporter splicing is a consequence of reduced *CG8108* function in *p{SuporP}CG8108*$^{-/-}$ animals, efforts were undertaken to generate a *CG8108* null allele. qRT-PCR indicated the *p{EPgy2}* p-element inserted in the *p{EPgy2}CG8108* allele specifically affected *CG8108* transcription, making it a suitable allele for p-element excision (Figure 4.3: A). The *CG8108* gene span in Figure 4.4 shows two isoforms of *CG8108* are produced, the sequences differ in their putative 5'UTRs, but their amino acid sequences are identical (www.flybase.org).

A *CG8108*-specific allele was generated by crossing *p{EPgy2}CG8108*$^{+/-}$ males to females expressing Δ*2-3* transposase and balancing candidate excision-event males. Genomic DNA was prepared from *yw*, *p{EPgy2}CG8108*$^{-/-}$, and homozygous-excision candidate larvae for PCR and sequencing analysis. Primers specific for regions spanning the *CG8108* and *CG6718* 5'UTRs (primer 1), the region flanking the *p{EPgy2}* p-element (primer 2), and the *CG8108* 3'UTR (primer 3) were used to identify lines with the desired excision event (Figure 4.4: B, compare lane 2 PCR products from *yw* and *CG8108Ex32*$^{-/-}$ larvae). One imprecise excision line was obtained *CG8108Ex32* (Figure 4.4). The *CG8108Ex32* line was initially identified by the failure to amplify a PCR product with *CG8108Ex32* genomic DNA using primer 2. To ensure the missing primer 2 PCR product from *CG8108Ex32*$^{-/-}$ animals was not due to incomplete excision of the *p{EPgy2}* p-element, *yw* and *CG8108Ex32*$^{-/-}$ genomic DNA was amplified with the same 5' primer and unique 3' primers spaced 500bp apart from each other and the PCR products were checked by electrophoresis to identify the 3' end of excision event (data

Figure 4.4: *CG8108Ex32*$^{-/-}$ clones weakly suppress ERSIA and *xbp1* splicing

[A] Gene span of *CG8108*. The elongated triangle glyph indicates the *p{EPgy2}* p-element insertion site in *p{EPgy2}CG8108*. The red, highlighted region marks span of the *CG8108Ex32* deletion. The olive-green shaded area covers the region which would yield an altered *CG8108* sequence if *CG8108Ex32*$^{-/-}$ RNA were produced. **[B]** PCRs from genomic DNA prepared from *yw* and *CG8108Ex32*$^{-/-}$ animals. *CG8108Ex32*$^{-/-}$ animals have a deletion which prevents the amplification of the region flanking the former *p{EPgy2}* insertion site (lane 2). Primer 1 amplifies the 5'UTRs of *CG6718* and *CG8108* and primer 3 amplifies the *CG8108* 3'UTR. **[C]** Gel of cDNA produced from RT-PCR reactions using primers for the *CG8108* ORF from *yw* (lane 1) and *CG8108Ex32*$^{-/-}$ (lane 2) total RNA. RNA from *CG8108Ex32*$^{-/-}$ animals is not amplified with *CG8108* ORF primers (lane 2), whereas *CG8108* cDNA is readily amplified from *yw* RNA (lane 1, white arrow). The turquoise arrows point to non-specific products. **[D-E'''']** DTT treated eye-antennal discs with *eyFLP* generated clones. Apoptotic cells are labeled by TUNEL (red). Wild-type or heterozygous tissues are marked by UbiGFP (green). **[D-D''']** *p{SuporP}CG8108*/*UbiGFP* disc incubated in S2 DTT has suppressed ERSIA in *CG8108*$^{-/-}$ clones (D''', see inset). **[E-E''']** DTT treated *CG8108Ex32*/*UbiGFP* disc. *CG8108Ex32*$^{-/-}$ clones are small and do not clearly suppress ERSIA (E''', see inset). **[F-G''']** Eye-antennal discs from animals expressing the Xbp1 reporter gene. ER stressed cells are labeled by EGFP (green). Wild-type or heterozygous clonal tissues are marked by GMRUASDsRed (red). **[F-F''']** DTT treated *p{SuporP}CG8108*/*UASDsRed* disc with delayed *xbp1* splicing in *CG8108*$^{-/-}$ clones. **[G-G''']** *CG8108Ex32*/*UASDsRed* disc treated with S2 DTT. *CG8108Ex32*$^{-/-}$ clones have weakly suppressed *xbp1* splicing.

Figure 4.4: ***CG8108Ex32*$^{-/-}$ clones weakly suppress ERSIA and *xbp1* splicing**

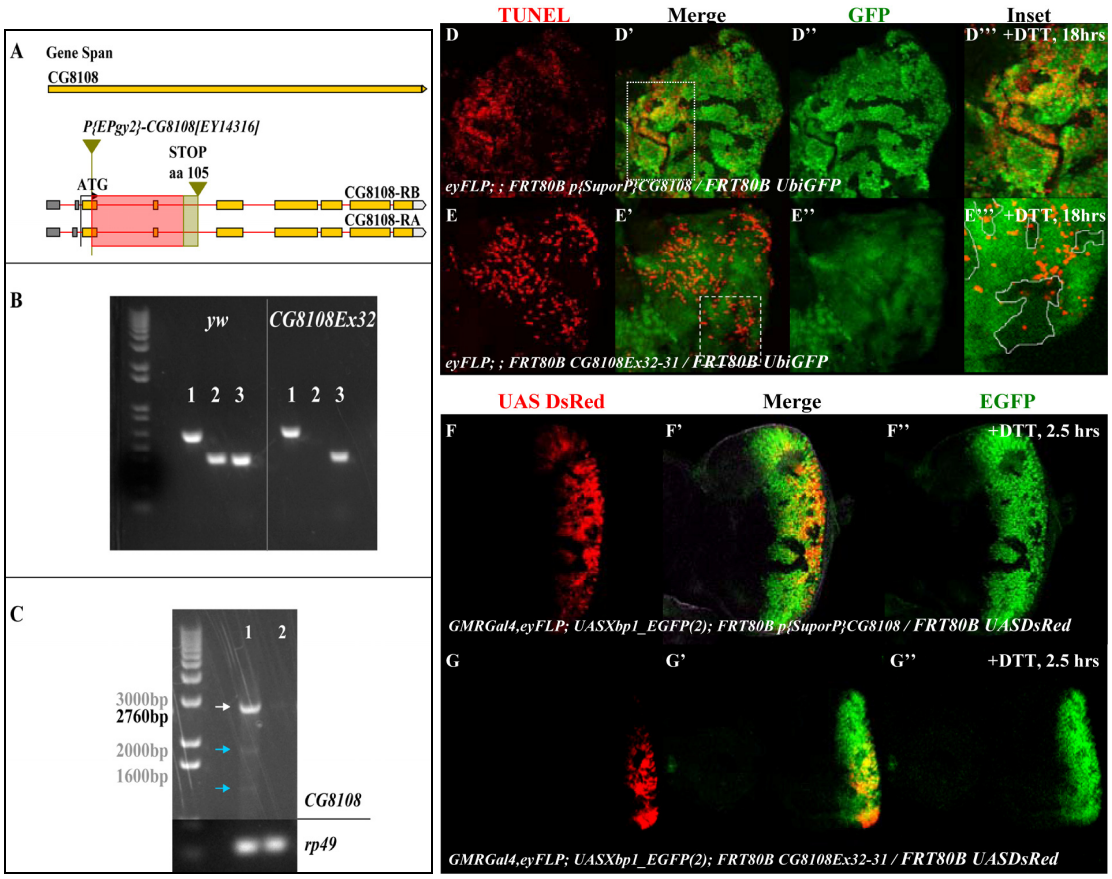

not shown).

The p-element excision event that generated the *CG8108Ex32* allele removed the last 77 bases of the first protein coding exon and 1.2kbp of *CG8108* which included the entire second protein coding exon (Figure 4.4: A, red area highlights deletion). Total RNA was isolated from *yw* and *CG8108Ex32*$^{-/-}$ larvae and RT-PCR was used to amplify the *CG8108* ORF (ATG to TGA). The expected size of *CG8108* is 2670bp and *yw* larvae generate a band corresponding to that size (Figure 4.4: C, lane 1 white arrows, the turquoise arrows point to non-specific products). In contrast, numerous preparations of *CG8108Ex32*$^{-/-}$ RNA did not yield a cDNA product (Figure 4.4: C, lane 2). It was possible that *CG8108* RNA was produced in *CG8108Ex32*$^{-/-}$ animals, but it was rapidly degraded. Sequencing of genomic DNA indicated a premature stop at amino acid 105 would be produced if the *CG8108* reading frame were maintained and *CG8108* RNA were produced in *CG8108Ex32*$^{-/-}$ animals (Figure 4.4: A, olive-green shaded region). Based on the RT-PCR and sequencing information gleaned from *CG8108Ex32*$^{-/-}$ RNA and DNA preparations, *CG8108Ex32* was classified as a strong loss-of-function and potentially null, *CG8108*-specific allele.

FRT80BCG8108Ex32 lines were generated by female recombination and four recombinants were tested for effects on ERSIA and *xbp1* splicing. *CG8108Ex32*$^{-/-}$ clones were very small and rarely survived the DTT assay limiting definitive conclusions regarding *CG8108* regulation of ERSIA (Figure 4.4: E-E'''). Homozygous *p{SuporP}CG8108* clones were small, but they could survive the DTT assay (Figure 4.4: D-D'''). *CG8108Ex32*$^{-/-}$ clones were subsequently assayed for their ability to delay *xbp1* splicing and *CG8108Ex32*$^{-/-}$ tissues occasionally showed evidence of hindered *xbp1*

reporter splicing during short incubations in S2 DTT (Figure 4.4: G-G''). *xbp1* reporter splicing suppression in *CG8108Ex32*$^{-/-}$ clones is detectable, but it pales in comparison to that of homozygous *p{SuporP}CG8108*$^{-/-}$ tissues (Figure 4.4: contrast the strong *xbp1* splicing delay in *p{SuporP}CG8108*$^{-/-}$ clones in F-F'' to *CG8108Ex32*$^{-/-}$ clones in G-G''). However, there were occasions when *CG8108Ex32-31*$^{-/-}$ clones exhibited increased *xbp1_EGFP* splicing compared to neighboring tissues after culture in S2 DTT (data not shown). *CG8108Ex32* is a strong hypomorph and it is likely a null allele. *CG8108* is a necessary gene and its requirement for viability hindered the analysis of ERSIA and *xbp1* splicing suppression in *CG8108Ex32*$^{-/-}$ tissues.

4.2.4 *CG8108* genomic rescue transgenes restore *CG8108* function

The *p{SuporP}CG8108* allele is a moderate hypomorph; *p{SuporP}CG8108*$^{-/-}$ third instar larvae developed melanotic tumors in the gut and the animals died during pupation. The strong hypomorphic and potentially null *CG8108Ex32* allele had increased mortality and *CG8108Ex32*$^{-/-}$ animals died during the late-first, early-second larval instars. Due to the *p{SuporP}* insertion affecting two genes and the increased mortality in *CG8108Ex32*$^{-/-}$ animals, genomic rescue transgenes were made for *CG6718* and *CG8108* (Figure 4.5: A-C). The genomic region for *CG8108* and *CG6718* is drawn to scale, it includes the various isoforms of their respective mRNAs, and the regions covered by the genomic rescue transgenes are outlined in Figure 4.5: A, B, C, respectively. The 5'UTRs are represented by dark gray boxes, introns are red lines, protein coding sequences are shaded rectangles (blue for *CG6718* and orange for *CG8108*), and the 3'UTRs are light gray pentagons (Figure 4.5: A). The black arrows in Figure 4.5: A show the direction of translation and the black arrows in Figure 4.5: B, C indicates the direction of transcription

Figure 4.5: *CG8108* genomic rescue transgenes restore tissue sensitivity to ERSIA

[A] Graphic representation of the *CG6718* and *CG8108* gene span. The isoforms of *CG6718* and *CG8108* are indicated. 5'UTRs are dark gray rectangles, 3'UTRs are light gray pentagons, protein coding sequences are blue (*CG6718*) or orange (*CG8108*) rectangles, and introns are depicted as red lines. The direction of translation is indicated by arrows underneath the respective "ATG". **[B]** Schematic for the *CG8108* genomic rescue construct: the black arrow indicates the direction of transcription, the dotted orange line corresponds to the putative *CG8108* promoter, the solid line encompasses the complete genomic region (introns/exons), and the gray dotted line corresponds to the 3' UTR and its 1kb extension. 1kb past the 3'UTR was included in the genomic rescue constructs to ensure the presence of transcriptional stop elements. **[C]** Schematic for the *CG6718* genomic rescue construct: the black arrow indicates the direction of transcription, the dotted blue line corresponds to the putative *CG6718* promoter, the solid line encompasses the complete genomic region (introns/exons), and the gray dotted line corresponds to the 3' UTR and its 1kb extension. **[D-E'''']** DTT treated eye-antennal discs with *eyFLP* generated clones. Apoptotic cells were labeled by TUNEL (red). Wild-type or heterozygous tissues were marked by GFP (green). **[D-D'''']** S2 DTT incubated *CG8108Ex32-31*/*UbiGFP* disc. *CG8108Ex32-31*$^{-/-}$ clones barely survive the DTT assay and did not clearly exhibit ERSIA suppression (inset). **[E-E'''']** S2 DTT incubated *CG8108* genomic rescue 1+2*; CG8108Ex32-31*/*UbiGFP* disc. *CG8108Ex32-31*$^{-/-}$ clones were prominent and exhibited ERSIA in animals carrying the genomic rescue construct (inset). Genomic rescue of *CG8108Ex32-31*$^{-/-}$ clones shows *CG8108* is necessary for cell viability and that the loss of *CG8108* function caused reduced clone size.

Figure 4.5: ***CG8108*** **genomic rescue transgenes restore tissue sensitivity to ERSIA**

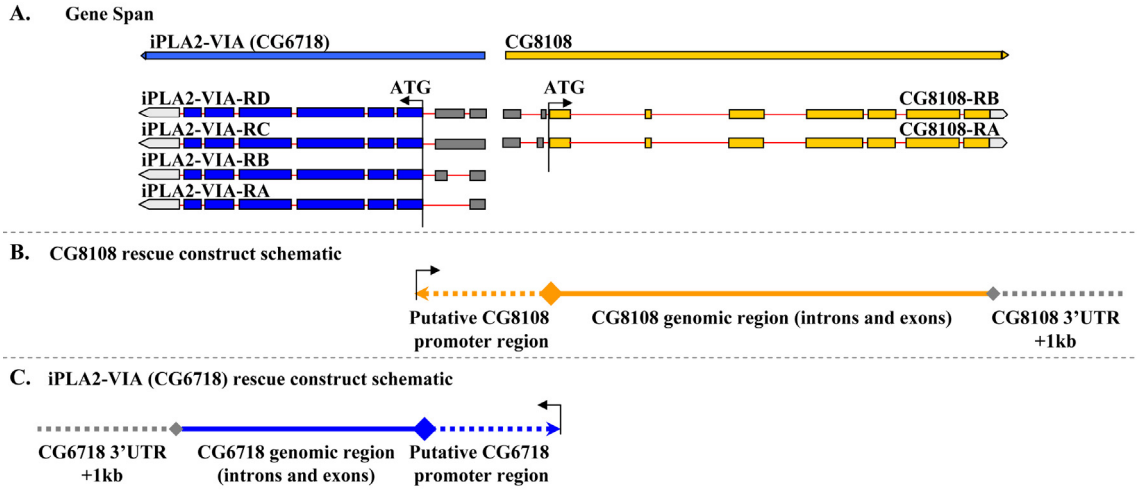

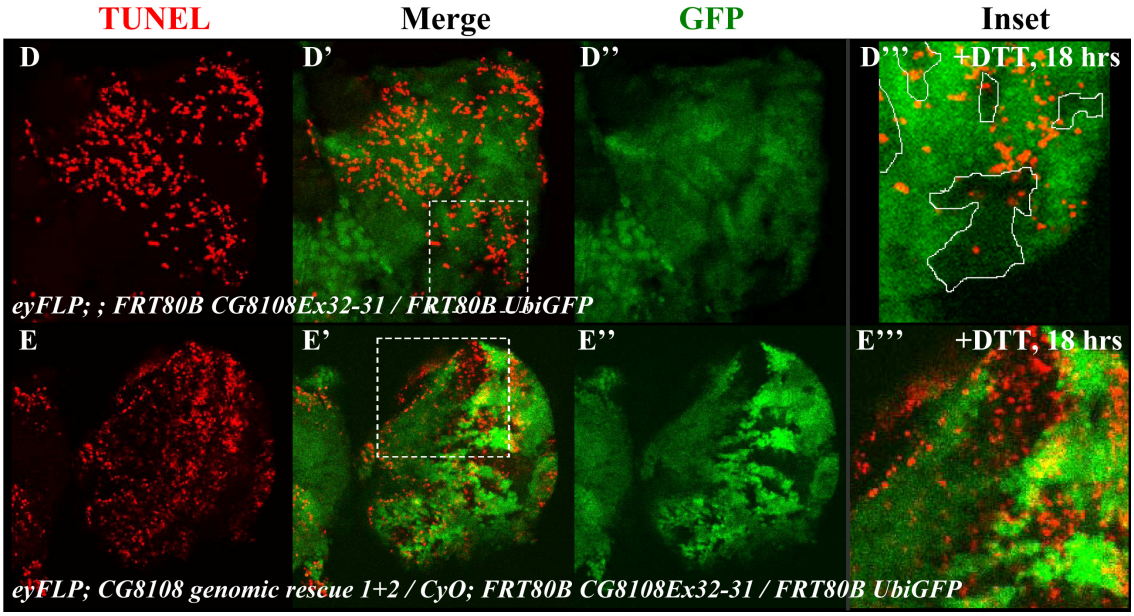

for the genomic rescue lines. The *CG8108* genomic rescue transgene encompassed the putative *CG8108* promoter region (the region from the *CG6718* ATG and the sequences inclusive of the *CG6718* and *CG8108* 5'UTRs), the entire *CG8108* genomic sequence (introns/exons) and 1kb past the predicted 3'UTR (Figure 4.5: A-B). The *CG6718* genomic transgene spanned from the putative *CG6718* promoter (the sequences from the *CG8108* ATG and the entire region including and between the *CG8108* and *CG6718* 5'UTRs), the complete *CG6718* genomic sequence (introns/exons) and 1kb past the predicted 3'UTR (Figure 4.5: A, C).

One *CG6718* and two independent *CG8108* genomic rescue transformant lines on the second chromosome were obtained and crossed to the *CG8108* alleles. The *CG6718* genomic rescue transgene failed to revert the lethality seen with the *p{SuporP}CG8108* line indicating *CG8108* deficiency was the cause of the pupal lethality seen in this line (Table 2). One copy of each of the *CG8108* genomic rescue transgenes reversed the lethality of the *p{SuporP}CG8108* line. Single copies of the individual *CG8108* rescue lines failed to rescue the lethality of *p{EPgy2}CG8108*$^{-/-}$ animals, the parental *CG8108Ex32* line, and two *FRT80BCG8108Ex32* lines (*Ex32-14*, *Ex32-28*) (Table 2). The *p{EPgy2}CG8108* stock is the progenitor of the *CG8108Ex32* excision line, raising the possibility the genomic rescue lines were missing elements necessary for *CG8108* function in strong *CG8108* alleles or a second-site mutation was on the FRT80B arm of *p{EPgy2}CG8108* derivatives. The two *CG8108* rescue lines were recombined to generate an animal that would have either two or four copies the *CG8108* transgene in an attempt to revert the lethality of *p{EPgy2}CG8108* derivatives. Since four copies of the *CG8108* rescue gene did not revert *p{EPgy2}CG8108* or *CG8108Ex32-*

Table 2: *CG8108* rescue transgenes rescue *CG8108* alleles to varying degrees

	Stage of lethality	Degree and stage of genomic transgene rescue			
***CG8108* alleles**	**No Transgene**	***CG8108* Transgene 1**	***CG8108* Transgene 2**	***CG8108* Transgenes 1+2[a]**	***CG6718* Transgene 1**
p{SuporP}CG8108$^{-/-}$	Third instar	Full rescue Adults eclose	Full rescue Adults eclose	Full rescue Adults eclose	No
p{EPgy2}CG8108$^{-/-}$	Late first, early second instar	Partial rescue Rare third instar	Partial rescue Rare third instar	Partial rescue Rare third instar	Not tested
CG8108Ex32$^{-/-}$ (not on an FRT)	Late first, early second instar	Not tested	Not tested	Partial rescue Third instar/pupae	Not tested
CG8108Ex32-14$^{-/-}$, *CG8108Ex32-28*$^{-/-}$	Late first, early second instar	Partial rescue Rare third instar	Partial rescue Rare third instar	Partial rescue Third instar/pupae	Not tested
CG8108Ex32-17$^{-/-}$	Late first, early second instar	Full rescue Adults eclose	Full rescue Adults eclose	Full rescue-adults eclose Pupal lethal (Mi55)[b]	Not tested
CG8108Ex32-31$^{-/-}$	Late first, early second instar	Full rescue Adults eclose	Full rescue Adults eclose	Full rescue Adults eclose (Mi55)[b]	Not tested

The *CG8108* and *CG6718* genomic rescue transgenes were tested for the ability to rescue the lethality associated with *CG8108* alleles generated by p-element insertion or p-element excision. One independent *CG6718* genomic rescue transgene stock and two *CG8108* genomic rescue lines were obtained by p-element transformation. Homologous recombination in females was used to generate flies simultaneously expressing both of the *CG8108* genomic rescue transgenes [a]. Full rescue was defined as the generation of viable and fertile adults with at least one copy of a genomic rescue transgene in a *CG8108*$^{-/-}$ background. Partial rescue was defined as extended viability for an allele without the production of viable adults in a *CG8108*$^{-/-}$ background. The first column indicates the genotype of the *CG8108* allele tested, the second column details the stage of lethality for each line and the subsequent columns show the degree and stage of rescue with the indicated rescue transgenes. *eyFLP;;FRT80BMi55UbiGFP* females crossed to *CG8108Ex32-17* and *CG8108Ex32-31* males expressing *CG8108* transgenes 1+2 were tested for their viability [b]. The *CG8108Ex32-31* stock is rescued by all *CG8108* rescue transgene conditions indicating it is least likely to have a second-site mutation which could obscure analysis of its function and that it can be used for future experimentation.

14(28) lethality, additional *CG8108Ex32* FRT lines were tested. The *CG8108Ex32-17 (31)* lines were rescued with one copy of the *CG8108* genomic transgene demonstrating the Bloomington Stock Center *p{EPgy2}CG8108* allele has a lethal second-site mutation on the FRT80B chromosome arm. Given that the second-site mutation affected viability and that *eyFLP* has leaky expression in non-eye-antennal tissues, *eyFLP*;;*FRT80B Mi55UbiGFP* females were mated to *CG8108Ex32-17*(*31*) males. It was hypothesized that animals with residual defects in the second-site mutation would fail to eclose in a *Minute* background even if they express *CG8108* rescue transgenes. *eyFLP*; *CG8108* genomic rescue 1+2*; FRT80BMi55UbiGFP/FRT80BCG8108Ex32-17* animals died as pupae and *eyFLP*; *CG8108* genomic rescue 1+2*; FRT80BCG8108Ex32-31/FRT80BMi55 UbiGFP* animals eclosed into fertile flies (Table 2). The *CG8108* genomic rescue results indicated the *CG8108Ex32-31* allele was least likely to have a deleterious second-site mutation and that it was the best line to use for loss-of-function analysis. Two copies of the *CG8108* genomic rescue construct restored clone size and tissue sensitivity to ERSIA in *CG8108Ex32-31*$^{-/-}$ tissues and it reversed the lethality seen in *CG8108Ex32-31*$^{-/-}$ animals (Figure 4.5: contrast D-D''' to E-E'''; Table 2). Genomic rescue of *xbp1* splicing in *CG8108Ex32-31*$^{-/-}$ tissues was not conducted due to the inability to generate stocks with the necessary genotypes.

4.2.5 CG8108 physically interacts with Xbp1 *in vitro* and *in vivo*

Based on the yeast-two-hybrid data which revealed *CG8108* physically interacts with Xbp1 and the delay of *xbp1* reporter splicing in *p{SuporP}CG8108*$^{-/-}$ and *CG8108Ex32-31*$^{-/-}$ clones, CG8108 was tested for its physical association with Xbp1 (Giot *et al*., 2003; Figure 4.4). FLAG tagged *UASCG8108* and HA tagged *UASXbp1U*

and *UASXbp1S* constructs were cloned and expressed in S2R$^+$ cells using the *actinGAL4* driver. S2R$^+$ cells were either mock transfected or transfected with equal amounts of plasmid: *UASCG8108_FLAG*, *UASCG8108_FLAG* + *UASXbp1S_HA*, *UASCG8108_FLAG* + *UASXbp1U_HA*, *UASXbp1U_HA*, *UASXbp1S_HA*, and lysates from the transfections were immunoprecipitated with CG8108 antibody and blotted for CG8108, FLAG, and/or HA (Figure 4.6). The CG8108 antibody immunoprecipitated both endogenous CG8108 and ectopic CG8108_FLAG (Figure 4.6: A, lanes 7-12, WB CG8108; lanes 8, 11-12, WB FLAG; 4.6: B, lanes 6-10, WB CG8108; lanes 7, 9-10 WB FLAG). IPs to detect the physical association between endogenous Xbp1 and CG8108 were not conducted due to the lack of Xbp1 antibodies. Both endogenous and ectopic CG8108 co-immunoprecipitated ectopically expressed UASXbp1U_HA and UASXbp1S_HA in S2R$^+$ cells (Figure 4.6: A, lanes 9-12, WB HA, bottom bands; 4.6: B, lanes 8-10, WB HA).

The *UASCG8108_FLAG* and *UASXbp1U_HA* constructs were introduced into flies and used to generate *GMRGal4*,*UASCG8108_FLAG*, *GMRGal4;;UASXbp1U_HA*, and *GMRGal4*,*UASCG8108_FLAG;UASXbp1U_HA* transformed stocks. Lysates from fly heads of the aforementioned lines were immunoprecipitated with CG8108 antibody and analyzed by western blot for CG8108 and HA. The CG8108 antibody failed to detect and immunoprecipitate endogenous CG8108 (Figure 4.6: C, lanes 1-2, 4-5, WB CG8108). However, the CG8108 antibody detected and immunoprecipitated ectopically expressed CG8108 (Figure 4.6: C, lanes 3, 6, WB CG8108). Ectopically expressed CG8108 and Xbp1U_HA physically associated *in vivo* when the proteins were produced under the control of the eye-specific *GMRGal4* driver (Figure 4.6: C, lane 6, WB HA).

Figure 4.6: CG8108 physically interacts with Xbp1

[A-B] CG8108 physically associated with Xbp1U and Xbp1S *in vitro*. **[A]** Endogenous and ectopic CG8108 physically interacted with Xbp1U in $S2R^+$ cells. Lanes 1-6, input fraction of S2 cell lysates used in a CG8108 and Xbp1U (co)-IP. Lanes 7-12, IP fraction of $S2R^+$ cell lysates immunoprecipitated with anti-CG8108 antibody. The constructs transfected into $S2R^+$ cells are listed and marked by a "+" sign. Endogenous and ectopic CG8108 was immunoprecipitated by the CG8108 antibody in S2 cells (lanes 7-12, WB CG8108; lanes 8, 11-12, WB FLAG). Endogenous and ectopic CG8108 physically interacted with UASXbp1U_HA (lanes 9-10 and 11-12, respectively, WB HA). **[B]** Endogenous and ectopic CG8108 immunoprecipitated Xbp1S in $S2R^+$ cells. Lanes 1-5, input fraction of $S2R^+$ cell lysates used in a CG8108 and Xbp1S (co)-IP. Lanes 6-10, IP fraction of $S2R^+$ cell lysates immunoprecipitated with anti-CG8108 antibody. The constructs transfected into $S2R^+$ cells are marked by a "+" sign. Endogenous and ectopic CG8108 physically interacts with UASXbp1S_HA (lane 8 and lanes 9-10, respectively, WB HA). **[C]** CG8108 interacted with Xbp1U *in vivo*. Lanes 1-3, input fraction of fly-head lysates. Lanes 4-6, IP fraction of fly-head lysates immunoprecipitated with CG8108 antibody. The transgenes expressed by the flies used to generate the input and IP lysates are marked by a "+" sign. Arrows point to the relevant western blot bands. Endogenous CG8108 was neither detected in nor immunoprecipitated from fly-head lysates with the CG8108 antibody (lanes 1-2 and 4-5, respectively, WB CG8108). Ectopic CG8108 was detected in and immunoprecipitated from fly-head lysates with the CG8108 antibody (lanes 3 and 6, WB CG8108). CG8108 physically associated with Xbp1U *in vivo* when both proteins are co-expressed in the fly eye using *GMRGal4* (lane 6, WB HA).

Figure 4.6: CG8108 physically interacts with Xbp1

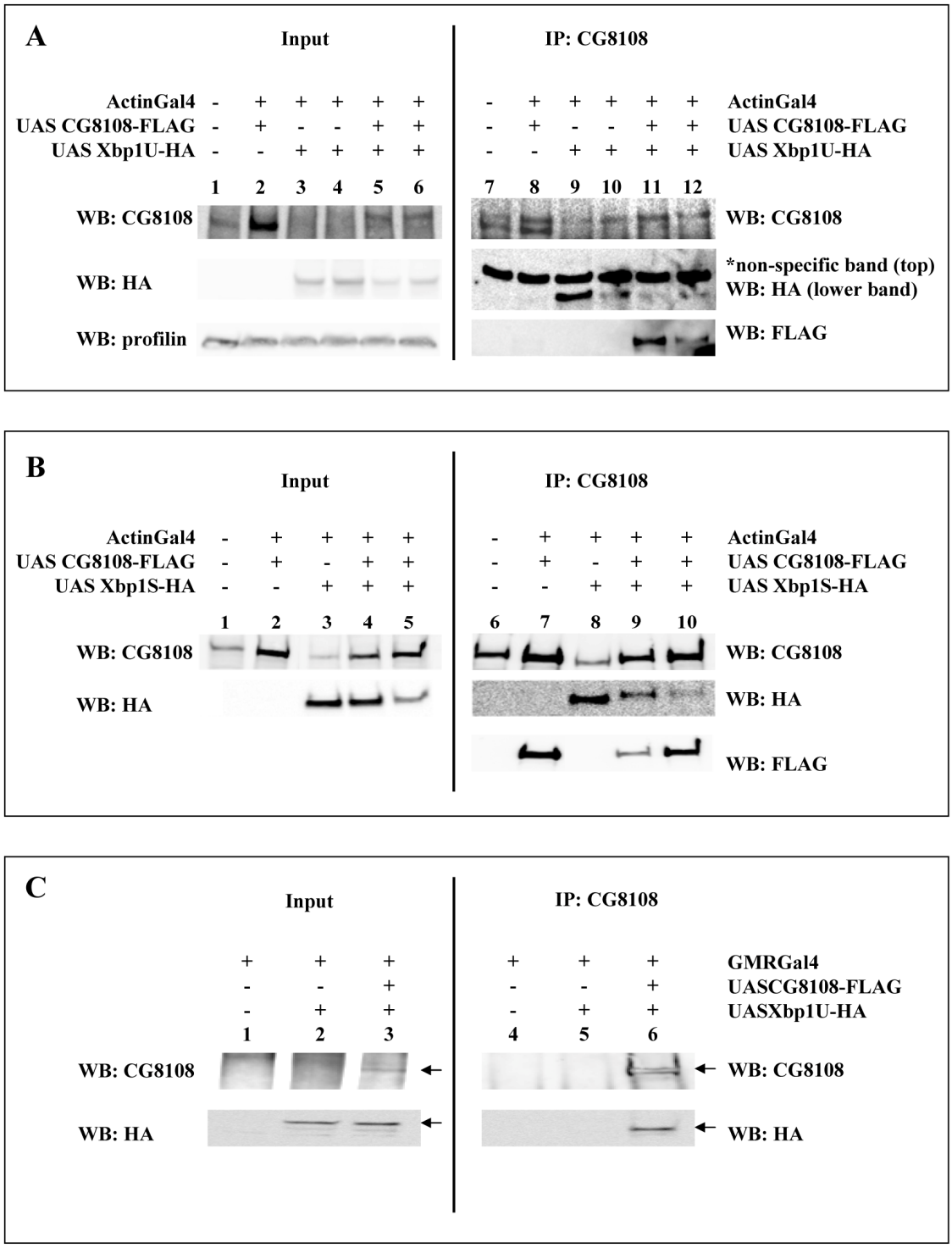

4.2.6 *CG8108* is necessary for X-ray induced cell death

In addition to chemicals such as DTT, ER stress can be induced by UV and ionizing radiation. UVB radiation upregulates CHOP expression in murine and human skin cells and ionizing radiation activates PERK signaling and *XBP1* splicing in rat intestinal epithelial cells (Anand *et al*., 2005; Zhang *et al*., 2010). Cells exposed to ionizing radiation can incur DNA damage that is potentially deleterious to cellular function. In order to prevent the propagation of renegade cells, the apoptotic program is activated in severely damaged cells (White *et al*., 1994; Zhou and Steller, 2003).

Since *CG8108* has an effect on the ER stress and cell death pathways, *CG8108* regulation of radiation-induced cell death was investigated using the *p{SuporP}CG8108* and *CG8108Ex32-31* lines (data not shown; Figure 4.7). Larvae were exposed to 0Gy or 40Gy of X-rays, allowed to recover for four hours, and discs were stained for cleaved caspase 3. X-rays induce cell death in two distinct bands corresponding to the rapidly dividing cells of the eye-antennal disc (Figure 4.7: B, C, E, F, white brackets). *CG8108Ex32-31*$^{-/-}$ clones have no or significantly reduced cleaved caspase 3 activity compared to neighboring wild-type and heterozygous tissues after irradiation (Figure 4.7: B-C'', white, turquoise arrows). The suppression of cell death seen in *CG8108Ex32-31*$^{-/-}$ clones was due to the mutation in *CG8108*. *CG8108Ex32-31*$^{-/-}$ tissues become responsive to X-rays when CG8108 expression was restored with one or two copies of the genomic rescue transgene (data not shown; Figure 4.7: E-E'', F-F''). *p{SuporP}CG8108*$^{-/-}$ tissues are resistant to X-irradiation and they become receptive to X-rays by precise excision of the *p{SuporP}* p-element or by the expression of *CG8108* genomic rescue transgenes (data not shown). The short duration needed to produce X-ray induced apoptosis enabled

Figure 4.7: ***CG8108Ex32-31$^{-/-}$*** **tissues have suppressed X-ray induced cell death**

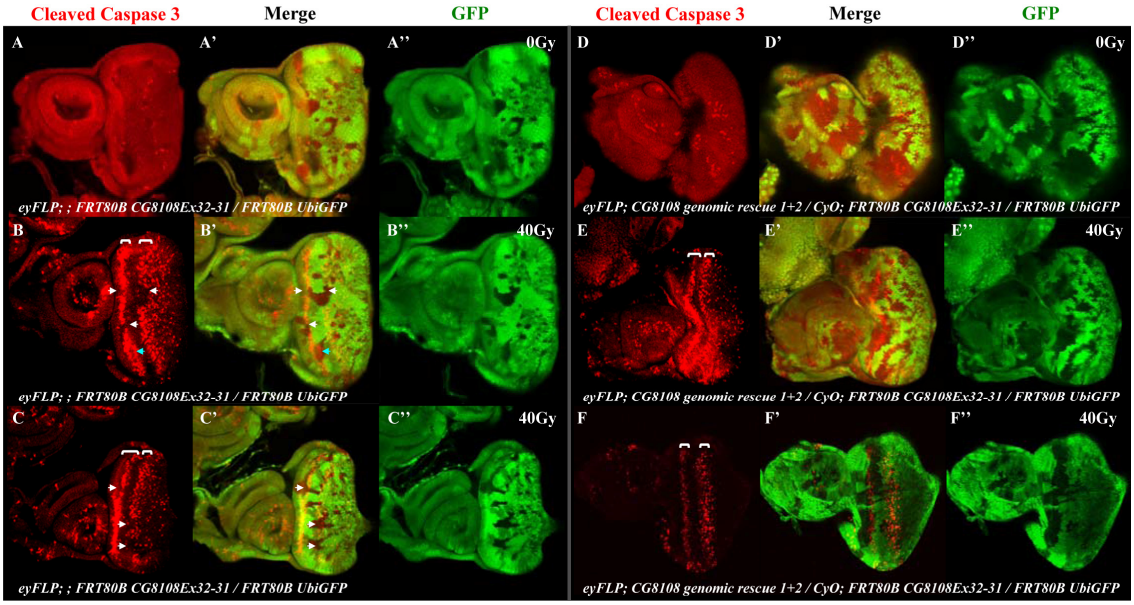

Figure 4.7: [A-F] *CG8108* was required for X-ray induced caspase activation. **[A-F]** Third instar eye-imaginal discs with *eyFLP* generated clones from larvae exposed to 0Gy (A-A'', D-D'') or 40Gy (B-C'', E-F'') X-ray radiation and allowed to recover for 4 hours. Apoptotic cells were labeled by cleaved caspase 3 (red). Wild-type and heterozygous cells were marked by UbiGFP (green). Homozygous-mutant tissues lack UbiGFP expression. White brackets point to stripes of dying X-ray responsive cells. **[A-A'']** Non-irradiated *CG8108Ex32-31*/*UbiGFP* disc had minute caspase activation. **[B-C'']** X-rayed *CG8108Ex32-31*/*UbiGFP* discs. *CG8108Ex32-31$^{-/-}$* clones had no (white arrows) or reduced (turquoise arrows) caspase activation after irradiation compared to wild-type and heterozygous tissues. **[D-D'']** *CG8108* genomic rescue 1+2; *CG8108Ex32-31*/*UbiGFP* disc displayed little caspase activity after mock irradiation. **[E-F'']** *CG8108* genomic rescue 1+2; *CG8108Ex32-31*/*UbiGFP* discs exposed to 40Gy X-ray radiation had significant caspase activation in all clonal genotypes. Two copies of the *CG8108* genomic rescue transgene restored *CG8108Ex32-31$^{-/-}$* tissue sensitivity to X-rays.

the use of the *CG8108Ex32-31* line for testing whether *CG8108* expression was necessary for X-ray induced cell death. In contrast to the results obtained with the *CG8108Ex32-31* allele using the DTT assay, *CG8108Ex32-31*$^{-/-}$ clones clearly exhibited reduced caspase activation after X-ray irradiation (compare Figures 4.4: E-E''' and 4.7: B-C''). *CG8108* is required for stress-induced cell deaths caused by ER stress and X-ray radiation.

rpr, *hid*, and *sickle* are upregulated in an age-dependent manner in irradiated embryos (White *et al*., 1994; Zhou *et al*., 2003; Zhang *et al*., 2008). Stage 9-11 embryos (4-7 AEL) are vastly sensitive to ionizing radiation and stage 13-17 embryos (9-17 AEL) are highly resistant to radiation exposure (Zhang *et al*., 2008). Since *CG8108* suppressed X-ray induced cell death in eye-antennal discs, the requirement for *CG8108* to elicit cell death was tested in *CG8108Ex32-31*$^{-/-}$ embryos. qRT-PCR was conducted on RNA prepared from *yw* and *CG8108Ex32-31*$^{-/-}$ embryos, exposed to 0Gy or 40Gy of X-ray radiation at 6-9 AEL (hours after egg laying) and allowed to recover for 2 hours. *CG8108Ex32-31*$^{-/-}$ and *yw* embryos upregulated *rpr* and *hid* upon X-irradiation, but the transcription of *rpr* and *hid* was slightly more elevated in *yw* animals (Table 3). *CG8108* mRNA was detected and translated in unfertilized and 0-2 hour embryos and it may be maternally deposited into embryos (Figure 4.8: G, upper RT-PCR; www.flybase.org; data not shown). The maternal contribution of *CG8108* may account for the mild suppression of *rpr* and *hid* transcription in *CG8108Ex32-31*$^{-/-}$ embryos after irradiation. *CG8108* expression affects *rpr* and *hid* transcription and it is necessary for caspase activation and radiation-induced cell death in embryonic and larval tissues (Figure 4.7; Table 3).

Table 3: *CG8108Ex32-31*$^{-/-}$ embryos suppress X-ray induced *rpr* and *hid*

Gene	Genotype	Fold Change			p-value
		Exp. 1	Exp. 2	Exp. 3	
rpr	*yw*	2.67	3.39	2.55	0.048754
	CG8108Ex32-31$^{-/-}$	2.30	2.27	1.92	
hid	*yw*	2.23	2.57	2.27	0.056007
	CG8108Ex32-31$^{-/-}$	1.17	2.04	1.85	

qRT-PCR was conducted on total RNA prepared from 6-9 hour old *yw* and *CG8108Ex32-31*$^{-/-}$ embryos exposed to 0Gy or 40Gy X-ray radiation and allowed to recover at 21^{o}C-25^{o}C for two hours. *CG8108Ex32-31*$^{-/-}$embryos had reduced upregulation of *rpr* and *hid* after irradiation compared to *yw* embryos. The fold increase of *rpr* and *hid* transcription after ionizing irradiation was determined by calculating the C_t difference of control and irradiated embryos normalized to *Act5C*. Each experiment was conducted in triplicate. The p-value is based on a two-sample unequal variance one-tailed Student's t-Test.

4.2.7 *CG8108* expression is tightly regulated and necessary for development

To date, *CG8108* expression data is based on large-scale mRNA or S2 cell and embryonic nuclear matrix protein profiling (www.flybase.org; Kallappagoudar *et al*., 2010). In order to gain further insight into the role of *CG8108* during development, *CG8108* expression was investigated using *in situ* hybridization, RT-PCR, *UASCG8108* constructs, clonal analysis in the eye, and a *CG8108mCherry* reporter (Figures 4.8, 4.9).

921bp antisense and sense *CG8108 in situ* hybridization probes corresponding to two unique regions of the *CG8108* cDNA sequence were used to probe for *CG8108* in embryonic and larval tissues. The *CG8108* mRNA pattern detected by fluorescent *in situ*

Figure 4.8: *CG8108* is broadly expressed during development

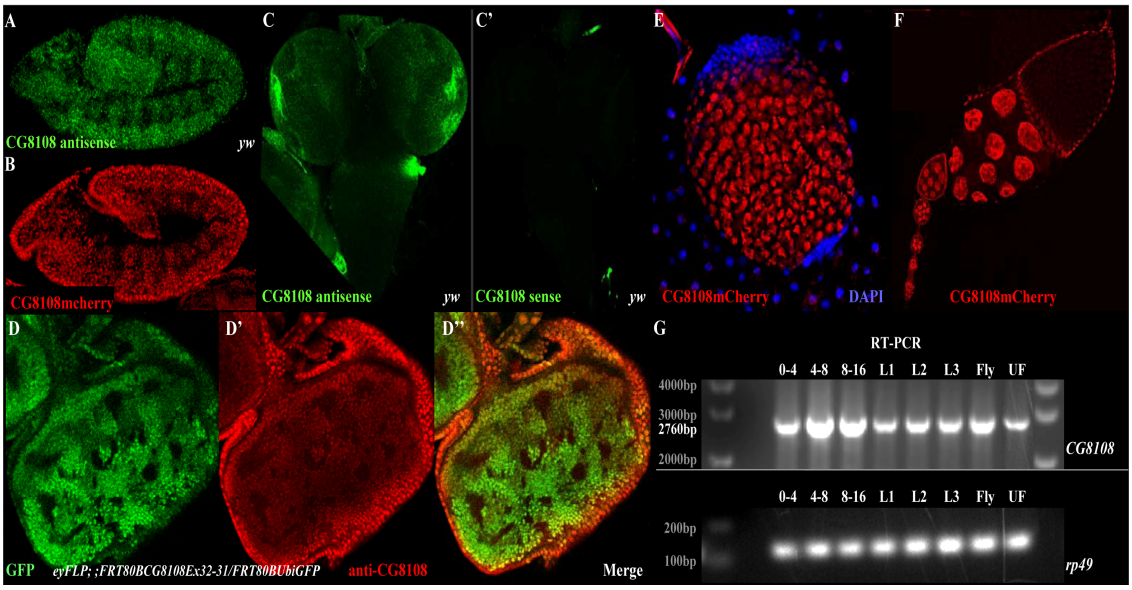

Figure 4.8: [A] Antisense *in situ* hybridization for *CG8108* in a *yw* embryo (green). **[B]** CG8108mCherry reporter expression (red) in a similarly staged embryo as in (A). The reporter consists of the putative *CG8108* promoter (Figure 4.5: B) and the *CG8108* ORF fused to mCherry. **[C]** Antisense *in situ* hybridization for *CG8108* in a *yw* third instar larval brain (green). **[C']** Sense *in situ* hybridization for *CG8108* in a *yw* third instar larval brain (green). **[D-D'']** Third instar eye-antennal disc with *eyFLP* induced clones from a *CG8108Ex32-31/UbiGFP* larva. Wild-type and heterozygous tissues are marked by UbiGFP (green) and anti-CG8108 antibody (red). **[E]** CG8108mCherry reporter immunofluorescence in a third instar larval future testis (red). Nuclei are labeled by DAPI (blue). **[F]** Adult female ovaries dissected from a fly expressing the *CG8108mCherry* reporter construct. **[G]** RT-PCRs for *CG8108* (upper gel) and *rp49* (lower gel) from RNA purified from embryos aged 0-4, 4-8, and 8-16 hours, first (L1), second (L2), and third (L3) instar larvae, whole flies, and unfertilized embryos (UF), respectively. *CG8108* is a maternally deposited gene that is expressed from embryogenesis through adult stages.

hybridization with both sets of antisense probes was identical and the sense probes failed to produce signal (data not shown; Figure 4.8: A, C-C'). *CG8108* mRNA was broadly expressed throughout embryogenesis; it was expressed prior to cellularization, enriched in a segment-polarity gene pattern during germ-band extension, and it was highly expressed in the nervous system at later stages of development (data not shown; Figure 4.8: A). *CG8108* mRNA was found in all third instar imaginal discs and the brain (data not shown; Figure 4.8: C). *CG8108* mRNA is widely expressed during embryonic and larval stages.

RT-PCR for *CG8108* on total RNA collected from *yw* embryos, larvae, and adult flies shows *CG8108* RNA was produced throughout development. *CG8108* mRNA was detected in 0-4, 4-8, 8-16 hour old embryos, first (L1), second (L2), and third (L3) instar larvae, mixed adult flies (fly), and unfertilized embryos (UF) (Figure 4.8: G, upper panel).

Antibodies for CG8108 were not available during the initial efforts to characterize CG8108 expression necessitating the generation of *UASCG8108* constructs to determine CG8108 protein localization. *UASCG8108_FLAG* driven by *actinGal4* in $S2R^{+}$ cells localizes to the nucleus and its overexpression is well tolerated in cell culture (data not shown). In contrast, ectopic expression of *CG8108* in the fly using the *enGal4*, *eyGal4*, or *armGal4* drivers induces organismal lethality (data not shown; Figure 4.9: H). Occasional *eyGal4_UASCG8108* escapers eclosed, but the animals lacked eyes, antennae, and/or large regions of the head, and died shortly after hatching (data not shown). One weak *UASCG8108* transgene insertion (*UASCG8108_FLAG2-7*) driven by *armGal4* survived to larval stages. *armGal4_UASCG8108_FLAG2-7* animals had atrophied

Figure 4.9: *CG8108* expression is tightly regulated and required for development

[A] *Canton S* fly head. **[B]** *eyFLP;;FRT80BMi55/TM6B* fly head. **[C]** *eyFLP; CG8108* genomic rescue 1+2*;TM6B/FRT80BCG8108Ex32-31* fly head. **[D-D']** *eyFLP;;FRT80B Mi55/F80BCG8108Ex32-31* fly heads. Clones generated from genes on chromosome arms containing *Minute* (*Mi55*) have a growth disadvantage compared to clones expressed on a *Minute*+ chromosome arm. Wild-type and heterozygous ommatidia are *white*$^{+}$. *CG8108Ex32-31*$^{-/-}$ clones are *white*$^{-}$. Loss of *CG8108* function in the eye induced severe defects in the eye, head, and antennal structures. Ommatidia devoid of *CG8108* did not form and were replaced with cuticle or heterozygous tissue (D; D', white arrow). The lack of proper *CG8108* expression occasionally led to the elimination or fusion of head structures (D, white arrow) as well as abnormal hairs by the eye (D', black arrow). **[E]** *eyFLP;CG8108* genomic rescue 1+2*;FRT80BMi55/FRT80BCG8108Ex32-31* fly head. The *CG8108* rescue transgene reverted all the *CG8108Ex32*$^{-/-}$ defects generated in a *Minute* background. Consequently, heterozygous tissues constituted a small fraction of eye tissue (white arrows). **[F-I]** Ectopic expression of *CG8108* induced developmental defects. **[F-G]** Flies expressing *GMRGal4_UASCG8108* had abnormal eyes or failed to eclose. **[H-I'']** Ectopic expression of *CG8108* with the *armGal4* driver led to tissue destruction and lethality. **[H]** Third instar larvae expressing *armGal4_CG8108* exhibited premature pupation. **[I-I'']** Salivary glands from animals ectopically expressing *CG8108* were extremely small (white outline). Cells expressing UASCG8108_FLAG were labeled in red and nuclei were marked by DAPI (blue). **[J-J'']** The expression of *CG8108_mCherry* did not adversely affect cell survival. Salivary glands from *CG8108_mCherry* animals were normal-sized unlike *armGal4_UASCG8108* glands.

Figure 4.9: ***CG8108*** **expression is tightly regulated and required for development**

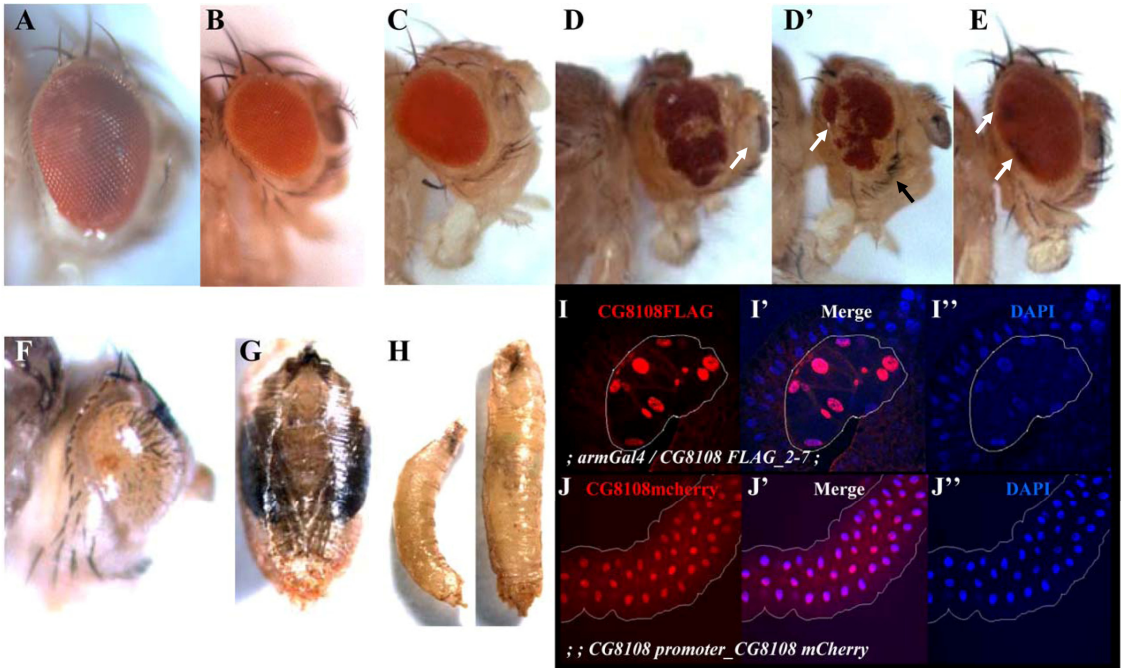

salivary glands surrounded by abnormal fat and the larvae underwent premature pupation (Figure 4.9: I-I'', H; data not shown). *GMRGal4* expression of *CG8108* led to a variety of eye phenotypes ranging from no phenotype, glossy eyes, rough eyes, depigmentation of the eye as animals age, and pupal death (data not shown; Figure 4.9: F, G). The rough eye and depigmentation phenotypes seen in *GMRGal4_UASCG8108* eyes were not suppressed by the pan-caspase inhibitor *p35* (data not shown). *CG8108* expression is tightly regulated and its misexpression is detrimental to animal survival.

The rough eye phenotype seen in *GMRGal4_UASCG8108* flies initiated an investigation into the consequences of eliminating *CG8108* in the developing eye. *CG8108Ex32-31* males were crossed to *eyFLP;;FRT80BMi55UbiGFP/TM6B* virgins and the eyes of adult flies were analyzed. *eyFLP;;FRT80BMi55UbiGFP/FRT80BCG8108 Ex32-31* flies were devoid of *CG8108Ex32-31*$^{-/-}$ ommatidia and they had severe head and antennal defects compared to wild-type flies (Figure 4.9: A-D'). The eyes of *eyFLP*;; *FRT80BMi55UbiGFP/TM6B* and *eyFLP*; *CG8108* genomic rescue 1+2; *TM6B/FRT80B CG8108Ex32-31* flies were grossly normal in appearance like CS flies (Figure 4.9: compare B-C to A). Two copies of the *CG8108* genomic rescue transgene restored *CG8108* function and normal head organization in *eyFLP; CG8108* genomic rescue 1+2*; FRT80BMi55UbiGFP/FRT80BCG8108Ex32-31* flies, confirming *CG8108* expression is necessary for the survival of eye tissues (Figure 4.9: E).

The lethality of ectopic *CG8108* expression during early development using *Gal4* drivers prompted the generation of tagged *CG8108* reporter lines. The *CG8108* reporter lines consisted of transgenic flies expressing the *CG8108* protein coding sequence (ORF) fused to mCherry (*CG8108_mCherry*) under the control of the putative

CG8108 promoter cloned into the pCasPeR4 vector. The *CG8108* promoter consisted of the sequences between the ATG of *CG6718* and the ATG of *CG8108* in the proper orientation for transcription of *CG8108* (Figure 4.5: B, black arrow and orange dotted line: the direction of transcription is indicated by the black arrow and the orange dotted line corresponds to the promoter sequences restricted to the area directly above in 4.5: A). Transgenic *CG8108_mCherry* reporter animals were viable and fertile. However, the lethality seen in *p{SuporP}CG8108*$^{-/-}$ and *CG8108Ex32-31*$^{-/-}$ animals was only partially rescued by the *CG8108_mCherry* transgene (data not shown). The CG8108_mCherry protein expression pattern matched the *CG8108* mRNA distribution in embryos and larval tissues (Figure 4.8: compare A and B; data not shown). CG8108_mCherry immunofluorescence was found in reproductive tissues and cells including the larval future testis, adult testis, and ovaries (Figure 4.8: E, F; data not shown). The salivary glands of *CG8108_mCherry* transgenic larvae were well formed and did not exhibit the defects seen in *armGal4_UASCG8108* salivary glands (data not shown; Figure 4.9: contrast I-I'' and J-J''). *CG8108* transcription and translation is carefully regulated and its global 'ectopic' expression during early developmental stages is only tolerated when *CG8108* is produced under its own promoter.

A CG8108 rabbit polyclonal antibody was subsequently generated and the immunofluorescence pattern obtained with the antibody matched that of the CG8108_mCherry reporter line in embryonic and larval tissues (data not shown). The CG8108 antibody was specific and CG8108 activity can be detected by immunohistochemistry in *eyFLP* generated wild-type and heterozygous clones in *eyFLP*; *CG8108Ex32-31/UbiGFP* animals (Figure 4.8: D-D''). The CG8108 antibody was also

sufficient for immunoprecipitation and western blotting in S2 cells and fly tissues over-expressing CG8108 and was used to demonstrate CG8108 physically associated with Xbp1 (Figure 4.6: A-C).

CG8108 is maternally deposited and the maternal contribution was sufficient for animal survival until the late-first, early-second larval instar (Figure 4.8: G, (UF); Table 2). CG8108 is broadly produced throughout the fly life cycle and its expression is tightly regulated. Misexpression of *CG8108* by either its loss or gain of function negatively impacts development and can lead to organismal death (Table 2; Figures 4.8, 4.9).

4.3 Discussion

This chapter describes the initial characterization of *CG8108* and its role in stress-induced apoptosis during *Drosophila* development. *CG8108* was identified in a screen for novel regulators of ERSIA and experiments were executed to determine if CG8108 acts at proximal as well as distal events during the UPR and ERSIA. CG8108 and Xbp1 were identified as interacting proteins in a large-scale yeast-two-hybrid screen of *Drosophila* proteins that favored the possibility that CG8108 regulated early ER stress events (Giot *et al*., 2003). CG8108 was also tested for regulation of X-ray induced cell death, since radiation exposure can activate components of the UPR (Anand *et al*., 2005; Zhang *et al*., 2010). Since all of the data on CG8108 function to date is based on sequence, RNA, or protein profiling, tools were generated to specifically determine CG8108 localization from embryogenesis through adult stages.

CG8108 regulation of proximal ER stress events was tested by assessing *xbp1* splicing with the *xbp1_EGFP* reporter. The *xbp1_EGFP* reporter consists of *xbp1U* sequence including the Ire1 splicing site fused to *EGFP*. In unstressed cells, EGFP is not expressed, but in stressed cells, EGFP is expressed due to Ire1 splicing of the reporter (Ryoo *et al*., 2007). *xbp1_EGFP* splicing was strongly suppressed in tissues of *p{SuporP}CG8108*$^{-/-}$ animals and delayed in *p{SuporP}CG8108*$^{-/-}$ clones in S2 DTT treated discs (Figure 4.1: contrast E' to D'; contrast B-B'' to C-C'', respectively). Control ;*armGal4,Xbp1_EGFP;* animals exhibited more reporter activity in eye discs than ;*armGal4,Xbp1_EGFP;p{SuporP}CG8108*$^{-/-}$ discs incubated in S2 DTT (Figure 4.1: contrast D' to E'). Unexpectedly, *xbp1_EGFP* reporter splicing in whole *p{SuporP}CG8108*$^{-/-}$ eye-antennal discs incubated in S2 DTT for 18 hours was much less

prominent than in mosaic *p{SuporP}CG8108*$^{-/-}$ discs incubated in S2 DTT for the same period of time. Nonautonomous *xbp1_EGFP* reporter splicing from wild-type and heterozygous tissues may account for the uniform EGFP signal in *GMRGal4,eyFLP; UASXbp1_EGFP;p{SuporP}CG8108*/*UASDsRed* mosaic eye-antennal discs incubated for 18 hours in S2 DTT. The disruption of CG8108 function by the *p{SuporP}* p-element insertion was responsible for the suppressed *xbp1* splicing seen in *p{SuporP}CG8108*$^{-/-}$ tissues. The precise excision of the *p{SuporP}* p-element in *p{SuporP}CG8108* reverted the *xbp1_EGFP* splicing phenotype. The delayed *xbp1* splicing seen in *p{SuporP}CG8108*$^{-/-}$ clones was not detected in homozygous clones of the precise excision line *p{SuporP}CG8108Ex69-14* (Figure 4.2: contrast the absence of Xbp1_EGFP in *p{SuporP}CG8108*$^{-/-}$ clones in D-D'', to the presence of Xbp1_EGFP in homozygous *p{SuporP}CG8108Ex69-14* clones in E-E''). In addition to restoring *xbp1_EGFP* reporter function, the precise excision of the *p{SuporP}* p-element in *p{SuporP}CG8108* sensitized tissues to the effects of ERSIA and reverted larval lethality (Figure 4.2: contrast caspase activation (red) in B, C; Table 2). CG8108 function is necessary for efficient *xbp1* splicing and mutations reducing CG8108 expression suppresses Xbp1_EGFP reporter activity.

During the course of this investigation, the *p{SuporP}* p-element insertion in *p{SuporP}CG8108* was found to affect the transcription of both *CG8108* and the neighboring gene *iPLA2-VIA* (*CG6718*). The 5'UTRs of *CG6718* and *CG8108* are separated by 246bp and they potentially have overlapping regulatory regions. qRT-PCR data revealed the *p{SuporP}* p-element reduced CG6718 transcription by 27% (Figure 4.3: A). Diminished CG6718 function indirectly impacts cardiolipin homeostasis in the

context of Barth syndrome (Malhotra *et al*., 2009). Cardiolipin is a component of the mitochondria and the finding that compromised *CG6718* expression could potentially affect the mitochondria raised many concerns. Cell death signaling via the Bcl-2 pathway involves the mitochondria and the ERSIA effects attributed to the *p{SuporP} CG8108* allele could have been due to reduced *CG6718* expression. In order to eliminate trepidation that CG6718 may be responsible for the phenotypes seen in the *p{SuporP}CG8108* allele, a null allele of *CG6718* was recombined onto an FRT and tested for suppression of *xbp1_EGFP* splicing and ERSIA. Loss of *CG6718* function was found to suppress neither ERSIA nor *xbp1_EGFP* splicing (Figure 4.3: B-C'' and D-E'', respectively). Therefore, the phenotypes seen with the *p{SuporP}CG8108* allele were due to the disruption of *CG8108*.

Since the p-element in the *p{SuporP}CG8108* allele affected two genes, a *CG8108*-specific allele was generated by imprecise excision of the *p{EPgy2}* p-element in *p{EPgy2}CG8108*. The *p{EPgy2}* p-element in *p{EPgy2}CG8108* was inserted in the first protein coding exon of *CG8108* and it specifically disrupted *CG8108* (Figure 4.3: A). One imprecise excision line was obtained by mobilization of the *p{EPgy2}* p-element. *CG8108Ex32* was produced by a deletion which removed the *p{EPgy2}* p-element and 1.2kb of *CG8108* sequence three-prime from the p-element insertion point (Figure 4.4: A, B). The *CG8108Ex32* line and its progenitor (*p{EPgy2}CG8108*) were also found to have a second-site mutation, but FRT-recombination and genomic rescue permitted the isolation of a clean *CG8108Ex32* allele (*CG8108Ex32-31*) (Figure 4.5; Table 2). *CG8108Ex32-31*$^{-/-}$ larvae did not produce full length *CG8108* RNA and died earlier than *p{SuporP}CG8108*$^{-/-}$ animals (Figure 4.4: C; Table 2).

p{SuporP} CG8108$^{-/-}$ animals develop melanotic tumors as third instar larvae and they die during pupation; in contrast, *CG8108Ex32-31*$^{-/-}$ animals die during the late-first, early-second instar (data not shown; Table 2). *CG8108Ex32-31*$^{-/-}$ clones are extremely small and do not survive the DTT assay preventing conclusive analysis with respect to ERSIA suppression (Figure 4.4: contrast D-D''' to E-E'''). *CG8108Ex32-31*$^{-/-}$ clones exhibit a weak delay in *xbp1* splicing compared to neighboring wild-type and heterozygous tissues, but the degree of suppression is much less pronounced than *p{SuporP}CG8108*$^{-/-}$ clones (Figure 4.4: contrast F-F'' to G-G''). The splicing seen in *CG8108Ex32-31*$^{-/-}$ clones may be due to nonautonomous splicing from the neighboring wild-type and heterozygous tissues. The consistent evidence that loss of *CG8108* function affects *xbp1_EGFP* splicing and the published yeast-two-hybrid data which demonstrated CG8108 physically associates with Xbp1 provoked immunoprecipitation experiments between CG8108 and Xbp1 (Figures: 4.1: D-E'; 4.4 F-G''; Giot *et al*., 2003).

CG8108 physically interacts with Xbp1U and Xbp1S *in vivo* and *in vitro*. Endogenous and ectopically expressed CG8108 in S2R^{+} cells physically associated with ectopically expressed Xbp1U and Xbp1S (Figure 4.6: A-B). In addition, CG8108 and Xbp1U were shown to co-immunoprecipitate in fly-head lysates from *GMRGal4*, *UASCG8108_FLAG;UASXbp1U_HA* animals (Figure 4.6: C). Immunofluorescence staining shows Xbp1U protein has both cytoplasmic and nuclear localization, while Xbp1S and CG8108 proteins have strictly nuclear localization in S2R^{+} cells (data not shown). Previous research has shown mammalian XBP1U protein has both nuclear export (NES) and nuclear localization (NLS) domains, which allows XBP1U to shuttle between the nucleus and cytoplasm (Yoshida *et al*., 2006). Xbp1U protein has a

degradation domain in its C-terminus that enables it to negatively regulate the UPR by targeting nuclear XBP1S and ATF6 for proteasomal degradation in the cytoplasm (Yoshida *et al*., 2006; Yoshida *et al*., 2009). The XBP1U degradation of XBPS and ATF6 is readily detectable when XBP1U is expressed at nine-fold excess compared to XBP1S and ATF6. XBP1U protein also targets its own mRNA to membranes to facilitate splicing by Ire1 (Yanagitani *et al*., 2009). The physical association of CG8108 with both forms of Xbp1 leaves many avenues for CG8108 regulation of Xbp1. It is possible CG8108 facilitates efficient *xbp1* splicing by favoring nuclear export of Xbp1U protein and the targeting of *xbp1* mRNA to membranes thereby increasing Xbp1S production. CG8108 could potentially activate *xbp1* transcription by binding to the *xbp1* promoter or by indirectly affecting the expression of an *xbp1* regulator. Alternatively, CG8108 may interact with the elusive metazoan RNA ligase that joins the spliced Xbp1U fragments that form Xbp1S. In yeast, the tRNA ligase Rlg1 connects $HAC1^{u}$ fragments spliced by Ire1 to produce $HAC1^{i}$, subsequently allowing the translation of mature HAC1 (Sidrauski *et al*., 1996; Mori *et al*., 2010). The metazoan ligase for *xbp1* has yet to be identified and CG8108 could potentially interact with and/or regulate this protein in the nucleus. CG8108 may influence Ire1 activity, but neither an appropriate antibody nor an Ire1 construct suitable for transfections was available for testing this possibility during the course of this study. The ectopic expression of the CG8108 in the eye does not induce *xbp1_EGFP* reporter splicing making it unlikely that CG8108 had a direct effect on Ire1 activation (data not shown). $p\{SuporP\}CG8108^{-/-}$ clones did not have altered protein levels of the ER chaperone Hsc3 (BiP) during 2.5 hour incubation periods in S2 DTT (data not shown). Although diminished Xbp1 function was shown to reduce Hsc3 protein

levels; the result that *p{SuporP}CG8108*$^{-/-}$ tissue did not suppress Hsc3 was not inconsistent with previous studies regarding chaperone activation in the absence of *xbp1* function (Ryoo *et al*., 2007; Lee *et al*., 2003). In mammals, BiP expression can be upregulated in the absence of IRE1/XBP1 branch activity (Lee *et al*., 2003). CG8108 is necessary for *xbp1* splicing, but the exact mechanism by which CG8108 regulates *xbp1* splicing has yet to be elucidated.

Loss of *CG8108* function suppressed ERSIA in *p{SuporP}CG8108*$^{-/-}$ tissues subjected to the DTT assay and precise excision of the p-element restored tissue sensitivity to prolonged culture in DTT (Figure 4.2: B-C). Previous research has shown radiation can induce components of the UPR such as eIF2α and *xbp1* splicing (Anand *et al*., 2005; Zhang *et al*., 2010). Although the *xbp1_EGFP* reporter is not activated in animals exposed to X-ray radiation, CG8108 was tested for an effect on radiation-induced cell death (data not shown; Figure 4.7; Table 3). *CG8108Ex32-31*$^{-/-}$ eye disc clones distinctly suppressed caspase activation after exposure to 40Gy of X-ray and γ-ray radiation (Figure 4.7: B-C'', white arrows; data not shown). The suppression of cell death in *CG8108Ex32-31*$^{-/-}$ clones was due to the loss of CG8108 function since *CG8108Ex32-31*$^{-/-}$ tissues are no longer refractory to X-rays in animals expressing CG8108 genomic rescue transgenes (Figure 4.7: E-F''). Since embryos are particularly sensitive to X-rays, *CG8108Ex32-31*$^{-/-}$ and *yw* 6-9 hour old embryos were X-irradiated and the level of Rpr and Hid transcriptional upregulation was quantified using qRT-PCR (Table 3). *CG8108Ex32-31*$^{-/-}$ embryos upregulated *rpr* and *hid* transcription to a lesser degree than *yw* embryos, but the effects of diminished CG8108 function in embryos was not as compelling as the cleaved caspase 3 suppression seen in eye discs. RT-PCR on

unfertilized embryo RNA, mRNA profiling of 0-2 hour embryos, and antibody staining revealed CG8108 was maternally deposited (Figure 4.8: G, top panel; www.flybase.org; data not shown). The maternal contribution of CG8108 in irradiated embryos may be sufficient for upregulation of Rpr and Hid to levels that marginally differ from wild-type. In eye-discs, the maternal CG8108 contribution titrates out in *CG8108Ex32-31*$^{-/-}$ tissues and reduced caspase activation as a consequence of reduced *rpr* and *hid* transcription was evident (Figure 4.7: B-C'', *CG8108Ex32-31*$^{-/-}$ clones had reduced cleaved caspase 3 activity; Figure 4.8: D-D'', immunoreactivity for CG8108 (red) was not detected in *CG8108Ex32-31*$^{-/-}$ clones). CG8108 function may be necessary for radiation-induced cell death in embryos and larval tissues.

CG8108 is required for viability and its expression is carefully regulated. Stronger CG8108 alleles exhibit earlier mortality (Table 2). Clones produced by the hypomorphic *p{SuporP}CG8108* allele were larger, survived the DTT assay, and showed a clear delay in *xbp1_EGFP* splicing (Figure 4.4: D-D'', F-F''). In contrast, *CG8108Ex32-31*$^{-/-}$ clones were small, rarely survived the DTT assay, and showed a weak delay or enhanced *xbp1_EGFP* splicing (Figure 4.4: E-E'', G-G''; data not shown). The small clone size and animal lethality associated with the *CG8108Ex32-31* allele could be rescued with two copies of the *CG8108* rescue transgene (Figure 4.7: D-D''; Table 2). CG8108 is expressed from embryogenesis through adult stages and its expression is tightly regulated (Figures 4.8, 4.9). The ectopic expression of *CG8108* using *enGal4*, *eyGal4*, *GMRGal4*, and *armGal4* led to abnormal development and lethality (data not shown; Figure 4.9: F-I''). In contrast, animals carrying a *CG8108* reporter transgene that expressed the *CG8108* ORF tagged with mCherry (*CG8108mCherry*) under the control

of the *CG8108* promoter did not display developmental defects (data not shown; Figures 4.8: B, E, F; 4.9: J-J''). The lack of CG8108 function negatively impacted development and the elimination of CG8108 expression in the eye in *eyFLP;;FRT80B Mi55UbiGFP/FRT80BCG8108Ex32-31* animals caused defects in eye and head structures (Figure 4.9: A-E). CG8108 activity is carefully controlled and maintenance of proper levels of CG8108 expression has great implications on development.

This study has shown that CG8108 is maternally deposited and that it is vital for *Drosophila* development and survival. The levels of CG8108 expression are carefully restricted and extreme fluctuations in CG8108 expression during early development are lethal to animals. CG8108 function was demonstrated to affect proximal and distal events during the UPR. CG8108 is necessary for proper splicing of the *xbp1_EGFP* reporter and for the activation of caspases during prolonged ER stress. Consequently, mutations that reduce CG8108 expression inhibit *xbp1* splicing during early stages of ER stress and suppress ERSIA during prolonged periods of ER stress. CG8108 physically associated with Xbp1U and Xbp1S and the three proteins could potentially engage in an auto-regulatory loop modulating the Ire1/Xbp1 arm of the UPR. CG8108 function was also shown to be necessary for caspase activation by Rpr and Hid after X-ray irradiation.

The aim of this thesis project was to find a gene that connected both the ER stress and apoptotic branches and would consequently regulate ERSIA. The DTT assay was optimized and utilized to screen 452 p-element lethal FRT lines that led to the identification of CG8108 as a loss-of-function suppressor of ERSIA. CG8108 is vital for development and it is a novel gene that impacts proximal and distal events during ER stress thereby connecting the ER stress and cell death pathways in *Drosophila*.

4.4 Materials and Methods

4.4.1 *Drosophila* stocks

P-element excision lines were generated by crossing Δ*2-3/CyO* transposase expressing females to red-eyed males from the following stocks obtained from the Bloomington Stock Center: *P{SUPor-P}CG8108*^{KG05452} (*p{SuporP}CG8108*), *P{EPgy2}CG8108*^{EY14316} (*p{EPgy2}CG8108*), and *P{EPgy2}iPLA2-VIA*^{EY05103} (*p{EPgy2}CG6718*). Males with mosaic eyes from the aforementioned crosses were mated to double balancer females, and individual stocks were generated from the resulting *white*$^{-}$/balancer male progeny. Precise and imprecise excision events were identified by comparing the size of PCR products amplified from genomic DNA preparations from candidate p-element excision lines to those from *yw* genomic DNA. PCR products less than 1kb produced by three or four primer pairs covering regions five-prime, spanning, and three-prime the p-element insertion sites were used to determine the nature of excision events. Precise excision events were expected to produce PCR products matching those produced from *yw* genomic DNA for all primer pairs. Imprecise excision events specific to the gene of interest were expected to yield PCR products which differed in size from *yw* genomic DNA amplified with primer pairs spanning and/or three-prime the p-element insertion site.

The *UASCG8108*, *UASCG8108_FLAG*, and *UASCG8108_mCherry* transgenic lines were generated by PCR amplification of the CG8108 ORF from the LD27033 cDNA clone (BACPAC resource center, (BPRC) at the Children's Hospital Oakland Research Institute) into the pUAST vector and the *UASCG8108* and *UASCG8108_FLAG* constructs were sent for p-element transformation by the BestGene company. The FLAG

tag sequence was incorporated in-frame into the three-prime *CG8108* primer to allow detection of CG8108 protein. The *UASCG8108_mCherry* transgene was generated by a two-step process first; the *CG8108* ORF was cloned into pUAST using a reverse primer which replaced the stop codon with a restriction site absent from *CG8108* and *mCherry* sequences generating a *UASCG8108_nonstop* construct. Second, the *mCherry* sequence was PCR amplified and cloned into the *UASCG8108_nonstop* construct to generate the *pUASCG8108_mCherry* construct. The *UASXbp1S* and *UASXbp1S_HA* constructs were made by re-cloning the *UASXbp1S* construct described in Ryoo *et al*., 2007 into pUAST and adding an HA tag to the three prime primer to make *UASXbp1S_HA*. The *UASXbp1U* and *UASXbp1U_HA* constructs were generated using a three-part PCR amplification cloning scheme utilizing the original *UASXbp1S*. First, the five-prime end of *xbp1* sequence common to *xbp1S* and *xbp1U,* up to the region where the 23nt sequence spliced out by Ire1 was amplified using a forward primer for the *xbp1* ORF and a reverse primer containing the 23nt splice sequence flanked by *xbp1S* sequence. Second, the three-prime end of *xbp1* just after the Ire1 splice site that is common to *xbp1U* and *xbp1S* was amplified using a five-prime primer with the 23nt splice sequence flanked by *xbp1S* sequence and reverse primers specific to *xbp1U* with or without the HA sequence. Third, the PCR products from the first and second PCR reactions mentioned above were combined and they served as a template for amplifying the complete Xbp1U ORF; using the forward primer from the first PCR reaction and the HA or tag-less reverse primer from the second PCR reaction. The PCR product from the third reaction was cloned into the pUAST vector. PCR products for the *UASCG8108*(*FLAG*) and *UASXbp1S*(*HA*) constructs were amplified using Easy-A High-Fidelity PCR Cloning Enzyme (Agilent),

gel purified with the QIAquick Gel Extraction kit (Qiagen), and TOPO cloned into the PCR 2.1 TOPO vector (Invitrogen/Life Technologies). TOPO colonies were mini-prepped using the QIAprep Spin Miniprep Kit (Qiagen) and DNA from candidate lines was sent for sequencing at the GENEWIZ facility. The sequenced *UASXbp1U*, *UASXbp1U_HA*, *UASXbp1S*, *UASXbp1S_HA* plasmids were midi-prepped with the HiSpeed Plasmid Midi Kit (Qiagen) and sent for p-element transformation at the BestGene company.

The *CG8108* and *CG6718* genomic rescue transgenes were cloned using the BACR07A05 genomic clone (BACPAC resource center, (BPRC) at the Children's Hospital Oakland Research Institute). The genomic rescue constructs were cloned piecemeal, using two or three separate PCR reactions amplifying 3-4kb blocks which were cloned into pBlueScriptSK$^+$ and sent for sequencing at the GENEWIZ facility. Once the three individual fragments were cloned into pBlueScriptSK$^+$, the pieces were subcloned one by one into pBlueScriptSK$^+$ to produce a full-length genomic rescue construct which could be subcloned into the pCasPeR4 vector. The start of the genomic rescue transgenes was the ATG (TAC) of the ORF of the adjacent gene and the end of the rescue construct was set at least 1kb after the putative 3'UTR described in FlyBase to ensure the *CG8108* transcription termination sequences were present in the construct. Once the complete genomic rescue construct was subcloned into pCasPeR4, it was re-sequenced, midi-prepped with the HiSpeed Plasmid Midi Kit (Qiagen) and sent for p-element transformation at the BestGene company.

The *CG8108_mCherry* reporter was made by a three-step method; the first step was the amplification and cloning the putative *CG8108* promoter into the pUAST vector

to generate the *pUASCG8108_prom* construct. The promoter region spanned the ATG (TAC) of the CG6718 ORF and the *CG8108* genomic sequence through the last base just before the ATG of the CG8108 ORF. In addition, a restriction site absent from the *CG8108* promoter, the CG8108 ORF, and mCherry was added to the end of the promoter. The second step was the subcloning of the *UASCG8108_mCherry* described above into the *pUASCG8108_prom* plasmid producing the *pUASCG8108_promCG8108_mCherry* construct. The last step involved subcloning the *CG8108_promCG8108_mCherry* portion of the *pUASCG8108_promCG8108_mCherry* into the pCasPeR4 vector. The final construct was sequenced, midi-prepped with the HiSpeed Plasmid Midi Kit (Qiagen), and sent for p-element transformation at the BestGene company.

4.4.2 DTT assay

The DTT assay was conducted as described in Chapter Three.

4.4.3 *xbp1* splicing assay

Fifteen to twenty eye-brain complexes, associated discs, and/or salivary glands of third instar larvae (mixed stages) expressing two copies of the *UASXbp1_EGFP* reporter construct transgene grown on regular or blue food were dissected in room temperature S2 media and transferred into a glass nine-well plate containing 400 µl S2 media. Once the dissections were complete, fresh S2 DTT (S2 media + 2 mM DTT) was made and the 400 µl S2 media containing the larval tissues was replaced with S2 or S2 DTT. Incubations in S2 (S2 DTT) were carried out in a humid chamber at 25^{o}C for 2.5 or 18 hours. After the incubations were complete, samples were fixed and antibody stained as described in Chapter Three. The primary antibodies used were chicken anti-GFP (1:200, Aves Labs) and/or rat anti-ELAV (1:40, DSHB) in PBTrN.

4.4.4 Embryo collection and fixation

The embryo collection and fixation procedure is an adaptation of the protocol used in Walrad *et al*., 2010. Embryos were collected by mating flies in cages containing a yeasted apple juice plate. Eggs deposited by females were removed from the apple juice plate by squirting 50% bleach onto the plates, gently dislodging the embryos with a soft paint brush, and transferring the bleach and embryos in into egg collection baskets. The embryos were dechorionated by gentle tapping and swirling of the egg collection baskets in a 50% bleach solution sufficient to cover the embryos. Dechorionated embryos were thoroughly rinsed inside the collection baskets with ddH_2O (for antibody staining procedures) or 1x PBS (for RNA extraction procedures).

Embryos were fixed by transferring dechorionated embryos into glass scintillation vials containing heptane and 10% PFA (0.5 ml heptane : 3.0 ml 10% PFA) and moderately shaking the vials for twenty minutes at room temperature on an orbital shaker. After twenty minutes, the aqueous phase of the heptane/PFA solution was removed with a glass Pasteur pipette and 4.0 ml of 100% methanol was added to the scintillation vials. Devitellinization of embryos was achieved by vigorously shaking the embryos in the heptane/methanol solution for 30-60 seconds by hand. The devitellinized embryos were allowed to settle to the bottom of the vial and then they were transferred to a microfuge tube using a cut-off 1.0 ml pipette tip. The embryos were rinsed three times with 1.0 ml of 100% methanol and stored in 1.0 ml 100% methanol at -20^{o}C until needed.

4.4.5 Antibody staining

Embryos were fixed for antibody staining following the embryo collection and fixation protocol as described above. Primary and secondary antibody staining of larval

tissues and embryos was conducted as described in Chapter Three. The mouse anti-mCherry (Clontech), mouse anti-FLAG (Sigma), and Cy3 anti-mouse (Jackson Laboratories) antibodies were used at a 1:200 dilution in PBTrN.

4.4.6 TUNEL staining

TUNEL staining was carried out as described in Chapter Three.

4.4.7 Genomic DNA preparation and sequencing

yw first- or second-instar larvae were used as controls. *CG8108* or *CG6718* mutant and excision alleles were maintained over the *TM6B*, *Sb*, *Dfd-YFP* balancer (Le *et al*., 2006) and homozygous-mutant larvae were identified by the absence of *YFP* fluorescence in the mouth hook region. Genomic DNA was prepared from at least fifty first- or second-instar larvae using the High Pure PCR Template Preparation Kit (Roche) following the manufacturers instructions. 100 μg of genomic DNA was amplified for PCR with Crimson Taq polymerase (NEB) using primers for the desired region of analysis.

Once candidate excision lines were identified, large-scale genomic DNA preparations for each line were made by running 4-8 50 μl PCR reactions that were gel purified using the QIAquick Gel Extraction kit (Qiagen). The genomic DNA was then sent for sequencing at the GENEWIZ sequencing facility to characterize excision events.

4.4.8 Fluorescent *in situ* hybridization

The fluorescent *in situ* hybridization (FISH) protocol used was a modification of the protocol described in Walrad *et al*., 2010. cDNA fragments were cloned into the PCR II TOPO vector (Life technologies/Invitrogen) that contains SP6 and T7 promoter sites. The PCR II TOPO vector was linearized and digoxigenin (DIG) labeled probes

were generated with the DIG RNA Labeling Kit (SP6/T7) (Roche) following the manufacturers instructions. DIG-labeled RNA was detected using anti-digoxigenin-POD (Roche) and Tyramide Signal Amplification (TSA) reagent (Perkin Elmer).

CG8108 RNA *in situ* probes were generated by PCR-amplifying the first and second 921bp sequences of the *CG8108* ORF from the LD27033 cDNA clone (BACPAC) as described above.

4.4.9 Generation of a CG8108 antibody

The rabbit anti-CG8108 antibody was generated by GenScript using a peptide corresponding to the following CG8108 amino acid sequence: TEEGDEDDHDDDKK.

4.4.10 X-ray and gamma-ray irradiation of imaginal discs and embryos

FRT80BUbiGFP virgin females were crossed to (*CG8108* genomic rescue 1+2); *FRT80B*(*CG8108*)*/TM6B* mutant allele males in vials containing standard media for imaginal disc irradiation experiments. At least 30 third instar larvae were transferred to 35 mm plates containing a moistened kimwipe and exposed to 0 Gy or 40 Gy of either X-ray or gamma-ray radiation. After irradiation, larvae were allowed to recover for two hours: one hour at 25^{o}C, and one hour at room temperature. Eye-brain complexes were dissected out of the larvae during the final hour of the recovery and they were transferred into a glass nine-well plate containing 400 µl PBS. The PBS was removed and dissected larval tissues were fully submerged in 4% PFA 10-15 minutes after the two hour recovery period and fixed overnight at 4^{o}C. After fixation, the discs were antibody and/or TUNEL stained as described in Chapter Three.

yw embryos were used for controls in embryo irradiation experiments. *CG8108Ex32-31* flies were balanced over the *TM3,Sb,Twi-GFP* balancer (Halfon *et al*.,

2002) to identify *CG8108Ex32-31*$^{-/-}$ embryos (non-GFP). *yw* and *CG8108Ex32-31/ TM3,Sb,Twi-GFP* flies were kept in cages with yeasted apple juice plates at 25^{o}C and used for collection over a period of one week. All plates used for embryo collection were pre-warmed to room temperature to encourage egg laying. Egg collections were conducted as follows: embryos were pre-collected for one hour at 25^{o}C, staged embryos were collected for three hours at 25^{o}C (0-3 hour plate), and the 0-3 hour collection plate was aged for an additional 5.25 hours at 25^{o}C. The embryos were dechorionated as described above and transferred to fresh room-temperature plates using a paint brush within a forty-five minute period. The then 6-9AEL embryos were irradiated with 0 Gy or 40 Gy X-ray radiation (uncovered, embryo side up). During the two hour recovery period, *yw* and fluorescent embryos were sorted and placed into a DNA Zap (Ambion) treated glass 9-well plate containing 500 µl 1X PBS using DNA Zap (Ambion) treated forceps (one pair of forceps per genotype, per condition). Embryos were transferred from the 9-well plate into labeled microfuge tubes where excess PBS was removed from the tube and the embryos were flash frozen in dry ice/ethanol and stored at -80^{o}C.

4.4.11 (q)RT-PCR sample preparation and analysis

Embryos for qRT-PCR were harvested, aged, and dechorionated as described above, then rinsed with 1X PBS, transferred to a microfuge tube, flash-frozen in dry ice-ethanol, and stored at -80^{o}C until ready for processing.

RNA was purified from embryos with the PureLink RNA Mini Kit (Life technologies/Invitrogen) using the manufacturers directions. qRT-PCR and RT-PCR reactions were carried out according to manufacturer instructions using the EXPRESS SYBR GreenER qPCR SuperMix Kit and SuperScript III One-Step RT-PCR System with

Platinum Taq (Life technologies/Invitrogen), respectively. p-values were calculated using the TTEST function in Microsoft Excel of RNAs normalized to Act5C.

4.4.12 Western blotting and immunoprecipitation

Samples for western blot or immunoprecipitation were comprised of frozen or fresh pellets (or tissues) resuspended in Triton X-100 buffer (20 mM Tris-HCl (pH 7.4), 420 mM NaCl, 10 mM $MgCl_2$, 2 mM EDTA, 10% glycerol, 1% Triton X-100, and cOmplete, Mini Protease Inhibitor Cocktail Tablets {Roche}). The resuspended cells were incubated for at least ten minutes on ice, sonicated twice for 10 seconds, and spun at 10,000 rcf for 30 minutes at 4^{o}C to pellet the cell debris. The supernatant was transferred to another tube and 1-2 μl of lysate was added to Bio-Rad Protein Assay (Bio-Rad) to determine the total protein concentration. 150-200 μg of total protein was used for western blotting and 400-1500 μg total protein was used for immunoprecipitations.

Western blot samples were boiled for five minutes after the addition of Red loading buffer for PAGE (NEB) and the samples were run at 80-100V on a 4-15% Ready Gel Tris-HCl Gel (Bio-Rad) in 1X Tricine running buffer (100 mM Tris, 100 mM Tricine and 0.1% SDS). Kaleidoscope marker (Bio-Rad) was used as a protein size standard. Proteins were transferred for 70 minutes at room temperature in transfer buffer (25 mM Tris, 192 mM Glycine) onto a Protran nitrocellulose membrane (Whatman). After transfer, the membrane was blocked for one hour in TBSTw (1X TBS, 0.05 M Tris. 0.15 M NaCl, and 0.1% Tween 20) containing 5% milk (Bio-Rad) on an orbital rotator. Blocked membranes were transferred to sandwich bags containing antibody diluted in TBSTw containing 5% milk or washed three times for ten minutes in TBSTw and then transferred to sandwich bags containing primary antibody diluted in TBSTw without

milk. Membranes were incubated on a nutator or orbital rotator overnight at 4°C. After incubation in primary antibody, membranes were washed three times for ten minutes on an orbital rotator. After incubation in primary antibody, membranes were washed three times for ten minutes in TBSTw. If a non-HRP conjugated primary antibody was used, the washed membrane was incubated for one hour in secondary antibody containing 5% milk diluted in TBSTw and subsequently washed three times for ten minutes in TBSTw. Membranes containing HRP-labeled antibodies were detected using ECL (Amersham ECL Western Blotting Detection Reagent (GE) or SuperSignal West Dura Substrate {Thermo Scientific}) and imaged on an ImageQuant imager (GE).

Sample preparation for immunoprecipitation was the same as described above. 400-1500 μg total protein lysate was incubated with 3 μl of primary antibody for 2-6 hours in microfuge tubes rotated end-over-end at 4°C. Protein A magnetic beads (NEB) (25-35 μl) were added to the lysate-antibody mixture and incubated overnight rotating end-over-end at 4°C. The immunoprecipitated proteins were isolated following the manufacturers instructions and 20 μl was analyzed by western blot (see above).

The following primary antibodies were incubated in TBSTw containing 5% milk: HRP-anti-FLAG (Sigma, 1:1000), HRP-anti-HA (Roche, 1:1000), and rabbit anti-CG8108 (lab generated, GenScript, 1:1000). The following primary antibodies were diluted in milk-free TBSTw: mouse anti-profilin (DSHB, 1:100). HRP-conjugated secondary antibodies were obtained from Jackson Laboratories.

4.4.13 S2 cell culture, transfection, and harvesting

$S2R^+$ cells (DGRC) were maintained in T25 or T75 flasks at 25°C in Shields and Sang M3 insect medium with L-glutamine and potassium bicarbonate (Sigma)

supplemented with 10% heat inactivated fetal bovine serum (HI-FBS, Gibco) and 1.0% penicillin/streptomycin (Mediatech).

$S2R^+$ cells were transfected using FectoFly insect cell transfection reagent (Polyplus) following the manufacturers instructions. First, 4.0 ml of complete media containing $5x10^6$ cells was added to a 10 cm plate and the cells were allowed to adhere for two hours. Second, working transfection reagent was prepared with a total of 25 μg DNA in 500 μl NaCl solution and 25 μl FectoFly transfection reagent in 500 μl NaCl solution. Working transfection reagent consisted of 4 μg *ActinGal4*, 1 μg *UASmitoGFP* or *UASDsRed*, and 10 μg empty pUAST vector + 10 μg vector of interest for single transfections or 10 μg each plasmid for double-transfections. Third, cells were incubated with working transfection reagent for four hours at 25°C. Fourth, 8.0 ml of complete media was added to the transfected cells after the four-hour incubation and the cells were harvested after 72 hours at 25°C.

$S2R^+$ cells were harvested by using cell a scrapper to initially dislodge the cells from 10 cm plates, gently resuspending the cells with a serological pipette, and transferring the cells to a 50 ml conical tube. The cells were spun at 1200 rcf at 4°C for five minutes, all the media was removed from the pelleted cells, and the pellets were flash frozen in dry ice/ethanol and stored at -20°C or processed for protein preparation.

4.4.14 Fly head lysate preparation

90-150 whole flies were collected and stored at -20°C in microfuge tubes. Flies were decapitated by placing the microfuge tube in liquid nitrogen and then vortexing the tube (repeated if needed). The fly carcasses and heads were sorted on a pad with a fine paintbrush and the heads were processed for immunoprecipitation as described in 4.4.12.

4.4.15 Primer list

		Cloning Primers			
	Primer Name	Sequence	Fwd. Res. Site	Rev. Res. Site	Cloning Plasmid
1	pUAST/GMR 3L-59F	5' GAGGAGCAATTGACCATGCGTGGACGCGGCGGATTCATTCC 3'	MfeI		pUAST
2	pUAST/GMR 3L-59R untag	5' GAGGAGAGATCTTTATTATTACTTGGAGTCGGCGGCTG CCGC 3'		BglII	pUAST
3	pUAS/GMRR3L-59FLAG R	5' GAGGAGAGATCTTTATTATTACTTGTCATCGTCGTCCTTGTAGTCCTTGGAG TCGGCGGCTGCCGC 3'		BglII	pUAST
4	CGISP 1-921 Fwd	5' GAGGAG GGATCCACCATGCGTGGACGCGGCGGATTC 3'	BamHI		pCRII TOPO
5	CGISP 1-921 Rev	5' CTCCTC TCTAGAGTCGTCGGATTCATCGCCTCCATC 3'		XbaI	pCRII TOPO
6	CGISP 921-1843 Fwd	5' GAGGAG GGATCCACCCGACGATGACGATGAAGAAGACGATG 3'	BamHI		pCRII TOPO
7	CGISP 921-1843 Rev	5' CTCCTC TCTAGACTATCTCGCGCTCATCCACGCTATC 3'		XbaI	pCRII TOPO
8	CGISP 1843-2760 Fwd	5' GAGGAG GGATCCACCGATTTGAATAAATTCCACACTGTAGACTCGGTG 3'	BamHI		pCRII TOPO
9	CGISP 1843-2760 Rev	5' CTCCTC TCTAGATCACTTGGAGTCGGCGGCTGC 3'		XbaI	pCRII TOPO
10	Xbp1U/S_fwd1-GJ	5' GAGGAGACCGAATTCATGGCACCCACAGCAAACACAGTGC3'	EcoRI		pUAST
11	Xbp1U_rev1	5' CCTGCGGCAGAGGGTCAGCTTTGGATGCTGCAGATCCAAGGTTGGTGGAC GCACAG 3'			
12	Xbp1U_fwd2	5' GGATCTGCAGCATCCAAAGCTGACCCTCTGCCGCAGGGTATACAACAGGT GGACAC 3'			
13	Xbp1U_rev2 UNTAG	5' CTCCTCAGATCTTCAGGCCATTAGCTCTATGCCCGTCGG 3'		BglII	pUAST
14	Xbp1U_rev2 HA	5' CTCCTCAGATCTTCAGAGGCTAGCATAATCAGGAACATCATAC GGATAGGCCATTAGCTCTATGCCCGTCGG 3'		BglII	pUAST
15	UASpcDNA3 Xbp1U/SFwd	5' GAGGAGACCGAATTCATGGCACCCACAGCAAACACAGTGC 3'	EcoRI		pUAST
16	UASpcDNA3 Xbp1UHARev	5' CTCCTCTCTAGATCAAGCATAATCAGGAACATCATACGGATAGGCCATTA GCTCTATGCCCGTC 3'		XbaI	pUAST
17	UASpBUFXbp1SHAR	5' CTCCTCACTAGTTCAAGCGTAGTCTGGGACGTCGTATGGGTAGATCAAAC TGGGAAACAGCTCGTC 3'		SpeI	pUAST
18	CG81ExtAFwd	5' GAGGAGACCGGTACCCATGACTCAAGGGTGCGGAATTTGC 3'	Acc65I		pUAST/ pCasPeR4
19	CG81rep-proR	5' CTCCTCGGTGAATTCGCGGCCGCACGCGTACGCATCTTTAATTCCAATC TCTTCCTGTTTGCAG 3'		MluI NotI EcoRI	pUAST
20	CG81cds_mchryF1	5' GAGGAGACCCAATTGACGCGTATGCGTGGACGCGGCGGATTCATTCC 3'	MfeI MluI		pUAST
21	cnCG81cds_mchryR1	5' CTCCTCGGTGTCGACCTTGGAGTCGGCGGCTGCCGC 3'		SalI	pUAST
22	CG81_mchrycdsF2	5' GAGGAGACCCTCGAGATGGTGAGCAAGGGCGAGGAG 3'	XhoI		pUAST
23	CG81_mchrycdsR2	5' CTCCTCGGTTCTAGAGGATCCTTATTATTACTTGTACAGCTCGTCCATGCCG 3'		BamHI XbaI	pUAST/ pCasPeR4
24	CG81ExtAFwd	5' GAGGAGACC GGTACCCATGACTCAAGGGTGCGGAATTTGC 3'	Acc65I		pBluescriptSK+/ pCasPeR4
25	CG81ExtARev	5' CTCCTCGGATCC GGTGTCGACCTTTGGGTATAGCGTGC 3'		SalI BamHI	pBluescriptSK+
26	CG81ExtBFwd	5' GAGGAG GGATCCACC GTCGACATATTAATTATGCATTAAGCCAATCGCC ATG 3'	SalI BamHI		pBluescriptSK+
27	CG81ExtBRev	5' CTCCTCCTTTAATGGCGGCCGCCGAAGT 3'		NotI	pBluescriptSK+
28	CG81ExtCFwd	5' GAGGAGACTTCGGCGGCCGCCATTAAAG 3'	NotI		pBluescriptSK+
29	CG81ExtCRev	5' CTCCTCCCGCGGGGGTGGATCCGACATTGTCTGACGGAGCACCAC 3'		BamHI SacII	pBluescriptSK+/ pCasPeR4
30	CG67ExtAFwd	5' GAGGAG CTCGAGACC CCTAGGGAATCCGCCGCGTCCACGCATC 3'	XhoI AvrII		pBluescriptSK+
31	CG67ExtARev	5' CTCCTCCCCGGGGGGTGTCGACTGGTGGTGGCCAG 3'		SalI XmaI	pBluescriptSK+
32	CG67ExtBFwd	5' GAGGAG CCCGGG CCACCAGTCGACAAATGATGGGTGG 3'	SalI XmaI		pBluescriptSK+
33	CG67ExtBRev	5' CTCCTCCCGCGGGGGTGCGGCCGCGCGGCAGGGCAAAGTGC 3'		NotI SacII	pBluescriptSK+/ pCasPeR4

	qRT-PCR Primers	
	Primer Name	**Sequence**
34	rp49qRT-PCRF [a]	5’ TACAGGCCCAAGATCGTGAAG 3’
35	rp49qRT-PCRR [a]	5’ GACGCACTCTGTTGTCGATACC 3’
36	JR362 hidqRT-PCR [a]	5’ CATCAGTCAGCAGCGACAGG 3’
37	JR363 hidqRT-PCR [a]	5’ ACGAAAACGGTCACAACAGTTG 3’
38	JR366 rprqRT-PCR [a]	5’ CCAGTTGTGTAATTCCGAACGA 3’
39	JR367 rprqRT-PCR [a]	5’ GGATCTGCTGCTCCTTCTGC 3’
40	Act 5C qRT-PCRF [b]	5' CCAGTCATTCCTTTCAAACCGTG 3'
41	Act 5C qRT-PCRR [b]	5' GCCGACCATCACACCCTG 3'
42	npCG81qRT-PCRF1	5’ CCCTATTGCGGCTCTTGCCATC 3’
43	npCG81qRT-PCRR1	5’ CATCCACGCTATCATCCGATCCG 3’
44	npCG67qRT-PCRF2	5’ GCAAGCCGGTCGATCTACATCTA 3’
45	npCG67qRT-PCRR2	5’ CAATTGTTCCGAAGGCTGAGGAG 3’
46	cnXbp1SqRT-PCRF1	5’ GCCAAGAACTCGCCGAACTG 3’
47	cnXbp1SqRT-PCRR1	5’ TACCCTGCGGCAGATCCAAG 3’
48	nXbp1UqRT-PCRF2	5’ AGCATCCAAAGCTGACCCTC 3’
49	cnXbp1UqRT-PCRR2	5’ TTGCTGCTCTTCAGCTGCTC 3’
50	cnhsc3qRT-PCRF2	5’ GCGAGGAGAAGAAGGAAAAGGA 3’
51	cnhsc3qRT-PCRR2	5’ TCAACGCGTCCGTTCTTGTA 3’

[a] Moon *et al*., 2008

[b] Mehrotra *et al.*, 2008

	Sequencing Primers	
	Primer Name	**Sequence**
52	CG81ExA 1F	5’ CACGGTCACACTTCACTTTGTTCG 3’
53	CG81ExA 1R	5’ CGAACAAAGTGAAGTGTGACCGTG 3’
54	3L-59 3’ Primer 1	5’ CTACGATAGCTTCAGAAATATGCCCAG 3’
55	3L-59 3’ Primer 1 Rev	5’ CTGGGCATATTTCTGAAGCTATCGTAG 3’
56	PCR Pmer (ISP1Fwd 1-921)	5’ GAGGAGGGATCCACCATGCGTGGACGCGGCGGATTC 3’
57	3L-59 3’ Primer 2	5’ GAACAGGTGCGTACTTATAAACGGCAC 3’
58	3L-59 3’ Primer 2 Rev	5’ GTGCCGTTTATAAGTACGCACCTGTTC 3’
59	3L-59 3’ Primer 3	5’ CGCGCTGACTCAAAGTTGCCAGAC 3’
60	3L-59 3’ Primer 3 Rev	5’ GTCTGGCAACTTTGAGTCAGCGCG 3’
61	3L-59 3’ Primer 4	5’ CAGCCAATTGTGAACTATATAACCCACAAC 3’
62	3L-59 3’ Primer 4 Rev	5’ GTTGTGGGTTATATAGTTCACAATTGGCTG 3’
63	3L-59 3’ Primer 5	5’ GCGCGTTGTGCGCACCAGG 3’
64	3L-59 3’ Primer 5 Rev	5’ CCTGGTGCGCACAACGCGC 3’
65	3L-59 3’ Primer 6	5’ CATCCTGCCACCCTGACATGACTTC 3’
66	3L-59 3’ Primer 6 Rev	5’ GAAGTCATGTCAGGGTGGCAGGATG 3’
67	3L-59 3’ Primer 7	5’ GTCAAGGTGAAGGGCGACGGTG 3’
68	3L-59 3’ Primer 7 Rev	5’ CACCGTCGCCCTTCACCTTGAC 3’
69	3L-59 3’ Primer 8	5’ GTCTGTGCCGCTTGGCCTACC 3’
70	3L-59 3’ Primer 8 Rev	5’ GTAGGCCAAGCGGCACAGAC
71	3L-59 3’ Primer 10	5’ GCCGGTGGCCAAGTCGCC 3’
72	3L-59 3’ Primer 10 Rev	5’ GGCGACTTGGCCACCGGC 3’
73	ISP3Fwd (1843-2670)	5’ GATTTGAATAAATTCCACACTGTAGACTCGGTG 3’
74	CG8108 3’ UTR-Pri11	5’ CAGGTTGGTTTAGTTAGGTCTAGACATTTATTAAGC 3’
75	3L-59 3’ Primer 12F	5’ CGATAAGAAAACCATTCGAGCCAACAAAGATG 3’
76	3L-59 3’ Primer 12Rev	5’ CATCTTTGTTGGCTCGAATGGTTTTCTTATCG 3’
77	CG67ExA 1F	5’ CGTTTGATGCAGTACCATCACTG 3’
78	CG67ExA 1R	5’ CAGTGATGGTACTGCATCAAACG 3’
79	CG67ExA 2F	5’ CGACTACAGTTCTACAGCGCC 3’
80	CG67ExA 2R	5’ GGCGCTGTAGAACTGTAGTCG 3’
81	CG67ExA 3F	5’ GCAAGCTGTACACACAGGACATG 3’
82	CG67ExA 3R	5’ CATGTCCTGTGTGTACAGCTTGC 3’
83	CG67ExB 1F	5’ CGCAACTATACGAGCGCCAG 3’
84	CG67ExB 1R	5’ CTGGCGCTCGTATAGTTGCG 3’
85	CG67ExB 2F	5’ GGTCTAAATCAGCTCACTCGCTG 3’
86	CG67ExB 2R	5’ CAGCGAGTGAGCTGATTTAGACC 3’
87	CG67ExB 3F	5’ GATAGTGTCCTCGCCAGAAGTTC 3’
88	CG67ExB 3R	5’ GAACTTCTGGCGAGGACACTATC 3’
89	(*CG8108*) YellowSeqPrimer-972	5' GACTTCGCCTGGTAAAAAACGCAACAAGTCG 3'
90	(*CG8108*) BlueSeqPrimer-1461	5' GGAGTATAACTACCATCTGAACTCGCGCTC 3'

	Sequencing Primers Continued	
	Primer Name	**Sequence**
91	(CG8108) MagentaSeqPrimer-1980	5' GATTGGACCGGACTATATAAAGGTCATAGAGGCATTC 3'
92	(CG8108) RedSeqPrimer-2461	5' GGCAAAGAGGAAGCGAACGGCGATAC 3'
93	(CG8108) Green'SeqPrimer-485	5' GCTCCTACCGCCCACGCGATG 3'
94	(CG8108) RedSeqPrimer-2461	5' GGCAAAGAGGAAGCGAACGGCGATAC 3'
95	CG6718 5' Primer	5' CGCCATCCACGCCATGACTCAAG 3'
96	CG6718 3' Primer	5' CTAGAAATATCGTTTGATGCAGTACCATCAC 3'
97	CG6718-CG8108 5' Primer	5' GTGATGGTACTGCATCAAACGATATTTCTAG 3'
98	CG6718-CG8108 3' Primer	5' CAGACTGAGCGTTCAGCGCAGC 3'
99	CG8108 5' Primer	5' CGATTTTAAGCACTGATTCCACAGAGCAC 3'
100	CG8108 5' UTR/5' Primer	5' GCTGCGCTGAACGCTCAGTCTG 3'
101	CG8108 3' Primer 1	5' CTGGGCATATTTCTGAAGCTATCGTAG 3'
102	CG8108 3' UTR-Pri11	5' CAGGTTGGTTTAGTTAGGTCTAGACATTTATTAAGC 3'
103	CG81Southern3'P1F	5' GTGCTGCTGTCAGCTCTTCCTGC 3'
104	CG81Southern3'P1R	5' GGATCGTATCGTATCGCATCGGATTAAATC 3'
105	CG81Southern3'P2F	5' GATGGTATACCCGCGTTTATCGACTTG 3'
106	CG81Southern3'P2R	5' GCATAACTGTCGAATACGAAGACCCATC 3'
107	Xbp1Sseq2F	5' CAACAGCAGCACAACACCAG 3'
108	Xbp1Sseq2R	5' CTGGTGTTGTGCTGCTGTTG 3'
109	Xbp1Sseq3F	5' CCACAGCAGCGCCAGCCTCG 3'
110	Xbp1Sseq3R	5' CGAGGCTGGCGCTGCTGTGG 3'
111	Xbp1Useq2F	5' CAGCAGCACAACACCAGATGC 3'
112	Xbp1Useq2R	5' GCATCTGGTGTTGTGCTGCTG 3'
113	pUAS seqF1	5' CAAGCGCAGCTGAACAAGC 3'
114	pUAS seqF2	5' GTAACCAGCAACCAAGTAAATC 3'
115	pUAS seqR1	5' CTCTGTAGGTAGTTTGTCC 3'
116	pUAS seqR2	5' CCCATTCATCAGTTCCATAG 3'

Chapter 5

Preliminary Data and Potential Future Experiments

5.1 Introduction

The ultimate goal of this thesis project was to find genes that connected both the ER stress and apoptotic pathways. 452 p-element lethal FRT lines were screened using a DTT assay that allowed for the identification of genes that differentially activated caspases compared to wild-type and heterozygous tissues. CG8108 was identified in the screen as a loss-of-function suppressor of caspase activation during ERSIA and it was tested for effects on proximal ER stress events. CG8108 was demonstrated to facilitate *xbp1* splicing during ER stress in experiments using an *xbp1_EGFP* reporter. Additionally, CG8108 was found to physically associate with Xbp1S *in vitro* and Xbp1U both *in vivo* and *in vitro*. CG8108 is vital for development and it is a novel gene which connects the ER stress and cell death pathways.

5.2 Preliminary data

5.2.1 CG8108 may activate *xbp1* transcription

During the course of this study, qRT-PCR for *xbp1U* was conducted on RNA from *p{SuporP}CG8108*$^{-/-}$ third instar larvae incubated in S2 media for varying periods of time (Table 4). The transcription of *xbp1U* in *p{SuporP}CG8108*$^{-/-}$ animals was significantly less than *yw* larvae. The preliminary qRT-PCR data points to CG8108 as a potential transcriptional activator of Xbp1. The *xbp1_EGFP* reporter splicing defect in a *CG8108* mutant background could be explained in the context of the research by the Kohno group who demonstrated XBP1U targets its own mRNA to membranes for efficient Ire1 splicing (Yanagitani *et al*., 2009). In a *CG8108*$^{-/-}$ background, less *xbp1U* RNA is transcribed and translated and the lower abundance of Xbp1U protein could prevent targeting of *xbp1_EGFP* reporter mRNA to membranes for splicing by Ire1. The

Table 4: *CG8108* expression is required for *xbp1U* transcription

Genotype	Gene analyzed	Duration of Incubation and C_t Value					p-value
		1 hr	2 hrs	4 hrs	6 hrs	16 hrs	
yw	*xbp1U*	20.13	20.78	20.54	20.84	21.10	0.005226
p{SuporP}CG8108$^{-/-}$		21.24	20.97	21.54	21.53	21.54	

qRT-PCR was conducted on total RNA from *yw* and *p{SuporP}CG8108*$^{-/-}$ eye-brain complexes incubated in S2 media for the indicated time periods. The C_t values for *xbp1U* are listed. The *xbp1U* C_t values from *p{SuporP}CG8108*$^{-/-}$ RNAs are consistently higher than wild-type animals. Higher C_t values represent a lower abundance of a particular RNA. *p{SuporP}CG8108*$^{-/-}$ animals have reduced *xbp1U* transcription. Each experiment was conducted in triplicate and *xbp1U* was normalized to *rp49*. The p-value is based on a two-sample unequal variance one-tailed Student's t-Test.

reduction in *xbp1U* mRNA in a *CG8108*$^{-/-}$ background should also retard the production of endogenous *xbp1S*. Preliminary qRT-PCRs for *xbp1U* and *xbp1S* on RNA prepared from *yw* and *p{SuporP}CG8108*$^{-/-}$ eye-brain complexes showed that levels of endogenous *xbp1U* and *xbp1S* mRNA are lower in *CG8108*$^{-/-}$ tissues (Table 4; data not shown).

5.2.2 Xbp1S may negatively regulate CG8108

In S2R^{+} culture experiments, ectopic Xbp1S frequently reduced the levels of endogenous and ectopically expressed CG8108 (Figure 4.6: B). In cells expressing ectopic Xbp1S the amount of endogenous CG8108 immunoprecipitated was less than non-transfected cells (Figure 4.6: B, contrast *CG8108* expression in lanes 6 and 8). Ectopic CG8108 expression was also suppressed by Xbp1S (Figure 4.6: B, contrast FLAG protein levels in non-transfected cells lane 7, to Xbp1S transfected cells lanes 9

and 10). The $S2R^{+}$ cell culture data indicated CG8108 could be negatively regulated by Xbp1S.

5.3 Potential model for CG8108 function

One possible mechanism for *CG8108* action during development is as follows: CG8108 either directly or indirectly activates the transcription of *xbp1U* mRNA (pre-mRNA), which affects the production of Xbp1U protein. Xbp1U protein targets *xbp1* pre-mRNA to membrane surfaces where it can be spliced into *xbp1S* by Ire1 during ER stress. Xbp1S is a potent transcription factor and it goes to the nucleus to activate chaperones and other UPR related genes. When the UPR is terminated, Xbp1S may interact with CG8108 in the nucleus where it also binds Xbp1U. Xbp1S, Xbp1U, and CG8108 could form a complex, and Xbp1U protein shuttles Xbp1S and CG8108 from the nucleus to the proteasome for degradation, thereby dampening the UPR (Figure 5.1: A). If ER stress is prolonged and a cell cannot recover, CG8108 activates the transcription of Rpr and Hid, which in turn causes caspase activation and cell death (Figure 5.1: B).

Another student in the lab, Brieann Fant, identified CG8108 in a screen for genes that influence *Hid-EGFP* localization. Brieann Fant noted that the levels and localization of ectopic and endogenous Hid protein decrease in the absence of CG8108 function in multiple *CG8108* alleles including *CG8108Ex32-31*. The defects in Hid expression and localization in $CG8108^{-/-}$ animals was due to the loss of *CG8108* function since the phenotypes were partially rescued in *CG8108* genomic rescue 1+2; $CG8108^{-/-}$ late-stage embryos. Previous research has shown that Hid targets Rpr to the mitochondria to effect efficient cell killing (Sandu *et al*., 2010). Brieann's findings regarding CG8108 function and its effects upon Hid localization in conjunction with the data indicating

Figure 5.1 Potential model for CG8108 function

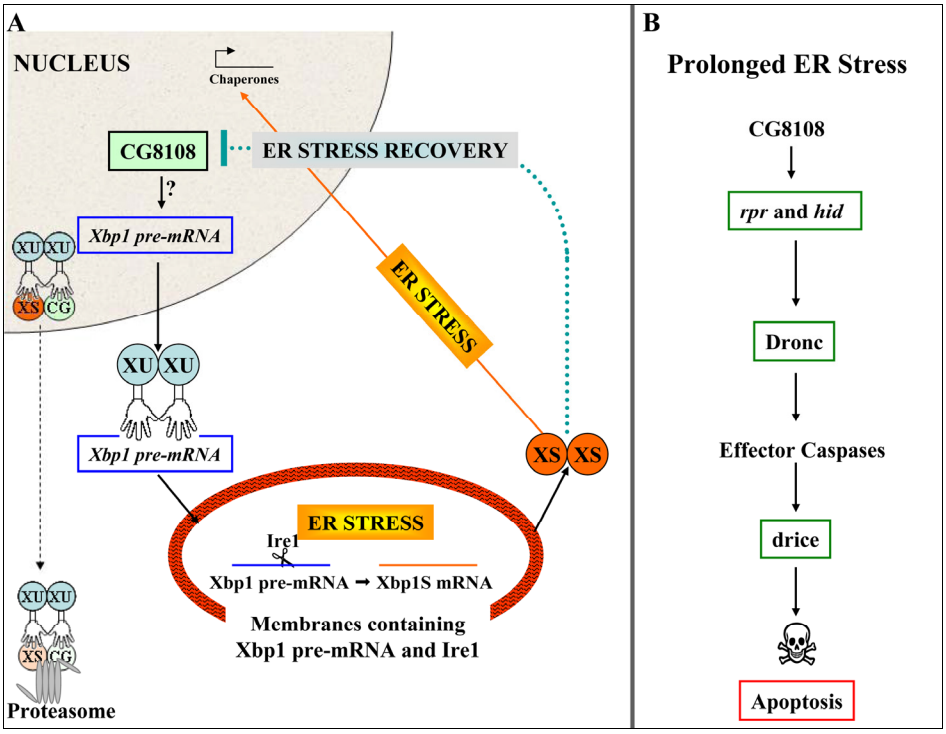

Figure 5.1: [A] Model for CG8108 function during normal development and ER stress. CG8108 is produced and localized in the nucleus (green square) where it indirectly or directly activates *xbp1* pre-mRNA transcription. Once *xbp1* pre-mRNA is transcribed (blue rectangle), Xbp1U protein (XU) transports *Xbp1* pre-mRNA to membrane surfaces (red and black oval) where Ire1 (scissors) is available to splice *xbp1* pre-mRNA (blue line) during ER stress into *xbp1S* mRNA (orange line). *xbp1S* mRNA is translated into Xbp1S protein (XS) and it translocates to the nucleus to activate chaperones during ER stress or to bind to CG8108 (CG). During ER stress recovery, Xbp1U binds to CG8108 and Xbp1S mediating their export to the cytosol for proteasomal degradation (dotted arrow). **[B]** Schematic of CG8108 upon apoptotic stimulus. CG8108 directly or indirectly mediates *rpr* and *hid* transcription allowing the activation of the initiator caspase *dronc* and effector caspases such as *drice* to induce apoptosis.

CG8108 can affect the transcription of *hid* upon irradiation (Table 3) suggests CG8108 may indirectly regulate Hid expression. It is possible CG8108 may modulate cell death by influencing the targeting of IAP antagonists at the mitochondrial outer membrane. Since ectopically expressed Hid-EGFP and CG8108_FLAG did not physically associate in $S2R^{+}$ cells, it seems unlikely CG8108 directly interacts with Hid to change its localization (data not shown). CG8108 could regulate another gene/protein which influences Hid targeting and/or levels in the cell. For example, CG8108 may suppress a factor which negatively regulates Hid. If CG8108 function is compromised, Hid may become degraded and caspase activation proceeds less efficiently.

5.4 Future characterization of *CG8108* function In order to confirm CG8108 affects *Xbp1* mRNA transcription, qRT-PCR would need to be conducted on RNA from *CG8108Ex32-31*$^{-/-}$, *CG8108* genomic rescue 1+2; *CG8108Ex32-31*$^{-/-}$, and *CG8108* genomic rescue 1+2; *p{SuporP}CG8108*$^{-/-}$ animals. The *CG8108* genomic rescue transgenes would be expected to restore Xbp1 levels. In addition, qRT-PCR for known Xbp1S targets such as *EDEM* and *hrd1* could be analyzed in mock incubated and S2 DTT treated *p{SuporP}CG8108*$^{-/-}$*, CG8108* genomic rescue 1+2; *p{SuporP}CG8108*$^{-/-}$, and *yw* tissues. If CG8108 specifically effects *xbp1* transcription, the loss of CG8108 function should strongly affect the upregulation of Xbp1S targets. qRT-PCR for *xbp1S* in stressed *p{SuporP}CG8108*$^{-/-}$ and *CG8108* genomic rescue 1+2; *p{SuporP}CG8108*$^{-/-}$ animals incubated in S2 DTT could also be utilized to confirm CG8108 affects endogenous *xbp1* splicing. The *CG8108Ex32-31* line may produce stronger phenotypes than *p{SuporP}CG8108* allele, but the early lethality of *CG8108Ex32-31*$^{-/-}$ larvae could complicate the execution of the DTT assay.

Xbp1 reporter constructs could provide a means to assess CG8108 regulation of Xbp1. One possible tool could involve a reporter line containing the *xbp1* promoter fused to a fluorescent protein. If CG8108 directly activates *xbp1* transcription, fluorescence should be readily detectable when CG8108 is ectopically expressed. Conversely, the reporter should be inactive or weakly expressed in *CG8108*$^{-/-}$ tissues. If the reporter line proves useful, deletions of the *xbp1* promoter region could be made and the *CG8108* binding sites could be identified. A second tool could consist of the *xbp1* promoter and the *xbp1* genomic region with an HA tag after the common *xbp1U/S* ATG and another tag (6x His) before the unique *xbp1S* stop codon. The production and conversion of Xbp1U and Xbp1S proteins could be analyzed by antibody staining for regions that are HA only (Xbp1U) and areas that have co-expression of HA and (6x His) (Xbp1S). The dual reporter could provide a clearer picture of Xbp1 production in a *CG8108*$^{-/-}$ and wild-type background.

In S2R^{+} cells, CG8108 physically interacts with Xbp1U and Xbp1S. The regions necessary for their interactions could be ascertained by creating deletion constructs for CG8108, Xbp1S, and Xbp1U and carrying out a series of immunoprecipitations. The deletion of important contact points would eliminate protein-protein interactions. In addition, individual and/or combinatorial site-directed mutagenesis of the CG8108 C2H2 zinc fingers would reveal if CG8108 interacts with Xbp1U/S through its C2H2 domains. CG8108 seems to be degraded by Xbp1S, but this phenomenon would need to be verified in S2R^{+} cells as well as in the fly. One way to test if CG8108 is degraded by the proteasome by Xbp1S is to add proteasome inhibitors such as MG132 to culture media, conduct an IP, and assess the levels of CG8108 expression.

In mammals, XBP1U mediates proteasomal degradation of XBP1S and ATF6 via an XBP1U C-terminal degradation domain (Yoshida *et al*., 2006; Yoshida *et al*., 2009). If CG8108 is not degraded by Xbp1S in the presence of MG132, CG8108 may undergo proteasomal degradation. The sequence similarity between Xbp1U and Xbp1S would make RNAi knock-down of *xbp1U* mRNA to distinguish between Xbp1S and Xbp1U protein contributions to CG8108 degradation a challenge in $S2R^+$ cells. One means to circumvent the $S2R^+$ *xbp1U/S* RNAi challenge is to over-express Xbp1S in *CG8108_mCherry* and $xbp1^{-/-}$; *CG8108_mCherry* tissues. If whole-eye $xbp1^{-/-}$ clones could be generated and Xbp1U is necessary for Xbp1S to degrade CG8108, ectopically expressed Xbp1S should have a stronger degradation effect in *CG8108_mCherry* eye-discs compared to $xbp1^{-/-}$; *CG8108_mCherry* discs. If $xbp1^{-/-}$ whole-eye clones cannot be generated, the degree of CG8108 degradation by Xbp1S could be tested in *Xbp1S* clones of over-expression generated in *CG8108_mCherry* and *xbp1/+*; *CG8108_mCherry* animals.

Another approach could involve the use of $xbp1^{d08698}$ flies which have a UAS sequence at the proximal end of the putative *xbp1* 5'UTR. Casas-Tinto *et al*. demonstrated that ectopic Xbp1 can be driven in the eye in $xbp1^{d08698}$ flies (Casas-Tinto *et al*., 2010). If *Gal4* expression is sufficient to promote *xbp1* transcription and *CG8108* does not directly activate Xbp1, $xbp1^{d08698}$*; p{SuporP}CG8108* (*CG8108 Ex32-31*) flies could be generated and tested for increased viability and *xbp1* splicing in $CG8108^{-/-}$ animals and tissues, respectively.

CG8108 regulation of *rpr* and *hid* could also be aided by reporter constructs. A former student in the lab Ann Tang generated a series of *rpr* reporter lines and they could

be used to determine if CG8108 directly activates *rpr*. If CG8108 directly activates *rpr*, the reporter lines could be used to identify CG8108 binding sites in the *rpr* promoter. It is very unlikely CG8108 indirectly activates *rpr,* as cleaved caspase 3 activity is not detected in the *GMR* region in *GMRGal4_UASCG8108* eye discs, (data not shown). Expanding the observations of Brieann Fant regarding CG8108 and Hid localization could also aid in understanding how CG8108 regulates cell death. Previous research has shown that Hid-mediated targeting of Rpr to the mitochondria is essential for effective cell killing (Sandu *et al*., 2010). If additional evidence demonstrating CG8108 directly or indirectly facilitates Hid localization were available, the cell death suppression phenotypes seen in $CG8108^{-/-}$ animals could be attributed to inefficient activation of apoptosis as consequence of misdirected IAP antagonists. CG8108 may associate with Hid specifically in the context of stress. In order to confirm whether CG8108 and Hid bind to each other, immunoprecipitation reactions would need to be conducted on mock treated and stressed (X-ray or DTT-treated) tissues *in vivo*. The analysis of tissues from animals expressing the *Hid-EGFP* transgene and *CG8108_mCherry* could also reveal whether CG8108 and Hid co-localize. Alternatively, CG8108 could function as a Diap1 suppressor during times of stress. If ideal sample preparation conditions were determined, it may be possible to use western blotting to show that levels of Diap1 are higher in DTT treated or irradiated $p\{SuporP\}CG8108^{-/-}$ tissues compared to *yw* eye-brain complexes. If CG8108 affected Diap1 expression, *CG8108* genomic rescue 1+2; $p\{SuporP\}CG8108^{-/-}$ tissues would be expected to have lower Diap1 levels after exposure to stress stimuli.

This study reveals a role of CG8108 during *Drosophila* development, and for the induction of apoptosis in response to stress and injury. CG8108 is a novel regulator

that connects the ER stress and cell death pathways. The current research will hopefully stimulate further work to elucidate the precise mechanism by which CG8108 activates apoptosis in response to stress and injury.

Bibliography

1. Abbott MK, Lengyel JA: **Embryonic head involution and rotation of male terminalia require the Drosophila locus head involution defective**. *Genetics* 1991, **129**(3):783-789.

2. Abdelwahid E, Yokokura T, Krieser RJ, Balasundaram S, Fowle WH, White K: **Mitochondrial disruption in Drosophila apoptosis**. *Developmental cell* 2007, **12**(5):793-806.

3. Abud HE: **Shaping developing tissues by apoptosis**. *Cell death and differentiation* 2004, **11**(8):797-799.

4. Acehan D, Jiang X, Morgan DG, Heuser JE, Wang X, Akey CW: **Three-dimensional structure of the apoptosome: implications for assembly, procaspase-9 binding, and activation**. *Molecular cell* 2002, **9**(2):423-432.

5. Acosta-Alvear D, Zhou Y, Blais A, Tsikitis M, Lents NH, Arias C, Lennon CJ, Kluger Y, Dynlacht BD: **XBP1 controls diverse cell type- and condition-specific transcriptional regulatory networks**. *Molecular cell* 2007, **27**(1):53-66.

6. Adachi Y, Yamamoto K, Okada T, Yoshida H, Harada A, Mori K: **ATF6 is a transcription factor specializing in the regulation of quality control proteins in the endoplasmic reticulum**. *Cell structure and function* 2008, **33**(1):75-89.

7. Ainscough JF, Rahman FA, Sercombe H, Sedo A, Gerlach B, Coverley D: **C-terminal domains deliver the DNA replication factor Ciz1 to the nuclear matrix**. *Journal of cell science* 2007, **120**(Pt 1):115-124.

8. Ali MM, Bagratuni T, Davenport EL, Nowak PR, Silva-Santisteban MC, Hardcastle A, McAndrews C, Rowlands MG, Morgan GJ, Aherne W *et al*: **Structure of the Ire1 autophosphorylation complex and implications for the unfolded protein response**. *The EMBO journal* 2011, **30**(5):894-905.

9. Amara JF, Lederkremer G, Lodish HF: **Intracellular degradation of unassembled asialoglycoprotein receptor subunits: a pre-Golgi, nonlysosomal endoproteolytic cleavage**. *The Journal of cell biology* 1989, **109**(6 Pt 2):3315-3324.

10. Anand S, Chakrabarti E, Kawamura H, Taylor CR, Maytin EV: **Ultraviolet light (UVB and UVA) induces the damage-responsive transcription factor CHOP/gadd153 in murine and human epidermis: evidence for a mechanism specific to intact skin**. *The Journal of investigative dermatology* 2005, **125**(2):323-333.

11. Aragon T, van Anken E, Pincus D, Serafimova IM, Korennykh AV, Rubio CA, Walter P: **Messenger RNA targeting to endoplasmic reticulum stress signalling sites**. *Nature* 2009, **457**(7230):736-740.

12. Arama E, Agapite J, Steller H: **Caspase activity and a specific cytochrome C are required for sperm differentiation in Drosophila**. *Developmental cell* 2003, **4**(5):687-697.

13. Arama E, Bader M, Rieckhof GE, Steller H: **A ubiquitin ligase complex regulates caspase activation during sperm differentiation in Drosophila**. *PLoS biology* 2007, **5**(10):e251.

14. Arama E, Bader M, Srivastava M, Bergmann A, Steller H: **The two Drosophila cytochrome C proteins can function in both respiration and caspase activation**. *The EMBO journal* 2006, **25**(1):232-243.

15. Arama E, Steller H: **Detection of apoptosis by terminal deoxynucleotidyl transferase-mediated dUTP nick-end labeling and acridine orange in Drosophila embryos and adult male gonads**. *Nature protocols* 2006, **1**(4):1725-1731.

16. Bader M, Steller H: **Regulation of cell death by the ubiquitin-proteasome system**. *Current opinion in cell biology* 2009, **21**(6):878-884.

17. Bailly-Maitre B, Fondevila C, Kaldas F, Droin N, Luciano F, Ricci JE, Croxton R, Krajewska M, Zapata JM, Kupiec-Weglinski JW *et al*: **Cytoprotective gene bi-1 is required for intrinsic protection from endoplasmic reticulum stress**

and ischemia-reperfusion injury. *Proceedings of the National Academy of Sciences of the United States of America* 2006, **103**(8):2809-2814.

18. Bartlett JD, Luethy JD, Carlson SG, Sollott SJ, Holbrook NJ: **Calcium ionophore A23187 induces expression of the growth arrest and DNA damage inducible CCAAT/enhancer-binding protein (C/EBP)-related gene, gadd153. Ca2+ increases transcriptional activity and mRNA stability**. *The Journal of biological chemistry* 1992, **267**(28):20465-20470.

19. Baum JS, Arama E, Steller H, McCall K: **The Drosophila caspases Strica and Dronc function redundantly in programmed cell death during oogenesis**. *Cell death and differentiation* 2007, **14**(8):1508-1517.

20. Bergmann A: **The role of ubiquitylation for the control of cell death in Drosophila**. *Cell death and differentiation* 2010, **17**(1):61-67.

21. Bergmann A, Agapite J, McCall K, Steller H: **The Drosophila gene hid is a direct molecular target of Ras-dependent survival signaling**. *Cell* 1998, **95**(3):331-341.

22. Bergmann A, Tugentman M, Shilo BZ, Steller H: **Regulation of cell number by MAPK-dependent control of apoptosis: a mechanism for trophic survival signaling**. *Developmental cell* 2002, **2**(2):159-170.

23. Bertolotti A, Zhang Y, Hendershot LM, Harding HP, Ron D: **Dynamic interaction of BiP and ER stress transducers in the unfolded-protein response**. *Nature cell biology* 2000, **2**(6):326-332.

24. Boatright KM, Renatus M, Scott FL, Sperandio S, Shin H, Pedersen IM, Ricci JE, Edris WA, Sutherlin DP, Green DR *et al*: **A unified model for apical caspase activation**. *Molecular cell* 2003, **11**(2):529-541.

25. Bobrovnikova-Marjon E, Hatzivassiliou G, Grigoriadou C, Romero M, Cavener DR, Thompson CB, Diehl JA: **PERK-dependent regulation of lipogenesis during mouse mammary gland development and adipocyte differentiation**. *Proceedings of the National Academy of Sciences of the United States of America* 2008, **105**(42):16314-16319.

26. Bommiasamy H, Back SH, Fagone P, Lee K, Meshinchi S, Vink E, Sriburi R, Frank M, Jackowski S, Kaufman RJ *et al*: **ATF6alpha induces XBP1-independent expansion of the endoplasmic reticulum**. *Journal of cell science* 2009, **122**(Pt 10):1626-1636.

27. Borderie VM, Baudrimont M, Vallee A, Ereau TL, Gray F, Laroche L: **Corneal endothelial cell apoptosis in patients with Fuchs' dystrophy**. *Investigative ophthalmology & visual science* 2000, **41**(9):2501-2505.

28. Calfon M, Zeng H, Urano F, Till JH, Hubbard SR, Harding HP, Clark SG, Ron D: **IRE1 couples endoplasmic reticulum load to secretory capacity by processing the XBP-1 mRNA**. *Nature* 2002, **415**(6867):92-96.

29. Call GB, Olson JM, Chen J, Villarasa N, Ngo KT, Yabroff AM, Cokus S, Pellegrini M, Bibikova E, Bui C *et al*: **Genomewide clonal analysis of lethal mutations in the Drosophila melanogaster eye: comparison of the X chromosome and autosomes**. *Genetics* 2007, **177**(2):689-697.

30. Carvalho P, Goder V, Rapoport TA: **Distinct ubiquitin-ligase complexes define convergent pathways for the degradation of ER proteins**. *Cell* 2006, **126**(2):361-373.

31. Casagrande R, Stern P, Diehn M, Shamu C, Osario M, Zuniga M, Brown PO, Ploegh H: **Degradation of proteins from the ER of S. cerevisiae requires an intact unfolded protein response pathway**. *Molecular cell* 2000, **5**(4):729-735.

32. Casas-Tinto S, Zhang Y, Sanchez-Garcia J, Gomez-Velazquez M, Rincon-Limas DE, Fernandez-Funez P: **The ER stress factor XBP1s prevents amyloid-beta neurotoxicity**. *Human molecular genetics* 2011, **20**(11):2144-2160.

33. Castillo K, Rojas-Rivera D, Lisbona F, Caballero B, Nassif M, Court FA, Schuck S, Ibar C, Walter P, Sierralta J *et al*: **BAX inhibitor-1 regulates autophagy by controlling the IRE1alpha branch of the unfolded protein response**. *The EMBO journal* 2011, **30**(21):4465-4478.

34. Chai J, Du C, Wu JW, Kyin S, Wang X, Shi Y: **Structural and biochemical basis of apoptotic activation by Smac/DIABLO**. *Nature* 2000, **406**(6798):855-862.

35. Chai J, Wu Q, Shiozaki E, Srinivasula SM, Alnemri ES, Shi Y: **Crystal structure of a procaspase-7 zymogen: mechanisms of activation and substrate binding**. *Cell* 2001, **107**(3):399-407.

36. Chai J, Yan N, Huh JR, Wu JW, Li W, Hay BA, Shi Y: **Molecular mechanism of Reaper-Grim-Hid-mediated suppression of DIAP1-dependent Dronc ubiquitination**. *Nature structural biology* 2003, **10**(11):892-898.

37. Challa M, Malladi S, Pellock BJ, Dresnek D, Varadarajan S, Yin YW, White K, Bratton SB: **Drosophila Omi, a mitochondrial-localized IAP antagonist and proapoptotic serine protease**. *The EMBO journal* 2007, **26**(13):3144-3156.

38. Chapman RE, Walter P: **Translational attenuation mediated by an mRNA intron**. *Current biology : CB* 1997, **7**(11):850-859.

39. Chen P, Nordstrom W, Gish B, Abrams JM: **grim, a novel cell death gene in Drosophila**. *Genes & development* 1996, **10**(14):1773-1782.

40. Chen P, Rodriguez A, Erskine R, Thach T, Abrams JM: **Dredd, a novel effector of the apoptosis activators reaper, grim, and hid in Drosophila**. *Developmental biology* 1998, **201**(2):202-216.

41. Claveria C, Caminero E, Martinez AC, Campuzano S, Torres M: **GH3, a novel proapoptotic domain in Drosophila Grim, promotes a mitochondrial death pathway**. *The EMBO journal* 2002, **21**(13):3327-3336.

42. Clem RJ, Fechheimer M, Miller LK: **Prevention of apoptosis by a baculovirus gene during infection of insect cells**. *Science* 1991, **254**(5036):1388-1390.

43. Clerc S, Hirsch C, Oggier DM, Deprez P, Jakob C, Sommer T, Aebi M: **Htm1 protein generates the N-glycan signal for glycoprotein degradation in the endoplasmic reticulum**. *The Journal of cell biology* 2009, **184**(1):159-172.

44. Colussi PA, Quinn LM, Huang DC, Coombe M, Read SH, Richardson H, Kumar S: **Debcl, a proapoptotic Bcl-2 homologue, is a component of the Drosophila melanogaster cell death machinery**. *The Journal of cell biology* 2000, **148**(4):703-714.

45. Conradt B, Horvitz HR: **The C. elegans protein EGL-1 is required for programmed cell death and interacts with the Bcl-2-like protein CED-9**. *Cell* 1998, **93**(4):519-529.

46. Conte D, Holcik M, Lefebvre CA, Lacasse E, Picketts DJ, Wright KE, Korneluk RG: **Inhibitor of apoptosis protein cIAP2 is essential for lipopolysaccharide-induced macrophage survival**. *Molecular and cellular biology* 2006, **26**(2):699-708.

47. Conze DB, Albert L, Ferrick DA, Goeddel DV, Yeh WC, Mak T, Ashwell JD: **Posttranscriptional downregulation of c-IAP2 by the ubiquitin protein ligase c-IAP1 in vivo**. *Molecular and cellular biology* 2005, **25**(8):3348-3356.

48. Coverley D, Marr J, Ainscough J: **Ciz1 promotes mammalian DNA replication**. *Journal of cell science* 2005, **118**(Pt 1):101-112.

49. Cox JS, Chapman RE, Walter P: **The unfolded protein response coordinates the production of endoplasmic reticulum protein and endoplasmic reticulum membrane**. *Molecular biology of the cell* 1997, **8**(9):1805-1814.

50. Cox JS, Shamu CE, Walter P: **Transcriptional induction of genes encoding endoplasmic reticulum resident proteins requires a transmembrane protein kinase**. *Cell* 1993, **73**(6):1197-1206.

51. Cox JS, Walter P: **A novel mechanism for regulating activity of a transcription factor that controls the unfolded protein response**. *Cell* 1996, **87**(3):391-404.

52. Credle JJ, Finer-Moore JS, Papa FR, Stroud RM, Walter P: **On the mechanism of sensing unfolded protein in the endoplasmic reticulum**. *Proceedings of the National Academy of Sciences of the United States of America* 2005, **102**(52):18773-18784.

53. Davidson FF, Steller H: **Blocking apoptosis prevents blindness in Drosophila retinal degeneration mutants**. *Nature* 1998, **391**(6667):587-591.

54. del Peso L, Gonzalez VM, Inohara N, Ellis RE, Nunez G: **Disruption of the CED-9.CED-4 complex by EGL-1 is a critical step for programmed cell**

death in Caenorhabditis elegans. *The Journal of biological chemistry* 2000, **275**(35):27205-27211.

55. del Peso L, Gonzalez VM, Nunez G: **Caenorhabditis elegans EGL-1 disrupts the interaction of CED-9 with CED-4 and promotes CED-3 activation**. *The Journal of biological chemistry* 1998, **273**(50):33495-33500.

56. Denic V, Quan EM, Weissman JS: **A luminal surveillance complex that selects misfolded glycoproteins for ER-associated degradation**. *Cell* 2006, **126**(2):349-359.

57. Deveraux QL, Roy N, Stennicke HR, Van Arsdale T, Zhou Q, Srinivasula SM, Alnemri ES, Salvesen GS, Reed JC: **IAPs block apoptotic events induced by caspase-8 and cytochrome c by direct inhibition of distinct caspases**. *The EMBO journal* 1998, **17**(8):2215-2223.

58. Deveraux QL, Takahashi R, Salvesen GS, Reed JC: **X-linked IAP is a direct inhibitor of cell-death proteases**. *Nature* 1997, **388**(6639):300-304.

59. Domingues C, Ryoo HD: **Drosophila BRUCE inhibits apoptosis through non-lysine ubiquitination of the IAP-antagonist REAPER**. *Cell death and differentiation* 2012, **19**(3):470-477.

60. Dorstyn L, Colussi PA, Quinn LM, Richardson H, Kumar S: **DRONC, an ecdysone-inducible Drosophila caspase**. *Proceedings of the National Academy of Sciences of the United States of America* 1999, **96**(8):4307-4312.

61. Dorstyn L, Read S, Cakouros D, Huh JR, Hay BA, Kumar S: **The role of cytochrome c in caspase activation in Drosophila melanogaster cells**. *The Journal of cell biology* 2002, **156**(6):1089-1098.

62. Dorstyn L, Read SH, Quinn LM, Richardson H, Kumar S: **DECAY, a novel Drosophila caspase related to mammalian caspase-3 and caspase-7**. *The Journal of biological chemistry* 1999, **274**(43):30778-30783.

63. Doumanis J, Quinn L, Richardson H, Kumar S: **STRICA, a novel Drosophila melanogaster caspase with an unusual serine/threonine-rich prodomain,**

interacts with DIAP1 and DIAP2. *Cell death and differentiation* 2001, **8**(4):387-394.

64. Du C, Fang M, Li Y, Li L, Wang X: **Smac, a mitochondrial protein that promotes cytochrome c-dependent caspase activation by eliminating IAP inhibition**. *Cell* 2000, **102**(1):33-42.

65. Ellgaard L, Helenius A: **Quality control in the endoplasmic reticulum**. *Nature reviews Molecular cell biology* 2003, **4**(3):181-191.

66. Ellis HM, Horvitz HR: **Genetic control of programmed cell death in the nematode C. elegans**. *Cell* 1986, **44**(6):817-829.

67. Fan Y, Bergmann A: **The cleaved-Caspase-3 antibody is a marker of Caspase-9-like DRONC activity in Drosophila**. *Cell death and differentiation* 2010, **17**(3):534-539.

68. Farny NG, Kedersha NL, Silver PA: **Metazoan stress granule assembly is mediated by P-eIF2alpha-dependent and -independent mechanisms**. *RNA* 2009, **15**(10):1814-1821.

69. Fernandez F, Jannatipour M, Hellman U, Rokeach LA, Parodi AJ: **A new stress protein: synthesis of Schizosaccharomyces pombe UDP--Glc:glycoprotein glucosyltransferase mRNA is induced by stress conditions but the enzyme is not essential for cell viability**. *The EMBO journal* 1996, **15**(4):705-713.

70. Fraser AG, Evan GI: **Identification of a Drosophila melanogaster ICE/CED-3-related protease, drICE**. *The EMBO journal* 1997, **16**(10):2805-2813.

71. Freel CD, Richardson DA, Thomenius MJ, Gan EC, Horn SR, Olson MR, Kornbluth S: **Mitochondrial localization of Reaper to promote inhibitors of apoptosis protein degradation conferred by GH3 domain-lipid interactions**. *The Journal of biological chemistry* 2008, **283**(1):367-379.

72. Friedlander R, Jarosch E, Urban J, Volkwein C, Sommer T: **A regulatory link between ER-associated protein degradation and the unfolded-protein response**. *Nature cell biology* 2000, **2**(7):379-384.

73. Fuchs Y, Steller H: **Programmed cell death in animal development and disease**. *Cell* 2011, **147**(4):742-758.

74. Gafuik C, Steller H: **A gain-of-function germline mutation in Drosophila ras1 affects apoptosis and cell fate during development**. *PloS one* 2011, **6**(8):e23535.

75. Gesellchen V, Kuttenkeuler D, Steckel M, Pelte N, Boutros M: **An RNA interference screen identifies Inhibitor of Apoptosis Protein 2 as a regulator of innate immune signalling in Drosophila**. *EMBO reports* 2005, **6**(10):979-984.

76. Gething MJ, Sambrook J: **Protein folding in the cell**. *Nature* 1992, **355**(6355):33-45.

77. Giot L, Bader JS, Brouwer C, Chaudhuri A, Kuang B, Li Y, Hao YL, Ooi CE, Godwin B, Vitols E *et al*: **A protein interaction map of Drosophila melanogaster**. *Science* 2003, **302**(5651):1727-1736.

78. Golic MM, Rong YS, Petersen RB, Lindquist SL, Golic KG: **FLP-mediated DNA mobilization to specific target sites in Drosophila chromosomes**. *Nucleic acids research* 1997, **25**(18):3665-3671.

79. Gottfried Y, Rotem A, Lotan R, Steller H, Larisch S: **The mitochondrial ARTS protein promotes apoptosis through targeting XIAP**. *The EMBO journal* 2004, **23**(7):1627-1635.

80. Goyal L, McCall K, Agapite J, Hartwieg E, Steller H: **Induction of apoptosis by Drosophila reaper, hid and grim through inhibition of IAP function**. *The EMBO journal* 2000, **19**(4):589-597.

81. Grether ME, Abrams JM, Agapite J, White K, Steller H: **The head involution defective gene of Drosophila melanogaster functions in programmed cell death**. *Genes & development* 1995, **9**(14):1694-1708.

82. Gu F, Nguyen DT, Stuible M, Dube N, Tremblay ML, Chevet E: **Protein-tyrosine phosphatase 1B potentiates IRE1 signaling during endoplasmic**

reticulum stress. *The Journal of biological chemistry* 2004, **279**(48):49689-49693.

83. Haining WN, Carboy-Newcomb C, Wei CL, Steller H: **The proapoptotic function of Drosophila Hid is conserved in mammalian cells**. *Proceedings of the National Academy of Sciences of the United States of America* 1999, **96**(9):4936-4941.

84. Halfon MS, Gisselbrecht S, Lu J, Estrada B, Keshishian H, Michelson AM: **New fluorescent protein reporters for use with the Drosophila Gal4 expression system and for vital detection of balancer chromosomes**. *Genesis* 2002, **34**(1-2):135-138.

85. Hampton RY, Gardner RG, Rine J: **Role of 26S proteasome and HRD genes in the degradation of 3-hydroxy-3-methylglutaryl-CoA reductase, an integral endoplasmic reticulum membrane protein**. *Molecular biology of the cell* 1996, **7**(12):2029-2044.

86. Han D, Lerner AG, Vande Walle L, Upton JP, Xu W, Hagen A, Backes BJ, Oakes SA, Papa FR: **IRE1alpha kinase activation modes control alternate endoribonuclease outputs to determine divergent cell fates**. *Cell* 2009, **138**(3):562-575.

87. Harding HP, Novoa I, Zhang Y, Zeng H, Wek R, Schapira M, Ron D: **Regulated translation initiation controls stress-induced gene expression in mammalian cells**. *Molecular cell* 2000, **6**(5):1099-1108.

88. Harding HP, Zeng H, Zhang Y, Jungries R, Chung P, Plesken H, Sabatini DD, Ron D: **Diabetes mellitus and exocrine pancreatic dysfunction in perk-/- mice reveals a role for translational control in secretory cell survival**. *Molecular cell* 2001, **7**(6):1153-1163.

89. Harding HP, Zhang Y, Ron D: **Protein translation and folding are coupled by an endoplasmic-reticulum-resident kinase**. *Nature* 1999, **397**(6716):271-274.

90. Harding HP, Zhang Y, Zeng H, Novoa I, Lu PD, Calfon M, Sadri N, Yun C, Popko B, Paules R *et al*: **An integrated stress response regulates amino acid**

metabolism and resistance to oxidative stress. *Molecular cell* 2003, **11**(3):619-633.

91. Harlin H, Reffey SB, Duckett CS, Lindsten T, Thompson CB: **Characterization of XIAP-deficient mice**. *Molecular and cellular biology* 2001, **21**(10):3604-3608.

92. Harvey NL, Daish T, Mills K, Dorstyn L, Quinn LM, Read SH, Richardson H, Kumar S: **Characterization of the Drosophila caspase, DAMM**. *The Journal of biological chemistry* 2001, **276**(27):25342-25350.

93. Hay BA, Wassarman DA, Rubin GM: **Drosophila homologs of baculovirus inhibitor of apoptosis proteins function to block cell death**. *Cell* 1995, **83**(7):1253-1262.

94. Haze K, Okada T, Yoshida H, Yanagi H, Yura T, Negishi M, Mori K: **Identification of the G13 (cAMP-response-element-binding protein-related protein) gene product related to activating transcription factor 6 as a transcriptional activator of the mammalian unfolded protein response**. *The Biochemical journal* 2001, **355**(Pt 1):19-28.

95. Haze K, Yoshida H, Yanagi H, Yura T, Mori K: **Mammalian transcription factor ATF6 is synthesized as a transmembrane protein and activated by proteolysis in response to endoplasmic reticulum stress**. *Molecular biology of the cell* 1999, **10**(11):3787-3799.

96. Hegde R, Srinivasula SM, Zhang Z, Wassell R, Mukattash R, Cilenti L, DuBois G, Lazebnik Y, Zervos AS, Fernandes-Alnemri T *et al*: **Identification of Omi/HtrA2 as a mitochondrial apoptotic serine protease that disrupts inhibitor of apoptosis protein-caspase interaction**. *The Journal of biological chemistry* 2002, **277**(1):432-438.

97. Helenius A, Marquardt T, Braakman I: **The endoplasmic reticulum as a protein-folding compartment**. *Trends in cell biology* 1992, **2**(8):227-231.

98. Hengartner MO: **The biochemistry of apoptosis**. *Nature* 2000, **407**(6805):770-776.

99. Hengartner MO, Ellis RE, Horvitz HR: **Caenorhabditis elegans gene ced-9 protects cells from programmed cell death**. *Nature* 1992, **356**(6369):494-499.

100. Hengartner MO, Horvitz HR: **The ins and outs of programmed cell death during C. elegans development**. *Philosophical transactions of the Royal Society of London Series B, Biological sciences* 1994, **345**(1313):243-246.

101. Hetz C, Bernasconi P, Fisher J, Lee AH, Bassik MC, Antonsson B, Brandt GS, Iwakoshi NN, Schinzel A, Glimcher LH *et al*: **Proapoptotic BAX and BAK modulate the unfolded protein response by a direct interaction with IRE1alpha**. *Science* 2006, **312**(5773):572-576.

102. Hetz C, Glimcher LH: **Fine-tuning of the unfolded protein response: Assembling the IRE1alpha interactome**. *Molecular cell* 2009, **35**(5):551-561.

103. Hollien J, Lin JH, Li H, Stevens N, Walter P, Weissman JS: **Regulated Ire1-dependent decay of messenger RNAs in mammalian cells**. *The Journal of cell biology* 2009, **186**(3):323-331.

104. Hollien J, Weissman JS: **Decay of endoplasmic reticulum-localized mRNAs during the unfolded protein response**. *Science* 2006, **313**(5783):104-107.

105. Hoozemans JJ, van Haastert ES, Eikelenboom P, de Vos RA, Rozemuller JM, Scheper W: **Activation of the unfolded protein response in Parkinson's disease**. *Biochemical and biophysical research communications* 2007, **354**(3):707-711.

106. Hoozemans JJ, van Haastert ES, Nijholt DA, Rozemuller AJ, Eikelenboom P, Scheper W: **The unfolded protein response is activated in pretangle neurons in Alzheimer's disease hippocampus**. *The American journal of pathology* 2009, **174**(4):1241-1251.

107. Horvitz HR, Shaham S, Hengartner MO: **The genetics of programmed cell death in the nematode Caenorhabditis elegans**. *Cold Spring Harbor symposia on quantitative biology* 1994, **59**:377-385.

108. Hosokawa N, Wada I, Hasegawa K, Yorihuzi T, Tremblay LO, Herscovics A, Nagata K: **A novel ER alpha-mannosidase-like protein accelerates ER-associated degradation**. *EMBO reports* 2001, **2**(5):415-422.

109. Huang Y, Rich RL, Myszka DG, Wu H: **Requirement of both the second and third BIR domains for the relief of X-linked inhibitor of apoptosis protein (XIAP)-mediated caspase inhibition by Smac**. *The Journal of biological chemistry* 2003, **278**(49):49517-49522.

110. Huh JR, Foe I, Muro I, Chen CH, Seol JH, Yoo SJ, Guo M, Park JM, Hay BA: **The Drosophila inhibitor of apoptosis (IAP) DIAP2 is dispensable for cell survival, required for the innate immune response to gram-negative bacterial infection, and can be negatively regulated by the reaper/hid/grim family of IAP-binding apoptosis inducers**. *The Journal of biological chemistry* 2007, **282**(3):2056-2068.

111. Hurtley SM, Bole DG, Hoover-Litty H, Helenius A, Copeland CS: **Interactions of misfolded influenza virus hemagglutinin with binding protein (BiP)**. *The Journal of cell biology* 1989, **108**(6):2117-2126.

112. Iwawaki T, Akai R, Yamanaka S, Kohno K: **Function of IRE1 alpha in the placenta is essential for placental development and embryonic viability**. *Proceedings of the National Academy of Sciences of the United States of America* 2009, **106**(39):16657-16662.

113. Jiang C, Lamblin AF, Steller H, Thummel CS: **A steroid-triggered transcriptional hierarchy controls salivary gland cell death during Drosophila metamorphosis**. *Molecular cell* 2000, **5**(3):445-455.

114. Jones G, Jones D, Zhou L, Steller H, Chu Y: **Deterin, a new inhibitor of apoptosis from Drosophila melanogaster**. *The Journal of biological chemistry* 2000, **275**(29):22157-22165.

115. Ju W, Valencia CA, Pang H, Ke Y, Gao W, Dong B, Liu R: **Proteome-wide identification of family member-specific natural substrate repertoire of caspases**. *Proceedings of the National Academy of Sciences of the United States of America* 2007, **104**(36):14294-14299.

116. Kallappagoudar S, Varma P, Pathak RU, Senthilkumar R, Mishra RK: **Nuclear matrix proteome analysis of Drosophila melanogaster**. *Molecular & cellular proteomics : MCP* 2010, **9**(9):2005-2018.

117. Kaneko M, Ishiguro M, Niinuma Y, Uesugi M, Nomura Y: **Human HRD1 protects against ER stress-induced apoptosis through ER-associated degradation**. *FEBS letters* 2002, **532**(1-2):147-152.

118. Kang MJ, Ryoo HD: **Suppression of retinal degeneration in Drosophila by stimulation of ER-associated degradation**. *Proceedings of the National Academy of Sciences of the United States of America* 2009, **106**(40):17043-17048.

119. Kanuka H, Sawamoto K, Inohara N, Matsuno K, Okano H, Miura M: **Control of the cell death pathway by Dapaf-1, a Drosophila Apaf-1/CED-4-related caspase activator**. *Molecular cell* 1999, **4**(5):757-769.

120. Kaplan Y, Gibbs-Bar L, Kalifa Y, Feinstein-Rotkopf Y, Arama E: **Gradients of a ubiquitin E3 ligase inhibitor and a caspase inhibitor determine differentiation or death in spermatids**. *Developmental cell* 2010, **19**(1):160-173.

121. Kawahara T, Yanagi H, Yura T, Mori K: **Endoplasmic reticulum stress-induced mRNA splicing permits synthesis of transcription factor Hac1p/Ern4p that activates the unfolded protein response**. *Molecular biology of the cell* 1997, **8**(10):1845-1862.

122. Kerr JF, Wyllie AH, Currie AR: **Apoptosis: a basic biological phenomenon with wide-ranging implications in tissue kinetics**. *British journal of cancer* 1972, **26**(4):239-257.

123. Khan FS, Fujioka M, Datta P, Fernandes-Alnemri T, Jaynes JB, Alnemri ES: **The interaction of DIAP1 with dOmi/HtrA2 regulates cell death in Drosophila**. *Cell death and differentiation* 2008, **15**(6):1073-1083.

124. Klee M, Pallauf K, Alcala S, Fleischer A, Pimentel-Muinos FX: **Mitochondrial apoptosis induced by BH3-only molecules in the exclusive presence of endoplasmic reticular Bak**. *The EMBO journal* 2009, **28**(12):1757-1768.

125. Knop M, Finger A, Braun T, Hellmuth K, Wolf DH: **Der1, a novel protein specifically required for endoplasmic reticulum degradation in yeast**. *The EMBO journal* 1996, **15**(4):753-763.

126. Kobayashi T, Tanaka K, Inoue K, Kakizuka A: **Functional ATPase activity of p97/valosin-containing protein (VCP) is required for the quality control of endoplasmic reticulum in neuronally differentiated mammalian PC12 cells**. *The Journal of biological chemistry* 2002, **277**(49):47358-47365.

127. Kondo S, Senoo-Matsuda N, Hiromi Y, Miura M: **DRONC coordinates cell death and compensatory proliferation**. *Molecular and cellular biology* 2006, **26**(19):7258-7268.

128. Korennykh AV, Egea PF, Korostelev AA, Finer-Moore J, Zhang C, Shokat KM, Stroud RM, Walter P: **The unfolded protein response signals through high-order assembly of Ire1**. *Nature* 2009, **457**(7230):687-693.

129. Kozutsumi Y, Segal M, Normington K, Gething MJ, Sambrook J: **The presence of malfolded proteins in the endoplasmic reticulum signals the induction of glucose-regulated proteins**. *Nature* 1988, **332**(6163):462-464.

130. Kuida K, Haydar TF, Kuan CY, Gu Y, Taya C, Karasuyama H, Su MS, Rakic P, Flavell RA: **Reduced apoptosis and cytochrome c-mediated caspase activation in mice lacking caspase 9**. *Cell* 1998, **94**(3):325-337.

131. Kurada P, White K: **Ras promotes cell survival in Drosophila by downregulating hid expression**. *Cell* 1998, **95**(3):319-329.

132. Laundrie B, Peterson JS, Baum JS, Chang JC, Fileppo D, Thompson SR, McCall K: **Germline cell death is inhibited by P-element insertions disrupting the dcp-1/pita nested gene pair in Drosophila**. *Genetics* 2003, **165**(4):1881-1888.

133. Le T, Liang Z, Patel H, Yu MH, Sivasubramaniam G, Slovitt M, Tanentzapf G, Mohanty N, Paul SM, Wu VM *et al*: **A new family of Drosophila balancer chromosomes with a w- dfd-GMR yellow fluorescent protein marker**. *Genetics* 2006, **174**(4):2255-2257.

134. Lee AH, Iwakoshi NN, Glimcher LH: **XBP-1 regulates a subset of endoplasmic reticulum resident chaperone genes in the unfolded protein response**. *Molecular and cellular biology* 2003, **23**(21):7448-7459.

135. Lee G, Wang Z, Sehgal R, Chen CH, Kikuno K, Hay B, Park JH: **Drosophila caspases involved in developmentally regulated programmed cell death of peptidergic neurons during early metamorphosis**. *The Journal of comparative neurology* 2011, **519**(1):34-48.

136. Lee K, Tirasophon W, Shen X, Michalak M, Prywes R, Okada T, Yoshida H, Mori K, Kaufman RJ: **IRE1-mediated unconventional mRNA splicing and S2P-mediated ATF6 cleavage merge to regulate XBP1 in signaling the unfolded protein response**. *Genes & development* 2002, **16**(4):452-466.

137. Lee KP, Dey M, Neculai D, Cao C, Dever TE, Sicheri F: **Structure of the dual enzyme Ire1 reveals the basis for catalysis and regulation in nonconventional RNA splicing**. *Cell* 2008, **132**(1):89-100.

138. Leulier F, Ribeiro PS, Palmer E, Tenev T, Takahashi K, Robertson D, Zachariou A, Pichaud F, Ueda R, Meier P: **Systematic in vivo RNAi analysis of putative components of the Drosophila cell death machinery**. *Cell death and differentiation* 2006, **13**(10):1663-1674.

139. Leulier F, Rodriguez A, Khush RS, Abrams JM, Lemaitre B: **The Drosophila caspase Dredd is required to resist gram-negative bacterial infection**. *EMBO reports* 2000, **1**(4):353-358.

140. Li P, Nijhawan D, Budihardjo I, Srinivasula SM, Ahmad M, Alnemri ES, Wang X: **Cytochrome c and dATP-dependent formation of Apaf-1/caspase-9 complex initiates an apoptotic protease cascade**. *Cell* 1997, **91**(4):479-489.

141. Lin JH, Li H, Yasumura D, Cohen HR, Zhang C, Panning B, Shokat KM, Lavail MM, Walter P: **IRE1 signaling affects cell fate during the unfolded protein response**. *Science* 2007, **318**(5852):944-949.

142. Lippincott-Schwartz J, Bonifacino JS, Yuan LC, Klausner RD: **Degradation from the endoplasmic reticulum: disposing of newly synthesized proteins**. *Cell* 1988, **54**(2):209-220.

143. Lisbona F, Rojas-Rivera D, Thielen P, Zamorano S, Todd D, Martinon F, Glavic A, Kress C, Lin JH, Walter P *et al*: **BAX inhibitor-1 is a negative regulator of the ER stress sensor IRE1alpha**. *Molecular cell* 2009, **33**(6):679-691.

144. Lisi S, Mazzon I, White K: **Diverse domains of THREAD/DIAP1 are required to inhibit apoptosis induced by REAPER and HID in Drosophila**. *Genetics* 2000, **154**(2):669-678.

145. Liu Y, Choudhury P, Cabral CM, Sifers RN: **Oligosaccharide modification in the early secretory pathway directs the selection of a misfolded glycoprotein for degradation by the proteasome**. *The Journal of biological chemistry* 1999, **274**(9):5861-5867.

146. Liu Y, Lehmann M: **A genomic response to the yeast transcription factor GAL4 in Drosophila**. *Fly* 2008, **2**(2):92-98.

147. Luo D, He Y, Zhang H, Yu L, Chen H, Xu Z, Tang S, Urano F, Min W: **AIP1 is critical in transducing IRE1-mediated endoplasmic reticulum stress response**. *The Journal of biological chemistry* 2008, **283**(18):11905-11912.

148. Luo S, Mao C, Lee B, Lee AS: **GRP78/BiP is required for cell proliferation and protecting the inner cell mass from apoptosis during early mouse embryonic development**. *Molecular and cellular biology* 2006, **26**(15):5688-5697.

149. Ma K, Vattem KM, Wek RC: **Dimerization and release of molecular chaperone inhibition facilitate activation of eukaryotic initiation factor-2 kinase in response to endoplasmic reticulum stress**. *The Journal of biological chemistry* 2002, **277**(21):18728-18735.

150. Malhotra A, Edelman-Novemsky I, Xu Y, Plesken H, Ma J, Schlame M, Ren M: **Role of calcium-independent phospholipase A2 in the pathogenesis of Barth syndrome**. *Proceedings of the National Academy of Sciences of the United States of America* 2009, **106**(7):2337-2341.

151. Malzer E, Daly ML, Moloney A, Sendall TJ, Thomas SE, Ryder E, Ryoo HD, Crowther DC, Lomas DA, Marciniak SJ: **Impaired tissue growth is mediated**

by checkpoint kinase 1 (CHK1) in the integrated stress response. *Journal of cell science* 2010, **123**(Pt 17):2892-2900.

152. Manion MK, Hockenbery DM: **Targeting BCL-2-related proteins in cancer therapy**. *Cancer biology & therapy* 2003, **2**(4 Suppl 1):S105-114.

153. Marciniak SJ, Ron D: **Endoplasmic reticulum stress signaling in disease**. *Physiological reviews* 2006, **86**(4):1133-1149.

154. Marciniak SJ, Yun CY, Oyadomari S, Novoa I, Zhang Y, Jungreis R, Nagata K, Harding HP, Ron D: **CHOP induces death by promoting protein synthesis and oxidation in the stressed endoplasmic reticulum**. *Genes & development* 2004, **18**(24):3066-3077.

155. McCall K, Steller H: **Facing death in the fly: genetic analysis of apoptosis in Drosophila**. *Trends in genetics : TIG* 1997, **13**(6):222-226.

156. McCarthy JV, Dixit VM: **Apoptosis induced by Drosophila reaper and grim in a human system. Attenuation by inhibitor of apoptosis proteins (cIAPs)**. *The Journal of biological chemistry* 1998, **273**(37):24009-24015.

157. McQuilton P, St Pierre SE, Thurmond J: **FlyBase 101--the basics of navigating FlyBase (www.flybase.com)**. *Nucleic acids research* 2012, **40**(Database issue):D706-714.

158. Mehrotra S, Maqbool SB, Kolpakas A, Murnen K, Calvi BR: **Endocycling cells do not apoptose in response to DNA rereplication genotoxic stress**. *Genes & development* 2008, **22**(22):3158-3171.

159. Meier P, Silke J, Leevers SJ, Evan GI: **The Drosophila caspase DRONC is regulated by DIAP1**. *The EMBO journal* 2000, **19**(4):598-611.

160. Mendes CS, Arama E, Brown S, Scherr H, Srivastava M, Bergmann A, Steller H, Mollereau B: **Cytochrome c-d regulates developmental apoptosis in the Drosophila retina**. *EMBO reports* 2006, **7**(9):933-939.

161. Mendes CS, Levet C, Chatelain G, Dourlen P, Fouillet A, Dichtel-Danjoy ML, Gambis A, Ryoo HD, Steller H, Mollereau B: **ER stress protects from retinal degeneration**. *The EMBO journal* 2009, **28**(9):1296-1307.

162. Mendes HF, van der Spuy J, Chapple JP, Cheetham ME: **Mechanisms of cell death in rhodopsin retinitis pigmentosa: implications for therapy**. *Trends in molecular medicine* 2005, **11**(4):177-185.

163. Meunier L, Usherwood YK, Chung KT, Hendershot LM: **A subset of chaperones and folding enzymes form multiprotein complexes in endoplasmic reticulum to bind nascent proteins**. *Molecular biology of the cell* 2002, **13**(12):4456-4469.

164. Miura M, Zhu H, Rotello R, Hartwieg EA, Yuan J: **Induction of apoptosis in fibroblasts by IL-1 beta-converting enzyme, a mammalian homolog of the C. elegans cell death gene ced-3**. *Cell* 1993, **75**(4):653-660.

165. Molinari M, Calanca V, Galli C, Lucca P, Paganetti P: **Role of EDEM in the release of misfolded glycoproteins from the calnexin cycle**. *Science* 2003, **299**(5611):1397-1400.

166. Moon NS, Di Stefano L, Morris EJ, Patel R, White K, Dyson NJ: **E2F and p53 induce apoptosis independently during Drosophila development but intersect in the context of DNA damage**. *PLoS genetics* 2008, **4**(8):e1000153.

167. Mori K: **Signalling pathways in the unfolded protein response: development from yeast to mammals**. *Journal of biochemistry* 2009, **146**(6):743-750.

168. Mori K, Kawahara T, Yoshida H, Yanagi H, Yura T: **Signalling from endoplasmic reticulum to nucleus: transcription factor with a basic-leucine zipper motif is required for the unfolded protein-response pathway**. *Genes to cells : devoted to molecular & cellular mechanisms* 1996, **1**(9):803-817.

169. Mori K, Ma W, Gething MJ, Sambrook J: **A transmembrane protein with a cdc2+/CDC28-related kinase activity is required for signaling from the ER to the nucleus**. *Cell* 1993, **74**(4):743-756.

170. Mori K, Ogawa N, Kawahara T, Yanagi H, Yura T: **Palindrome with spacer of one nucleotide is characteristic of the cis-acting unfolded protein response element in Saccharomyces cerevisiae**. *The Journal of biological chemistry* 1998, **273**(16):9912-9920.

171. Mori K, Ogawa N, Kawahara T, Yanagi H, Yura T: **mRNA splicing-mediated C-terminal replacement of transcription factor Hac1p is required for efficient activation of the unfolded protein response**. *Proceedings of the National Academy of Sciences of the United States of America* 2000, **97**(9):4660-4665.

172. Mori K, Sant A, Kohno K, Normington K, Gething MJ, Sambrook JF: **A 22 bp cis-acting element is necessary and sufficient for the induction of the yeast KAR2 (BiP) gene by unfolded proteins**. *The EMBO journal* 1992, **11**(7):2583-2593.

173. Mori T, Ogasawara C, Inada T, Englert M, Beier H, Takezawa M, Endo T, Yoshihisa T: **Dual functions of yeast tRNA ligase in the unfolded protein response: unconventional cytoplasmic splicing of HAC1 pre-mRNA is not sufficient to release translational attenuation**. *Molecular biology of the cell* 2010, **21**(21):3722-3734.

174. Morris JA, Dorner AJ, Edwards CA, Hendershot LM, Kaufman RJ: **Immunoglobulin binding protein (BiP) function is required to protect cells from endoplasmic reticulum stress but is not required for the secretion of selective proteins**. *The Journal of biological chemistry* 1997, **272**(7):4327-4334.

175. Muller P, Kuttenkeuler D, Gesellchen V, Zeidler MP, Boutros M: **Identification of JAK/STAT signalling components by genome-wide RNA interference**. *Nature* 2005, **436**(7052):871-875.

176. Muro I, Berry DL, Huh JR, Chen CH, Huang H, Yoo SJ, Guo M, Baehrecke EH, Hay BA: **The Drosophila caspase Ice is important for many apoptotic cell deaths and for spermatid individualization, a nonapoptotic process**. *Development* 2006, **133**(17):3305-3315.

177. Muro I, Means JC, Clem RJ: **Cleavage of the apoptosis inhibitor DIAP1 by the apical caspase DRONC in both normal and apoptotic Drosophila cells**. *The Journal of biological chemistry* 2005, **280**(19):18683-18688.

178. Nadanaka S, Yoshida H, Kano F, Murata M, Mori K: **Activation of mammalian unfolded protein response is compatible with the quality control system operating in the endoplasmic reticulum**. *Molecular biology of the cell* 2004, **15**(6):2537-2548.

179. Nikawa J, Yamashita S: **IRE1 encodes a putative protein kinase containing a membrane-spanning domain and is required for inositol phototrophy in Saccharomyces cerevisiae**. *Molecular microbiology* 1992, **6**(11):1441-1446.

180. Nishitoh H, Matsuzawa A, Tobiume K, Saegusa K, Takeda K, Inoue K, Hori S, Kakizuka A, Ichijo H: **ASK1 is essential for endoplasmic reticulum stress-induced neuronal cell death triggered by expanded polyglutamine repeats**. *Genes & development* 2002, **16**(11):1345-1355.

181. Nordstrom W, Chen P, Steller H, Abrams JM: **Activation of the reaper gene during ectopic cell killing in Drosophila**. *Developmental biology* 1996, **180**(1):213-226.

182. Normington K, Kohno K, Kozutsumi Y, Gething MJ, Sambrook J: **S. cerevisiae encodes an essential protein homologous in sequence and function to mammalian BiP**. *Cell* 1989, **57**(7):1223-1236.

183. Novoa I, Zeng H, Harding HP, Ron D: **Feedback inhibition of the unfolded protein response by GADD34-mediated dephosphorylation of eIF2alpha**. *The Journal of cell biology* 2001, **153**(5):1011-1022.

184. Novoa I, Zhang Y, Zeng H, Jungreis R, Harding HP, Ron D: **Stress-induced gene expression requires programmed recovery from translational repression**. *The EMBO journal* 2003, **22**(5):1180-1187.

185. Oda Y, Hosokawa N, Wada I, Nagata K: **EDEM as an acceptor of terminally misfolded glycoproteins released from calnexin**. *Science* 2003, **299**(5611):1394-1397.

186. Oikawa D, Kimata Y, Kohno K: **Self-association and BiP dissociation are not sufficient for activation of the ER stress sensor Ire1**. *Journal of cell science* 2007, **120**(Pt 9):1681-1688.

187. Okada T, Yoshida H, Akazawa R, Negishi M, Mori K: **Distinct roles of activating transcription factor 6 (ATF6) and double-stranded RNA-activated protein kinase-like endoplasmic reticulum kinase (PERK) in transcription during the mammalian unfolded protein response**. *The Biochemical journal* 2002, **366**(Pt 2):585-594.

188. Okamura K, Kimata Y, Higashio H, Tsuru A, Kohno K: **Dissociation of Kar2p/BiP from an ER sensory molecule, Ire1p, triggers the unfolded protein response in yeast**. *Biochemical and biophysical research communications* 2000, **279**(2):445-450.

189. Olson MR, Holley CL, Gan EC, Colon-Ramos DA, Kaplan B, Kornbluth S: **A GH3-like domain in reaper is required for mitochondrial localization and induction of IAP degradation**. *The Journal of biological chemistry* 2003, **278**(45):44758-44768.

190. Olson MR, Holley CL, Yoo SJ, Huh JR, Hay BA, Kornbluth S: **Reaper is regulated by IAP-mediated ubiquitination**. *The Journal of biological chemistry* 2003, **278**(6):4028-4034.

191. Peterson C, Carney GE, Taylor BJ, White K: **reaper is required for neuroblast apoptosis during Drosophila development**. *Development* 2002, **129**(6):1467-1476.

192. Pincus D, Chevalier MW, Aragon T, van Anken E, Vidal SE, El-Samad H, Walter P: **BiP binding to the ER-stress sensor Ire1 tunes the homeostatic behavior of the unfolded protein response**. *PLoS biology* 2010, **8**(7):e1000415.

193. Plongthongkum N, Kullawong N, Panyim S, Tirasophon W: **Ire1 regulated XBP1 mRNA splicing is essential for the unfolded protein response (UPR) in Drosophila melanogaster**. *Biochemical and biophysical research communications* 2007, **354**(3):789-794.

194. Pomar N, Berlanga JJ, Campuzano S, Hernandez G, Elias M, de Haro C: **Functional characterization of Drosophila melanogaster PERK eukaryotic initiation factor 2alpha (eIF2alpha) kinase**. *European journal of biochemistry / FEBS* 2003, **270**(2):293-306.

195. Potts PR, Singh S, Knezek M, Thompson CB, Deshmukh M: **Critical function of endogenous XIAP in regulating caspase activation during sympathetic neuronal apoptosis**. *The Journal of cell biology* 2003, **163**(4):789-799.

196. Pourkarimi E, Greiss S, Gartner A: **Evidence that CED-9/Bcl2 and CED-4/Apaf-1 localization is not consistent with the current model for C. elegans apoptosis induction**. *Cell death and differentiation* 2012, **19**(3):406-415.

197. Prasanthi JR, Larson T, Schommer J, Ghribi O: **Silencing GADD153/CHOP gene expression protects against Alzheimer's disease-like pathology induced by 27-hydroxycholesterol in rabbit hippocampus**. *PloS one* 2011, **6**(10):e26420.

198. Prostko CR, Brostrom MA, Malara EM, Brostrom CO: **Phosphorylation of eukaryotic initiation factor (eIF) 2 alpha and inhibition of eIF-2B in GH3 pituitary cells by perturbants of early protein processing that induce GRP78**. *The Journal of biological chemistry* 1992, **267**(24):16751-16754.

199. Puthalakath H, O'Reilly LA, Gunn P, Lee L, Kelly PN, Huntington ND, Hughes PD, Michalak EM, McKimm-Breschkin J, Motoyama N *et al*: **ER stress triggers apoptosis by activating BH3-only protein Bim**. *Cell* 2007, **129**(7):1337-1349.

200. Quan EM, Kamiya Y, Kamiya D, Denic V, Weibezahn J, Kato K, Weissman JS: **Defining the glycan destruction signal for endoplasmic reticulum-associated degradation**. *Molecular cell* 2008, **32**(6):870-877.

201. Quinn L, Coombe M, Mills K, Daish T, Colussi P, Kumar S, Richardson H: **Buffy, a Drosophila Bcl-2 protein, has anti-apoptotic and cell cycle inhibitory functions**. *The EMBO journal* 2003, **22**(14):3568-3579.

202. Quinn LM, Dorstyn L, Mills K, Colussi PA, Chen P, Coombe M, Abrams J, Kumar S, Richardson H: **An essential role for the caspase dronc in developmentally programmed cell death in Drosophila**. *The Journal of biological chemistry* 2000, **275**(51):40416-40424.

203. Reed JC, Doctor KS, Godzik A: **The domains of apoptosis: a genomics perspective**. *Science's STKE : signal transduction knowledge environment* 2004, **2004**(239):re9.

204. Reimold AM, Etkin A, Clauss I, Perkins A, Friend DS, Zhang J, Horton HF, Scott A, Orkin SH, Byrne MC *et al*: **An essential role in liver development for transcription factor XBP-1**. *Genes & development* 2000, **14**(2):152-157.

205. Reimold AM, Iwakoshi NN, Manis J, Vallabhajosyula P, Szomolanyi-Tsuda E, Gravallese EM, Friend D, Grusby MJ, Alt F, Glimcher LH: **Plasma cell differentiation requires the transcription factor XBP-1**. *Nature* 2001, **412**(6844):300-307.

206. Renatus M, Stennicke HR, Scott FL, Liddington RC, Salvesen GS: **Dimer formation drives the activation of the cell death protease caspase 9**. *Proceedings of the National Academy of Sciences of the United States of America* 2001, **98**(25):14250-14255.

207. Richardson CE, Kinkel S, Kim DH: **Physiological IRE-1-XBP-1 and PEK-1 signaling in Caenorhabditis elegans larval development and immunity**. *PLoS genetics* 2011, **7**(11):e1002391.

208. Richardson CE, Kooistra T, Kim DH: **An essential role for XBP-1 in host protection against immune activation in C. elegans**. *Nature* 2010, **463**(7284):1092-1095.

209. Rodriguez A, Oliver H, Zou H, Chen P, Wang X, Abrams JM: **Dark is a Drosophila homologue of Apaf-1/CED-4 and functions in an evolutionarily conserved death pathway**. *Nature cell biology* 1999, **1**(5):272-279.

210. Rodriguez J, Lazebnik Y: **Caspase-9 and APAF-1 form an active holoenzyme**. *Genes & development* 1999, **13**(24):3179-3184.

211. Ron D, Walter P: **Signal integration in the endoplasmic reticulum unfolded protein response**. *Nature reviews Molecular cell biology* 2007, **8**(7):519-529.

212. Roy N, Deveraux QL, Takahashi R, Salvesen GS, Reed JC: **The c-IAP-1 and c-IAP-2 proteins are direct inhibitors of specific caspases**. *The EMBO journal* 1997, **16**(23):6914-6925.

213. Rutkowski DT, Hegde RS: **Regulation of basal cellular physiology by the homeostatic unfolded protein response**. *The Journal of cell biology* 2010, **189**(5):783-794.

214. Ryoo HD, Bergmann A, Gonen H, Ciechanover A, Steller H: **Regulation of Drosophila IAP1 degradation and apoptosis by reaper and ubcD1**. *Nature cell biology* 2002, **4**(6):432-438.

215. Ryoo HD, Domingos PM, Kang MJ, Steller H: **Unfolded protein response in a Drosophila model for retinal degeneration**. *The EMBO journal* 2007, **26**(1):242-252.

216. Ryu EJ, Harding HP, Angelastro JM, Vitolo OV, Ron D, Greene LA: **Endoplasmic reticulum stress and the unfolded protein response in cellular models of Parkinson's disease**. *The Journal of neuroscience : the official journal of the Society for Neuroscience* 2002, **22**(24):10690-10698.

217. Safer B: **2B or not 2B: regulation of the catalytic utilization of eIF-2**. *Cell* 1983, **33**(1):7-8.

218. Sandu C, Ryoo HD, Steller H: **Drosophila IAP antagonists form multimeric complexes to promote cell death**. *The Journal of cell biology* 2010, **190**(6):1039-1052.

219. Sato N, Imaizumi K, Manabe T, Taniguchi M, Hitomi J, Katayama T, Yoneda T, Morihara T, Yasuda Y, Takagi T *et al*: **Increased production of beta-amyloid and vulnerability to endoplasmic reticulum stress by an aberrant spliced form of presenilin 2**. *The Journal of biological chemistry* 2001, **276**(3):2108-2114.

220. Scheuner D, Song B, McEwen E, Liu C, Laybutt R, Gillespie P, Saunders T, Bonner-Weir S, Kaufman RJ: **Translational control is required for the unfolded protein response and in vivo glucose homeostasis**. *Molecular cell* 2001, **7**(6):1165-1176.

221. Schile AJ, Garcia-Fernandez M, Steller H: **Regulation of apoptosis by XIAP ubiquitin-ligase activity**. *Genes & development* 2008, **22**(16):2256-2266.

222. Schindler AJ, Schekman R: **In vitro reconstitution of ER-stress induced ATF6 transport in COPII vesicles**. *Proceedings of the National Academy of Sciences of the United States of America* 2009, **106**(42):17775-17780.

223. Schuck S, Prinz WA, Thorn KS, Voss C, Walter P: **Membrane expansion alleviates endoplasmic reticulum stress independently of the unfolded protein response**. *The Journal of cell biology* 2009, **187**(4):525-536.

224. Shaffer AL, Shapiro-Shelef M, Iwakoshi NN, Lee AH, Qian SB, Zhao H, Yu X, Yang L, Tan BK, Rosenwald A *et al*: **XBP1, downstream of Blimp-1, expands the secretory apparatus and other organelles, and increases protein synthesis in plasma cell differentiation**. *Immunity* 2004, **21**(1):81-93.

225. Shaham S, Horvitz HR: **Developing Caenorhabditis elegans neurons may contain both cell-death protective and killer activities**. *Genes & development* 1996, **10**(5):578-591.

226. Shaham S, Horvitz HR: **An alternatively spliced C. elegans ced-4 RNA encodes a novel cell death inhibitor**. *Cell* 1996, **86**(2):201-208.

227. Shamu CE, Walter P: **Oligomerization and phosphorylation of the Ire1p kinase during intracellular signaling from the endoplasmic reticulum to the nucleus**. *The EMBO journal* 1996, **15**(12):3028-3039.

228. Shen J, Chen X, Hendershot L, Prywes R: **ER stress regulation of ATF6 localization by dissociation of BiP/GRP78 binding and unmasking of Golgi localization signals**. *Developmental cell* 2002, **3**(1):99-111.

229. Shen X, Ellis RE, Lee K, Liu CY, Yang K, Solomon A, Yoshida H, Morimoto R, Kurnit DM, Mori K *et al*: **Complementary signaling pathways regulate the unfolded protein response and are required for C. elegans development**. *Cell* 2001, **107**(7):893-903.

230. Shen X, Ellis RE, Sakaki K, Kaufman RJ: **Genetic interactions due to constitutive and inducible gene regulation mediated by the unfolded protein response in C. elegans**. *PLoS genetics* 2005, **1**(3):e37.

231. Shi Y: **Mechanisms of caspase activation and inhibition during apoptosis**. *Molecular cell* 2002, **9**(3):459-470.

232. Shi Y, Vattem KM, Sood R, An J, Liang J, Stramm L, Wek RC: **Identification and characterization of pancreatic eukaryotic initiation factor 2 alpha-subunit kinase, PEK, involved in translational control**. *Molecular and cellular biology* 1998, **18**(12):7499-7509.

233. Shinya S, Kadokura H, Imagawa Y, Inoue M, Yanagitani K, Kohno K: **Reconstitution and characterization of the unconventional splicing of XBP1u mRNA in vitro**. *Nucleic acids research* 2011, **39**(12):5245-5254.

234. Shiozaki EN, Shi Y: **Caspases, IAPs and Smac/DIABLO: mechanisms from structural biology**. *Trends in biochemical sciences* 2004, **29**(9):486-494.

235. Shiu RP, Pouyssegur J, Pastan I: **Glucose depletion accounts for the induction of two transformation-sensitive membrane proteinsin Rous sarcoma virus-transformed chick embryo fibroblasts**. *Proceedings of the National Academy of Sciences of the United States of America* 1977, **74**(9):3840-3844.

236. Sidrauski C, Cox JS, Walter P: **tRNA ligase is required for regulated mRNA splicing in the unfolded protein response**. *Cell* 1996, **87**(3):405-413.

237. Silke J, Kratina T, Ekert PG, Pakusch M, Vaux DL: **Unlike Diablo/smac, Grim promotes global ubiquitination and specific degradation of X chromosome-linked inhibitor of apoptosis (XIAP) and neither cause apoptosis**. *The Journal of biological chemistry* 2004, **279**(6):4313-4321.

238. Smith MH, Ploegh HL, Weissman JS: **Road to ruin: targeting proteins for degradation in the endoplasmic reticulum**. *Science* 2011, **334**(6059):1086-1090.

239. Song Z, Guan B, Bergman A, Nicholson DW, Thornberry NA, Peterson EP, Steller H: **Biochemical and genetic interactions between Drosophila caspases and the proapoptotic genes rpr, hid, and grim**. *Molecular and cellular biology* 2000, **20**(8):2907-2914.

240. Song Z, McCall K, Steller H: **DCP-1, a Drosophila cell death protease essential for development**. *Science* 1997, **275**(5299):536-540.

241. Sonnenfeld MJ, Jacobs JR: **Apoptosis of the midline glia during Drosophila embryogenesis: a correlation with axon contact**. *Development* 1995, **121**(2):569-578.

242. Sood R, Porter AC, Ma K, Quilliam LA, Wek RC: **Pancreatic eukaryotic initiation factor-2alpha kinase (PEK) homologues in humans, Drosophila melanogaster and Caenorhabditis elegans that mediate translational control in response to endoplasmic reticulum stress**. *The Biochemical journal* 2000, **346 Pt 2**:281-293.

243. Souid S, Lepesant JA, Yanicostas C: **The xbp-1 gene is essential for development in Drosophila**. *Development genes and evolution* 2007, **217**(2):159-167.

244. Sriburi R, Bommiasamy H, Buldak GL, Robbins GR, Frank M, Jackowski S, Brewer JW: **Coordinate regulation of phospholipid biosynthesis and secretory pathway gene expression in XBP-1(S)-induced endoplasmic reticulum biogenesis**. *The Journal of biological chemistry* 2007, **282**(10):7024-7034.

245. Srinivasula SM, Datta P, Kobayashi M, Wu JW, Fujioka M, Hegde R, Zhang Z, Mukattash R, Fernandes-Alnemri T, Shi Y *et al*: **sickle, a novel Drosophila death gene in the reaper/hid/grim region, encodes an IAP-inhibitory protein**. *Current biology : CB* 2002, **12**(2):125-130.

246. Srivastava M, Scherr H, Lackey M, Xu D, Chen Z, Lu J, Bergmann A: **ARK, the Apaf-1 related killer in Drosophila, requires diverse domains for its apoptotic activity**. *Cell death and differentiation* 2007, **14**(1):92-102.

247. Steller H: **Mechanisms and genes of cellular suicide**. *Science* 1995, **267**(5203):1445-1449.

248. Sulston JE, Horvitz HR: **Post-embryonic cell lineages of the nematode, Caenorhabditis elegans**. *Developmental biology* 1977, **56**(1):110-156.

249. Suzanne M, Petzoldt AG, Speder P, Coutelis JB, Steller H, Noselli S: **Coupling of apoptosis and L/R patterning controls stepwise organ looping**. *Current biology : CB* 2010, **20**(19):1773-1778.

250. Tan Y, Yamada-Mabuchi M, Arya R, St Pierre S, Tang W, Tosa M, Brachmann C, White K: **Coordinated expression of cell death genes regulates neuroblast apoptosis**. *Development* 2011, **138**(11):2197-2206.

251. Tenev T, Zachariou A, Wilson R, Ditzel M, Meier P: **IAPs are functionally non-equivalent and regulate effector caspases through distinct mechanisms**. *Nature cell biology* 2005, **7**(1):70-77.

252. Tenev T, Zachariou A, Wilson R, Paul A, Meier P: **Jafrac2 is an IAP antagonist that promotes cell death by liberating Dronc from DIAP1**. *The EMBO journal* 2002, **21**(19):5118-5129.

253. Thompson CB: **Apoptosis in the pathogenesis and treatment of disease**. *Science* 1995, **267**(5203):1456-1462.

254. Thuerauf DJ, Morrison L, Glembotski CC: **Opposing roles for ATF6alpha and ATF6beta in endoplasmic reticulum stress response gene induction**. *The Journal of biological chemistry* 2004, **279**(20):21078-21084.

255. Tirasophon W, Lee K, Callaghan B, Welihinda A, Kaufman RJ: **The endoribonuclease activity of mammalian IRE1 autoregulates its mRNA and is required for the unfolded protein response**. *Genes & development* 2000, **14**(21):2725-2736.

256. Tirasophon W, Welihinda AA, Kaufman RJ: **A stress response pathway from the endoplasmic reticulum to the nucleus requires a novel bifunctional protein kinase/endoribonuclease (Ire1p) in mammalian cells**. *Genes & development* 1998, **12**(12):1812-1824.

257. Travers KJ, Patil CK, Wodicka L, Lockhart DJ, Weissman JS, Walter P: **Functional and genomic analyses reveal an essential coordination between the unfolded protein response and ER-associated degradation**. *Cell* 2000, **101**(3):249-258.

258. Tsujimoto Y, Gorham J, Cossman J, Jaffe E, Croce CM: **The t(14;18) chromosome translocations involved in B-cell neoplasms result from mistakes in VDJ joining**. *Science* 1985, **229**(4720):1390-1393.

259. Urano F, Calfon M, Yoneda T, Yun C, Kiraly M, Clark SG, Ron D: **A survival pathway for Caenorhabditis elegans with a blocked unfolded protein response**. *The Journal of cell biology* 2002, **158**(4):639-646.

260. Urano F, Wang X, Bertolotti A, Zhang Y, Chung P, Harding HP, Ron D: **Coupling of stress in the ER to activation of JNK protein kinases by transmembrane protein kinase IRE1**. *Science* 2000, **287**(5453):664-666.

261. Vashist S, Ng DT: **Misfolded proteins are sorted by a sequential checkpoint mechanism of ER quality control**. *The Journal of cell biology* 2004, **165**(1):41-52.

262. Vembar SS, Brodsky JL: **One step at a time: endoplasmic reticulum-associated degradation**. *Nature reviews Molecular cell biology* 2008, **9**(12):944-957.

263. Verhagen AM, Ekert PG, Pakusch M, Silke J, Connolly LM, Reid GE, Moritz RL, Simpson RJ, Vaux DL: **Identification of DIABLO, a mammalian protein that promotes apoptosis by binding to and antagonizing IAP proteins**. *Cell* 2000, **102**(1):43-53.

264. Vernooy SY, Chow V, Su J, Verbrugghe K, Yang J, Cole S, Olson MR, Hay BA: **Drosophila Bruce can potently suppress Rpr- and Grim-dependent but not Hid-dependent cell death**. *Current biology : CB* 2002, **12**(13):1164-1168.

265. Vucic D, Kaiser WJ, Harvey AJ, Miller LK: **Inhibition of reaper-induced apoptosis by interaction with inhibitor of apoptosis proteins (IAPs)**. *Proceedings of the National Academy of Sciences of the United States of America* 1997, **94**(19):10183-10188.

266. Vucic D, Kaiser WJ, Miller LK: **Inhibitor of apoptosis proteins physically interact with and block apoptosis induced by Drosophila proteins HID and GRIM**. *Molecular and cellular biology* 1998, **18**(6):3300-3309.

267. Walker NP, Talanian RV, Brady KD, Dang LC, Bump NJ, Ferenz CR, Franklin S, Ghayur T, Hackett MC, Hammill LD *et al*: **Crystal structure of the cysteine protease interleukin-1 beta-converting enzyme: a (p20/p10)2 homodimer**. *Cell* 1994, **78**(2):343-352.

268. Walrad PB, Hang S, Joseph GS, Salas J, Gergen JP: **Distinct contributions of conserved modules to Runt transcription factor activity**. *Molecular biology of the cell* 2010, **21**(13):2315-2326.

269. Walter P, Ron D: **The unfolded protein response: from stress pathway to homeostatic regulation**. *Science* 2011, **334**(6059):1081-1086.

270. Wang SL, Hawkins CJ, Yoo SJ, Muller HA, Hay BA: **The Drosophila caspase inhibitor DIAP1 is essential for cell survival and is negatively regulated by HID**. *Cell* 1999, **98**(4):453-463.

271. Wang XZ, Harding HP, Zhang Y, Jolicoeur EM, Kuroda M, Ron D: **Cloning of mammalian Ire1 reveals diversity in the ER stress responses**. *The EMBO journal* 1998, **17**(19):5708-5717.

272. White K, Grether ME, Abrams JM, Young L, Farrell K, Steller H: **Genetic control of programmed cell death in Drosophila**. *Science* 1994, **264**(5159):677-683.

273. White K, Tahaoglu E, Steller H: **Cell killing by the Drosophila gene reaper**. *Science* 1996, **271**(5250):805-807.

274. Williams DW, Kondo S, Krzyzanowska A, Hiromi Y, Truman JW: **Local caspase activity directs engulfment of dendrites during pruning**. *Nature neuroscience* 2006, **9**(10):1234-1236.

275. Wilson KP, Black JA, Thomson JA, Kim EE, Griffith JP, Navia MA, Murcko MA, Chambers SP, Aldape RA, Raybuck SA *et al*: **Structure and mechanism of interleukin-1 beta converting enzyme**. *Nature* 1994, **370**(6487):270-275.

276. Wilson R, Goyal L, Ditzel M, Zachariou A, Baker DA, Agapite J, Steller H, Meier P: **The DIAP1 RING finger mediates ubiquitination of Dronc and is indispensable for regulating apoptosis**. *Nature cell biology* 2002, **4**(6):445-450.

277. Wing JP, Zhou L, Schwartz LM, Nambu JR: **Distinct cell killing properties of the Drosophila reaper, head involution defective, and grim genes**. *Cell death and differentiation* 1998, **5**(11):930-939.

278. Woehlbier U, Hetz C: **Modulating stress responses by the UPRosome: a matter of life and death**. *Trends in biochemical sciences* 2011, **36**(6):329-337.

279. Wu G, Chai J, Suber TL, Wu JW, Du C, Wang X, Shi Y: **Structural basis of IAP recognition by Smac/DIABLO**. *Nature* 2000, **408**(6815):1008-1012.

280. Wu J, Rutkowski DT, Dubois M, Swathirajan J, Saunders T, Wang J, Song B, Yau GD, Kaufman RJ: **ATF6alpha optimizes long-term endoplasmic reticulum function to protect cells from chronic stress**. *Developmental cell* 2007, **13**(3):351-364.

281. Wu JN, Nguyen N, Aghazarian M, Tan Y, Sevrioukov EA, Mabuchi M, Tang W, Monserrate JP, White K, Brachmann CB: **grim promotes programmed cell death of Drosophila microchaete glial cells**. *Mechanisms of development* 2010, **127**(9-12):407-417.

282. Wu JW, Cocina AE, Chai J, Hay BA, Shi Y: **Structural analysis of a functional DIAP1 fragment bound to grim and hid peptides**. *Molecular cell* 2001, **8**(1):95-104.

283. Xu D, Li Y, Arcaro M, Lackey M, Bergmann A: **The CARD-carrying caspase Dronc is essential for most, but not all, developmental cell death in Drosophila**. *Development* 2005, **132**(9):2125-2134.

284. Xu D, Wang Y, Willecke R, Chen Z, Ding T, Bergmann A: **The effector caspases drICE and dcp-1 have partially overlapping functions in the apoptotic pathway in Drosophila**. *Cell death and differentiation* 2006, **13**(10):1697-1706.

285. Xu Y, Condell M, Plesken H, Edelman-Novemsky I, Ma J, Ren M, Schlame M: **A Drosophila model of Barth syndrome**. *Proceedings of the National Academy of Sciences of the United States of America* 2006, **103**(31):11584-11588.

286. Yamamoto K, Sato T, Matsui T, Sato M, Okada T, Yoshida H, Harada A, Mori K: **Transcriptional induction of mammalian ER quality control proteins is mediated by single or combined action of ATF6alpha and XBP1**. *Developmental cell* 2007, **13**(3):365-376.

287. Yamamoto K, Yoshida H, Kokame K, Kaufman RJ, Mori K: **Differential contributions of ATF6 and XBP1 to the activation of endoplasmic reticulum stress-responsive cis-acting elements ERSE, UPRE and ERSE-II**. *Journal of biochemistry* 2004, **136**(3):343-350.

288. Yan N, Wu JW, Chai J, Li W, Shi Y: **Molecular mechanisms of DrICE inhibition by DIAP1 and removal of inhibition by Reaper, Hid and Grim**. *Nature structural & molecular biology* 2004, **11**(5):420-428.

289. Yan W, Frank CL, Korth MJ, Sopher BL, Novoa I, Ron D, Katze MG: **Control of PERK eIF2alpha kinase activity by the endoplasmic reticulum stress-induced molecular chaperone P58IPK**. *Proceedings of the National Academy of Sciences of the United States of America* 2002, **99**(25):15920-15925.

290. Yanagitani K, Imagawa Y, Iwawaki T, Hosoda A, Saito M, Kimata Y, Kohno K: **Cotranslational targeting of XBP1 protein to the membrane promotes cytoplasmic splicing of its own mRNA**. *Molecular cell* 2009, **34**(2):191-200.

291. Yang X, Chang HY, Baltimore D: **Essential role of CED-4 oligomerization in CED-3 activation and apoptosis**. *Science* 1998, **281**(5381):1355-1357.

292. Yang X, Chang HY, Baltimore D: **Autoproteolytic activation of pro-caspases by oligomerization**. *Molecular cell* 1998, **1**(2):319-325.

293. Ye J, Rawson RB, Komuro R, Chen X, Dave UP, Prywes R, Brown MS, Goldstein JL: **ER stress induces cleavage of membrane-bound ATF6 by the same proteases that process SREBPs**. *Molecular cell* 2000, **6**(6):1355-1364.

294. Ye Y, Shibata Y, Yun C, Ron D, Rapoport TA: **A membrane protein complex mediates retro-translocation from the ER lumen into the cytosol**. *Nature* 2004, **429**(6994):841-847.

295. Yin VP, Thummel CS: **A balance between the diap1 death inhibitor and reaper and hid death inducers controls steroid-triggered cell death in Drosophila**. *Proceedings of the National Academy of Sciences of the United States of America* 2004, **101**(21):8022-8027.

296. Yoo SJ, Huh JR, Muro I, Yu H, Wang L, Wang SL, Feldman RM, Clem RJ, Muller HA, Hay BA: **Hid, Rpr and Grim negatively regulate DIAP1 levels through distinct mechanisms**. *Nature cell biology* 2002, **4**(6):416-424.

297. Yorimitsu T, Nair U, Yang Z, Klionsky DJ: **Endoplasmic reticulum stress triggers autophagy**. *The Journal of biological chemistry* 2006, **281**(40):30299-30304.

298. Yoshida H, Haze K, Yanagi H, Yura T, Mori K: **Identification of the cis-acting endoplasmic reticulum stress response element responsible for transcriptional induction of mammalian glucose-regulated proteins. Involvement of basic leucine zipper transcription factors**. *The Journal of biological chemistry* 1998, **273**(50):33741-33749.

299. Yoshida H, Matsui T, Hosokawa N, Kaufman RJ, Nagata K, Mori K: **A time-dependent phase shift in the mammalian unfolded protein response**. *Developmental cell* 2003, **4**(2):265-271.

300. Yoshida H, Matsui T, Yamamoto A, Okada T, Mori K: **XBP1 mRNA is induced by ATF6 and spliced by IRE1 in response to ER stress to produce a highly active transcription factor**. *Cell* 2001, **107**(7):881-891.

301. Yoshida H, Okada T, Haze K, Yanagi H, Yura T, Negishi M, Mori K: **ATF6 activated by proteolysis binds in the presence of NF-Y (CBF) directly to the cis-acting element responsible for the mammalian unfolded protein response**. *Molecular and cellular biology* 2000, **20**(18):6755-6767.

302. Yoshida H, Oku M, Suzuki M, Mori K: **pXBP1(U) encoded in XBP1 pre-mRNA negatively regulates unfolded protein response activator pXBP1(S) in**

mammalian ER stress response. *The Journal of cell biology* 2006, **172**(4):565-575.

303. Yoshida H, Uemura A, Mori K: **pXBP1(U), a negative regulator of the unfolded protein response activator pXBP1(S), targets ATF6 but not ATF4 in proteasome-mediated degradation**. *Cell structure and function* 2009, **34**(1):1-10.

304. Yuan J, Kroemer G: **Alternative cell death mechanisms in development and beyond**. *Genes & development* 2010, **24**(23):2592-2602.

305. Yuan J, Shaham S, Ledoux S, Ellis HM, Horvitz HR: **The C. elegans cell death gene ced-3 encodes a protein similar to mammalian interleukin-1 beta-converting enzyme**. *Cell* 1993, **75**(4):641-652.

306. Yuan J, Yankner BA: **Apoptosis in the nervous system**. *Nature* 2000, **407**(6805):802-809.

307. Yuan JY, Horvitz HR: **The Caenorhabditis elegans genes ced-3 and ced-4 act cell autonomously to cause programmed cell death**. *Developmental biology* 1990, **138**(1):33-41.

308. Zachariou A, Tenev T, Goyal L, Agapite J, Steller H, Meier P: **IAP-antagonists exhibit non-redundant modes of action through differential DIAP1 binding**. *The EMBO journal* 2003, **22**(24):6642-6652.

309. Zhang B, Wang Y, Pang X, Su Y, Ai G, Wang T: **ER stress induced by ionising radiation in IEC-6 cells**. *International journal of radiation biology* 2010, **86**(6):429-435.

310. Zhang K, Wong HN, Song B, Miller CN, Scheuner D, Kaufman RJ: **The unfolded protein response sensor IRE1alpha is required at 2 distinct steps in B cell lymphopoiesis**. *The Journal of clinical investigation* 2005, **115**(2):268-281.

311. Zhang P, McGrath B, Li S, Frank A, Zambito F, Reinert J, Gannon M, Ma K, McNaughton K, Cavener DR: **The PERK eukaryotic initiation factor 2 alpha kinase is required for the development of the skeletal system, postnatal**

growth, and the function and viability of the pancreas. *Molecular and cellular biology* 2002, **22**(11):3864-3874.

312. Zhang Y, Lin N, Carroll PM, Chan G, Guan B, Xiao H, Yao B, Wu SS, Zhou L: **Epigenetic blocking of an enhancer region controls irradiation-induced proapoptotic gene expression in Drosophila embryos**. *Developmental cell* 2008, **14**(4):481-493.

313. Zhou L, Hashimi H, Schwartz LM, Nambu JR: **Programmed cell death in the Drosophila central nervous system midline**. *Current biology : CB* 1995, **5**(7):784-790.

314. Zhou L, Schnitzler A, Agapite J, Schwartz LM, Steller H, Nambu JR: **Cooperative functions of the reaper and head involution defective genes in the programmed cell death of Drosophila central nervous system midline cells**. *Proceedings of the National Academy of Sciences of the United States of America* 1997, **94**(10):5131-5136.

315. Zhou L, Song Z, Tittel J, Steller H: **HAC-1, a Drosophila homolog of APAF-1 and CED-4 functions in developmental and radiation-induced apoptosis**. *Molecular cell* 1999, **4**(5):745-755.

316. Zhou L, Steller H: **Distinct pathways mediate UV-induced apoptosis in Drosophila embryos**. *Developmental cell* 2003, **4**(4):599-605.

317. Zhou R, Hotta I, Denli AM, Hong P, Perrimon N, Hannon GJ: **Comparative analysis of argonaute-dependent small RNA pathways in Drosophila**. *Molecular cell* 2008, **32**(4):592-599.

318. Zinszner H, Kuroda M, Wang X, Batchvarova N, Lightfoot RT, Remotti H, Stevens JL, Ron D: **CHOP is implicated in programmed cell death in response to impaired function of the endoplasmic reticulum**. *Genes & development* 1998, **12**(7):982-995.

319. Zou H, Li Y, Liu X, Wang X: **An APAF-1.cytochrome c multimeric complex is a functional apoptosome that activates procaspase-9**. *The Journal of biological chemistry* 1999, **274**(17):11549-11556.